

Shape Analysis of the Human Brain: A Brief Survey

Matthew J. Nitzken, *Member, IEEE*, Manuel F. Casanova, Georgy Gimel'farb, Tamer Inanc, *Member, IEEE*, Jacek M. Zurada, *Life Fellow, IEEE*, and Ayman El-Baz, *Member, IEEE*

Abstract—The survey outlines and compares popular computational techniques for quantitative description of shapes of major structural parts of the human brain, including medial axis and skeletal analysis, geodesic distances, Procrustes analysis, deformable models, spherical harmonics, and deformation morphometry, as well as other less widely used techniques. Their advantages, drawbacks, and emerging trends, as well as results of applications, in particular, for computer-aided diagnostics, are discussed.

Index Terms—Brain, diagnostics, shape analysis.

I. INTRODUCTION

THE human brain belongs to the most complex anatomical structure in the human body. Individual brains vary substantially, and therefore analyzing the brain presents a real challenge [1]. Fig. 1 illustrates the complexity of the brain represented in a three-dimensional (3-D) mesh format. Computer-aided medical diagnostics call for the quantitative analysis of many structural parts of the brain, such as the cortex, ventricles, corpus callosum, hippocampus, brain stem, and gyrfications.

This survey focuses primarily on applications of various shape analysis techniques to the human brain. Methods of shape analysis for the human brain include techniques such as medial axis and skeletal analysis, geodesic distances, Procrustes analysis, deformable models, SPHARM, deformation-based morphometry, symmetry-based analysis, Laplace-Beltrami operators, and homologous modeling, among other techniques.

In 1979, Lande [3] proposed to analyze the shape of the brain by measuring the brain volume. While the volumetric analysis of brain scans arguably does not yield sound discriminatory features, it was a key starting point for shape analysis related to the brain. Later on, Desimone *et al.* [4] and Martin *et al.* [5]

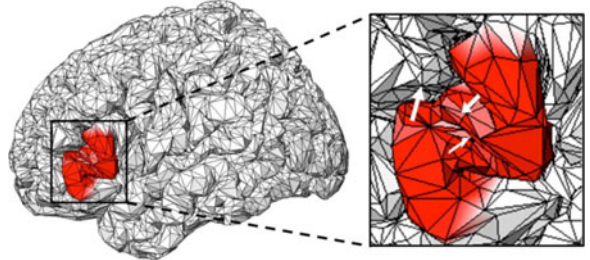


Fig. 1. 3-D mesh brain representation (the expanded section details its complexity and variability due to multiple different structures and gyrfications). Courtesy of Barras *et al.* [2].

proposed two more elaborate shape analysis frameworks. The first framework examined color, shape, and texture of the cortex on 2-D scans of the brain. The second framework performed a more advanced analysis, by examining pregenerated mesh models of the brain ventricles. To more accurately represent the brain, the meshes were decomposed using eigenvectors, that were obtained in a way similar to conventional principal component analysis (PCA). These early frameworks for examining the shapes of brain constructs did not produce reliable descriptors of brain-related health or behavioral disorders, such as autism and Alzheimer's disorder. However, they inspired extensive subsequent research that helped to push the current field of brain shape analysis into the forefront of research and development for computer-assisted medical diagnostics.

Generally, shape analysis is applied to digital geometric models of surfaces and/or volumes of objects-of-interest in order to detect similarities or differences between the objects [6]. Typically, shape analysis is fully automated or is a combination of automated and manual processing, and it is closely paired with some kind of object segmentation. Segmented objects are represented in a variety of digital formats including volumes, point clouds, and meshes. Most typically, the outer boundary (or surface) of an object, or a manifold representing this object, is examined.¹

Surface analysis, formally called surface interrogation, and computer-aided design systems, explicitly examine intrinsic and extrinsic geometric properties of surfaces of objects and manifolds, including visual pleasantness, technical smoothness, and geometric constraints [8]. It is often used to detect surface imperfections, analyze shapes, or visualize different forms.

Shape analysis techniques can be primarily classified into first- and second-order types, each containing large numbers of congruency-based, intrinsic, and graph-based shape descriptors [8]. The first-order methods typically rely on surface normal

Manuscript received March 25, 2013; revised September 12, 2013 and November 08, 2013; accepted December 20, 2013. Date of publication; date of current version.

M. J. Nitzken and A. El-Baz are with the BioImaging Laboratory, Bioengineering Department, University of Louisville, Louisville, KY 40292 USA (e-mail: mjnitz02@louisville.edu; aselba01@louisville.edu).

M. F. Casanova is with the Department of Psychiatry, University of Louisville, Louisville, KY 40202 USA (e-mail: m0cas02@louisville.edu).

G. Gimel'farb is with the Department of Computer Science, University of Auckland, Auckland 1142, New Zealand (e-mail: g.gimelfarb@auckland.ac.nz).

T. Inanc is with the Department of Electrical and Computer Engineering, University of Louisville, Louisville, KY 40292 USA (e-mail: t.inanc@louisville.edu).

J. M. Zurada is with the Electrical and Computer Engineering Department, University of Louisville, Louisville, KY 40292 USA and also with the Spoleczna Akademia Nauk, 90-011 Lodz, Poland (e-mail: jacek.zurada@louisville.edu).

Color versions of one or more of the figures in this paper are available online at <http://ieeexplore.ieee.org>.

Digital Object Identifier 10.1109/JBHI.2014.2298139

¹By Henri Poincaré [7], a manifold is the level set of a continuously differentiable function between Euclidean spaces that satisfies the non-degeneracy hypothesis of the implicit function theorem. In a simplified version, it can be thought of as an object with no holes or discontinuities.

vectors, inflections, and other intrinsic descriptors, obtained, e.g., by the Laplace–Beltrami analysis or the more popular geodesic path analysis. Some congruency methods fall into this category, such as the shape distribution and symmetry analysis.

Second-order analysis generally is based on the surface curvature and second derivatives. Typical descriptors are produced by moment analysis, spherical harmonics (SPHARMs), and Procrustes analysis, being invariant with respect to congruency and medial axis, skeletal, and Reeb graph analysis, which also heavily rely on the curvature. Importantly, many second-order analysis methods incorporate first-order techniques.

Both categories of shape analysis depend critically on shape interrogation, or extraction of structural characteristics of a shape from its geometric model [8], and remeshing, i.e., repartitioning of primitive components to fit best the original shape. Most commonly, vertex–vertex or face–vertex methods are used to construct the meshes. The vertex–vertex method deals with a point cloud, where the points relate to critical junctures in an object, while the face–vertex method exploits faces that interconnect vertices in a specific and controlled manner [9]. A widely known example of the latter is Delaunay triangulation, in which every face is a triangle and the final mesh consists of a large number of interconnected triangular faces. While the remeshing helps to preserve the original shape of the object, it can also be used to enhance some features of the shape. A primitive (such as a triangle that minimally characterizes the shape) can locally fit any such feature.

Some of the most popular shape analysis techniques, for application to the human brain, are detailed and compared below. These include 1) the medial axis and skeletal analysis, which is commonly used for surface (2-D) and volume (3-D) reconstruction in complex models; 2) geodesic distances to compare different brains in detail by using intrinsic and graph based analysis; 3) Procrustes analysis that can provide accurate and quick statistical evaluation of shapes in rigid objects; 4) deformable models evolving to fit boundaries of complex objects; 5) more recent 3-D surface approximation with SPHARMs in order to analyze the brain shape in detail; 6) the use of morphometry-based techniques to accurately analyze the volume of objects; 7) an examination of alternative and lesser used techniques.

II. MEDIAL AXIS AND SKELETAL ANALYSIS

Medial axes of complex 2-D/3-D graphical models are widely used for surface reconstruction and dimensionality reduction. A medial axis, or a skeleton of an object, is defined as the set of internal points with more than one closest point on the object's surface (see Fig. 2). Generally, it is represented by a polygon or a similar simple construction of concatenated arcs and parabolas that follow the would-be centerline of the object. The medial axis and skeletal graphs facilitate indexing, matching, segmenting, or associating objects with one another. Medial axis analysis has a wide range of uses that can be used in many anatomical applications outside of the brain, such as virtual colonoscopies.

The notion of a skeleton of a 2-D or 3-D shape was first introduced by Blum *et al.* [11], [12]. The underlying idea was to place a primitive shape inside an object, such as a ball. The

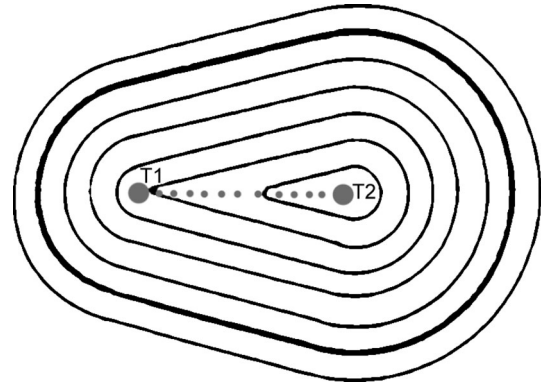


Fig. 2. Medial axis of a 2-D object: the outer black line shows the boundary of the object and the central dark line connecting the points T1 and T2. Inner isolines indicate the same distances from the boundary [10].

TABLE I
AUTOMATED (A) OR SEMIAUTOMATED (SA) MEDIAL AXIS ANALYSIS: GROUND TRUTH (GT) FROM CLINICIAN (C) OR NONCLINICIAN (N) EXPERTS; DIMENSIONALITY (DIM) AND SIZES (#) OF EXPERIMENTAL IMAGE DATABASES

| Publication | Year | Mode | Dim | # | GT |
|-----------------------------|------|------|-----|-----|----|
| Naf <i>et al</i> [13] | 1996 | A | 3D | n/a | N |
| Golland <i>et al</i> [14] | 1999 | A | 2D | 66 | C |
| Pizer <i>et al</i> [15] | 1999 | SA | 2D | 20 | C |
| Golland <i>et al</i> [16] | 2001 | A | 3D | 30 | C |
| Styner <i>et al</i> [17] | 2001 | A | 3D | 20 | C |
| Gorcowski <i>et al</i> [18] | 2007 | A | 3D | 70 | C |
| Elnakib <i>et al</i> [19] | 2011 | A | 3D | 34 | C |
| Paniagua <i>et al</i> [20] | 2013 | A | 3D | 90 | C |

primitive is then inflated it until reaching the object's surface, and this process is repeated until the object is filled with the maximum-size primitives. Connected centers of the primitives form the skeleton that represents geometric properties of the object's interior, such as bends and elongations, and reveals the geometric structure, or constituent parts of the object, and gives information about the object's position, orientation, and size.

Table I indexes applications of skeletons for human brain analysis, starting from the novel proposal by Naf *et al.* [13]. Naf classified various organs, including the brain, after characterizing their structure in 3-D images with Voronoi diagrams and skeletons. Excepting [15], all the methods in Table I were used for medical diagnostics or classification.

Golland *et al.* [14] analyzed skeletons of the corpus callosum in 2-D images in order to classify cases of schizophrenia. The initial skeletons were refined using snakes, or active contours, which evolved from different randomly chosen starting points. Then, the curvature angles and the width of the skeleton were used as discriminatory features. The angles were calculated between each set of adjacent points along the sampled medial axis, and the width was defined as the radial distance from the medial axis point to the surface boundary. Sampling more points of the skeleton provided finer details, but also increased the analysis time. The approach was tested on clinical datasets for normal and schizophrenic patients. A relatively high accuracy (more than 70% in the best case) was obtained for identifying schizophrenia in patients by statistical shape analysis of the corpus callosum and hippocampus [16] (the accuracy of a linear

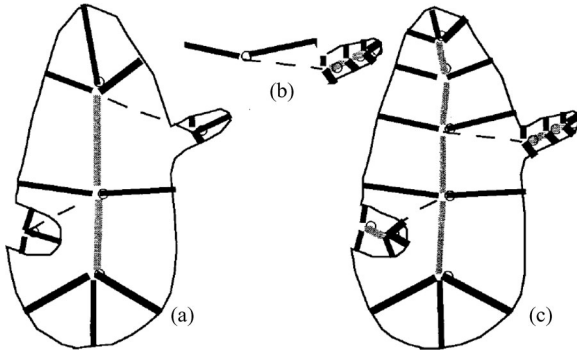


Fig. 3. Shown is a visual representation of Pizer's [15] medial axis approach. Due to the complexity of the shape, it is initialized with three skeletons (a). These are then individually examined (b) to create a composite skeleton of the parent figure (c).

classifier in determining schizophrenic patients on the training data proved to be consistently higher than the one using cross validation).

As noted in [14] and [16], the main advantages and drawbacks of skeletons relate to their compact and intuitive shape representation that can be used for segmentation, tracking, and object recognition, as well as their high sensitivity to noise in the object's boundary, respectively. The complex and spatially variant structure of the brain leads to a large amount of noise along the typical shape boundary. To overcome this challenge, frequently the typical general shapes of the objects are known in advance from segmented training samples and methods using fixed topology skeletons have been proposed in [14] and [16]. The significant benefit of such skeletons is that they can be adjusted to each current object of similar shape and optimized for accuracy.

Pizer *et al.* [15] proposed another method of quantifying object shapes in 2-D images that can be used in a variety of applications, including different brain structures. In this case, the skeletons were used to register brain shapes and compare the brain ventricles and brain stem. These structures could then be quantitatively described using a combination of the medial axes and distance analysis.

Golland's works [14], [16] dealt primarily with the corpus callosum of the shape that typically featured no extending appendages. Contrastingly, Pizer's medial axis analysis was focused on the brain ventricles, shapes of which (and thus their skeletons) often have one or more appendages. The skeletal appendages extend outward to include additional information about the more complex shapes. In Pizer's case, the medial axis analysis was modified to incorporate intersection points where multiple skeletons can be fused together, as, e.g., in Fig. 3. The resulting more complex skeletons proved to be useful for solving various problems, including segmentation and image registration [15]. Both Pizer's and Golland's approaches can be easily extended from 2-D to 3-D objects, at the expense of increased computational time due to the calculation of 3-D distances.

Styner and Gerig [17] expanded Pizer's concepts and analyzed the brain ventricles in 3-D images using Voronoi skeletons and PCA to obtain discriminatory features of shape changes and

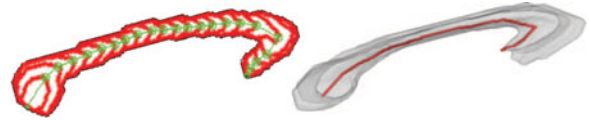


Fig. 4. Elnakib *et al.* [19] skeleton extraction method showing the centerline extraction method on the left and the final extracted centerline on the right.

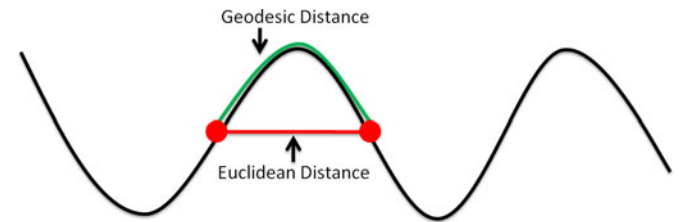


Fig. 5. Visual representation of a simple geodesic distance. The two points on the curve (shown as red circles) are connected by Euclidean (red straight line) and geodesic (green curved line) distance lines. Note how the geodesic distance follows the arc of the curve.

locality. SPHARMs were used to analyze similarities between the skeletons and compare twin ventricles. Similar to Pizer's implementation, Styner and Gerig's skeletons contain many detailed branches and intersections that represented the shape of the object. To reduce the effect of the noise in the outer object's boundary of the shape, the shape was smoothed by using PCA to include only dominant characteristics of shapes. After this initial simplification, the Voronoi skeleton was constructed using standard medial axis computation. Then PCA was used once again to "prune" smaller and less important branches of the skeleton.

Gorcowski *et al.* [18] used skeletons to analyze shapes and poses of five brain structures in order to classify autism. The mean classification accuracy on the basis of only poses, only shapes, or combined poses and shapes was 56%, 60%, and 64%, respectively, for an image database of 46 autistic and 24 control subjects. Although the combined features gave better results, the overall classification rate was rather low.

Elnakib *et al.* [19] obtained notably better classification accuracy, using a method shown in Fig. 4, for autistic and control subjects by analyzing the corpus callosum centerline: the study correctly classified 94% autistic and 88% control subjects at the 85% confidence level, 94% autistic and 82% control subjects at the 90% confidence level, and 82% autistic and 76.5% control subjects at the 95% confidence level for the database of 17 autistic and 17 normal subjects. They further extended their centerline extraction implementations [21]–[24] to examine more aspects of the corpus callosum and its 3-D centerline as applied to autism and dyslexia. This study was also explored by Casanova *et al.* [25], [26] and El-Baz *et al.* [27].

Paniagua *et al.* [20] used SPHARMs to calculate the mean latitude axis of ventricles in neonates. While this is not a full medial axis computation, it can be computed in a straightforward manner when using SPHARM. Importantly, Paniagua introduced a fusion of the medial axis technique with SPHARM analysis to achieve a diagnostic classification in neonatal subjects. This is

consistent with the modern trend of combining techniques for better accuracy.

In total, the medial axis and skeletal analysis are important for examining basic locations and shapes of structural parts of the brain. The main advantages of this method are that it creates simple representations of objects along with similarity measures and accurate descriptions for very complex shapes. These are useful in applications such as object classification and matching for medical diagnostics or understanding of object structure and construction. The limited use of the object's surface is the major drawback of the skeletal analysis that significantly decreases the usefulness of the medial axes and skeletons in applications dealing with the surface characteristics and/or small variations in shapes.

III. GEODESIC DISTANCES

Of primary interest in the analysis of the brain is the ability to make detailed comparisons of different brains. This often requires some form of nonrigid registration of the two surfaces of interest, or surface matching. A popular approach to this shape analysis problem is the use of geodesic distances. Geodesic distances can serve as an important geometric measurement of the brain and can help to provide a means of understanding complex shapes. Geodesic distances can serve to deliver a wealth of information about the surface geometry of a shape [8]. One of the first uses of geodesic distances, as applied to the brain, was by Griffin [28] in 1994. Griffin proposed the use of geodesic distance to characterize the cortical shape of the brain. This was later expanded on by Khaneja [29] who used geodesic distance to examine the curvature of sulci in the brain.

Geodesic distance is a combination of intrinsic and graph-based analysis. It is defined as the length of the graph of a geodesic between two vertices within an object [30]. It is the shortest path between two points that can be found in a curved space (such as the surface of a sphere) and has a wide array of practical uses. If you have ever boarded a plane to travel between continents there is a strong likelihood that you have traveled on a geodesic path, because these are the shortest distances between two points. In the sulci of the brain, geodesic paths that connect two points in a single sulcus will often follow the curvature of the sulcus [31]. The detection of geodesic paths is also heavily utilized on the surfaces of meshes for common graphics operations such as mesh segmentation, watermarking, editing, and smoothing [8].

Table II lists the applications of geodesic distance to the human brain analysis. Early application methods by Wang *et al.* [31] analyze the individual sulci of the brain. No methods that are primarily based on geodesic distance analysis have been used solely for medical diagnostics or classification.

The geodesic distance can be defined in a number of ways, although the most common calculations are for the Gaussian curvature and the mean surface curvature of an object. These metrics allow features of the brain, such as the gyrus and sulcus, to be easily calculated by examining each point. Information about the convex and concave areas of the sulci can be determined by examining the sign of the Gaussian curvature to

TABLE II
AUTOMATED (A) OR SEMIAUTOMATED (SA) GEODESIC DISTANCE ANALYSIS:
GROUND TRUTH (GT) FROM CLINICIAN (C) OR NONCLINICIAN (N) EXPERTS;
DIMENSIONALITY (DIM) AND SIZES (#) OF EXPERIMENTAL IMAGE DATABASES

| Publication | Year | Mode | Dim | # | GT |
|--------------------|------|------|-----|-----|----|
| Wang et al [31] | 2003 | A | 3D | n/a | N |
| Pastore et al [32] | 2005 | SA | 2D | 200 | N |
| Huang et al [33] | 2006 | A | 3D | 36 | C |
| Mio et al [34] | 2007 | A | 3D | 14 | C |
| Butman et al [35] | 2008 | SA | 3D | 12 | C |
| Hua et al [36] | 2008 | A | 3D | 20 | N |
| Liang et al [37] | 2008 | A | 3D | 34 | C |
| Joshi et al [38] | 2012 | A | 3D | 12 | N |

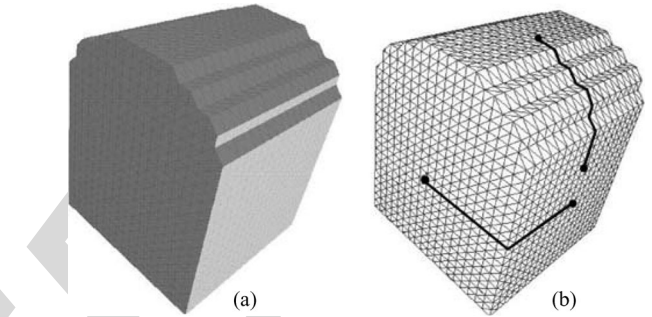


Fig. 6. Illustration showing the calculated geodesic distance between two points on a synthetic surface. (a) Original synthetic surface. (b) Synthetic surface overlayed with geodesic distances between four example points, calculated using the fast marching method [31], [41].

determine if the value is greater than or less than the mean surface curvature.

Once the points of interest are determined, the geodesic distance can be computed using a number of different methods [39]–[41]. One of the most popular is the fast marching method proposed by Kimmel and Sethian [41]. This method has gained wide acceptance due to the speed of the calculations, and its easy applicability to a vast array of applications, which include 2- and 3-D structures. An example of the result of the fastmarching method is illustrated on a synthetic surface in Fig. 6.

Wang *et al.* [31] proposed the use of geodesic distance analysis to analyze the sulci and gyral fissures of the brain for matching brains. Locations were classified and compared between subjects. Areas where the sulci and gyri were similar could then be detected in the brain. Their results showed that surface correspondences could be found between brains, and that the fissures could be consistently identified across brains. Pastore *et al.* [32] used geodesic distances to improve the segmentation accuracy (see Fig. 7) of the sulci and gyri in the brain. They found that geodesic distances proved to be a precise, efficient, and versatile method for segmenting the external boundary of the brain because the gyrfications of the brain have large curvatures and this feature is carried over into the MRI images.

Huang *et al.* [33] proposed a method for the extraction of brain for comparison of contours using geodesic distances. Results they obtained showed that geodesic distances could aid in making extractions consistent across datasets, and the proposed method achieved a tight brain mask around the brain cortex.

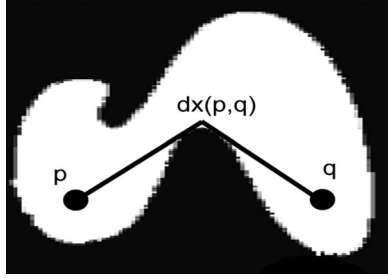


Fig. 7. Example of a geodesic distance calculation between two points (p and q) on the boundary of a 2-D MRI scan [32]. The area has been zoomed and binarized so that the curvature can be clearly seen.

Mio *et al.* [34] used geodesic distances to compare brains by comparing the decomposed geodesic curvature of each brain. Their work illustrated how geodesic distance could be successfully used to quantify morphological similarity and differences, and to identify particular regions where shape similarity and divergence were the most pronounced.

Butman *et al.* [35] identified the brain ventricles and computed the volume of hydrocephalus in subjects using geodesic distance. Similar to the results of Huang, Butman showed that segmentation results were robust throughout datasets and able to classify hydrocephalus.

Hua *et al.* [36] combined geodesic distances with vector image diffusion, a method of examining intrinsic geometric characteristics (e.g., mean curvatures) using a multiscale diffusion and scale space, to match brains of different subjects. This method was shown to be superior to anisotropic diffusion and SIFT curvature matching algorithms in finding stable keypoints. Liang *et al.* [37] approximated the curved cingulum bundle using diffusion tensor imaging (DTI) tractography and geodesic distances. Although there were many limitations found, a significant reduction in fractional anisotropy values, within specific anatomical regions, were detected when using geodesic distances.

Joshi *et al.* [38] analyzed the sulcal curvature in the cortex of the human brain using geodesic curvature. They concluded that geodesic curvature showed promising prospects for analyzing the sulcal curvature in case of small temporal lobe lesions. In the literature and application, geodesic distances are most often used to examine the curvatures of locations of the brain and to locate key points that can be identified due to their curved nature. Geodesic distances have proven to be a useful shape analysis tool in segmentation, registration, and analysis, and are also unique in that they incorporate aspects of first- and second-order analysis.

Geodesic distances have a large number of applications, but primary advantages are their applications in segmentation and the identification of locations in the shapes of brains. This method provides an excellent metric for examining curvature and localized areas of objects, and can provide many discriminatory metrics for classification. Their major drawbacks are their generally localized nature, and the fact that it is difficult to examine large and complex objects that have numerous inflections in their curvature. Three-dimensional analysis of shapes

TABLE III
AUTOMATED (A) OR SEMIAUTOMATED (SA) PROCRUSTES ANALYSIS: GROUND TRUTH (GT) FROM CLINICIAN (C) OR NONCLINICIAN (N) EXPERTS; DIMENSIONALITY (DIM) AND SIZES (#) OF EXPERIMENTAL IMAGE DATABASES

| Publication | Year | Mode | Dim | # | GT |
|---------------------|------|------|-----|-----|----|
| Duta et al [44] | 1999 | A | 2D | 28 | C |
| Penin et al [45] | 2002 | SA | 3D | N/A | N |
| Bienvenu et al [46] | 2011 | A | 3D | 144 | N |

such as the cortex and white matter of the brain prove more challenging for a solely geodesic analysis.

IV. PROCRUSTES ANALYSIS

Procrustes analysis is a statistical form of congruent shape analysis that primarily focuses on the distributions of sets of shapes. It is interesting to note that Procrustes was a rogue and bandit who was the son of Poseidon in ancient Greek mythology [42]. He was known for either stretching people or cutting off their limbs to force them to fit within a statically sized iron bed. The process of Procrustes analysis thereby refers to shape analysis in which properties such as translation, rotation, and scaling are removed so that the shape can be fit into a common reference frame. The process is inherently congruent. Procrustes analysis is most commonly performed by superimposing shapes on top of one another and then applying uniform properties so that geometric transformation of the objects are removed and the shapes can be compared. Procrustes analysis has also served an important role in shape warping, especially as applied to the brain [43].

Table III exemplifies applications of procrustes analysis to brain analysis. It includes methods starting with the early application by Duta *et al.* [44] which analyzes the properties of the skull structure. Bienvenu *et al.* [46] used Procrustes analysis primarily for medical diagnostics or classification.

Nicolae Duta *et al.* [44] proposed a method for the basis of Procrustes analysis in 2-D shape models in medical image analysis. Duta defines the main reasons for the use of Procrustes analysis as a convenient way to compute a prototype (average shape) from a set of simultaneously aligned shapes. Once the point correspondences are found, there exists an analytical or exact solution to the alignment problem.

Mathematically, Procrustes analysis seeks a solution to the following problem: assume we are given a set of m shape instances where $S_k = (x_i^k, y_i^k)_{i=1 \dots n_k}^{k=1 \dots m}$ that is represented by a set of landmarks or boundary points. This set is partitioned into a set of clusters and for each shape cluster a mean shape, or prototype, must be computed. The set of prototypes can then be used for segmentation or the calculation of other metrics. One such metric is a Procrustes residual, which is defined as a deviation in landmarks on a specific object from the consensus of a group, or the prototypes. Duta illustrated the usage of Procrustes analysis for the segmentation of objects and registration of different objects following segmentation. They also introduced algorithms for global and local similarity measures using Procrustes analysis.

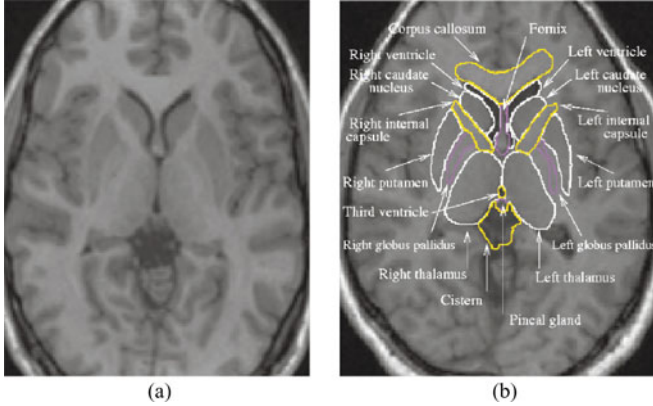


Fig. 8. (a) Magnetic resonance image of the human brain. Neuroanatomic structures of the brain are highlighted by a neuroanatomist (b) Structures shown in yellow are able to be accurately classified by Procrustes analysis. Image courtesy of Duta *et al.* [47].

Penin *et al.* [45] proposed a method for the study of the skull of humans and brains as compared to other primates through the use of tri-dimensional Procrustes analysis. In this study, 29 key features were identified as common landmarks between the different skulls, and the shapes were defined as Procrustes residuals. A Procrustes residual is a deviation in a landmark from the consensus of a group. One downside noted by Penin was that in Procrustes analysis the size and shape are calculated as independent vectors when using traditional shape theory, meaning that normalization of objects is often required during preprocessing.

Bienvenu *et al.* [46] proposed a similar method for examining endocranial variations. Bienvenu found that Procrustes analysis was more favorable in examining the skull, as it has less variability than the cortical surface itself, and is therefore less subjective to the noise introduced by the large differences in the cortex. Similar to Penin, Bienvenu selected specific landmarks commonly found on the enocranial surface and generated a prototype. This prototype was then used to examine the differences between males and females of different species. It was found that Procrustes analysis was capable of determining not only the gender, but the species as well due to the large variation in the landmarks of the prototypes.

In a follow up to his previous work, Duta examined the automated construction of shape models using Procrustes analysis [47]. This study determined that the major advantage of Procrustes analysis, as applied to the brain, is that Procrustes analysis is a reliable method of classifying and segmenting anatomical structures in relatively rigid objects including the ventricles and corpus callosum of the brain (see Fig. 8). It struggles with more complex structures of the brain, specifically the gray and white matter. Procrustes analysis therefore provides an accurate and fast method of analysis in objects that do not have significant variation. This limits its applicability to only specific cases; however, it is a useful measure for examining the shape of the brain and its more rigid structures.

One of the more direct problems related to Procrustes analysis is the method of selecting landmarks on the brain. Because of

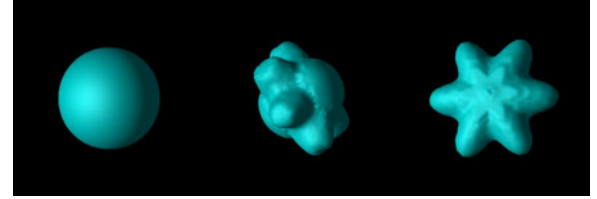


Fig. 9. Illustration of a 3-D deformable model as it contracts on a star-like object [50]. Three frames of progression are shown starting at the left with the original spherical model. The model gradually deforms around the object until it has converged on the star in the center.

the variability in sulci and notable landmarks on the brain, there may be an impact on the resulting analysis. Furthermore, the selection of landmarks could introduce a bias into the analysis. If landmarks are not appropriately located, areas may either be over- or undercompensated for, adding an additional degree of complication to this form of analysis. It is likely one of the driving reasons that this methodology has only seen moderate modern adoption.

Procrustes analysis, while useful, does not provide an in-depth analysis of complex objects as some other methods. Discussion of deformable models and SPHARMs will illustrate examples of some of the more popular techniques for identifying mathematical differences between 3-D shapes that the human eye is unlikely to be able to classify.

V. DEFORMABLE MODELS

Deformable models, also known as active surfaces, are a model-based technique that combines geometry, physics, and approximation theory in order to offer a unique and powerful approach to image analysis [48]. Deformable models have proven useful in a variety of applications for the brain including segmentation, shape representation, matching, and motion tracking. Unlike more rigid methods of analysis, deformable models are capable of accommodating for significant variability in shapes (see Fig. 9), like the brain, over time and across different individuals. While deformable models were originally used in the field of computer vision, their application to the analysis of complex medical objects, such as the brain, was quickly realized by the scientific community. In their 2-D forms, deformable models are often referred to as active contours or snakes [49], [50].

Deformable models have mathematical foundations in geometry, physics, and shape approximation theory [48]–[50]. Geometry is used to represent an object's shape, and deformable models commonly make use of complex geometric representations, such as splines, that offer flexibility and many degrees of freedom. Physics is applied to impose constraints controlling how that shape can vary, with respect to properties such as space and time. The name “deformable models” is most closely associated with the incorporation of this elasticity theory at a physical level. Therefore, deformable models are most commonly constructed inside a Lagrangian dynamics setting that is able to respond naturally to constraints and applied forces. As a model deforms in the Lagrangian setting, the deformation energy will give rise to internal elastic forces. Potential energy functions for the external model are defined so that the model

TABLE IV

AUTOMATED (A) OR SEMIAUTOMATED (SA) DEFORMABLE MODEL ANALYSIS:
GROUND TRUTH (GT) FROM CLINICIAN (C) OR NONCLINICIAN (N) EXPERTS;
DIMENSIONALITY (DIM) AND SIZES (#) OF EXPERIMENTAL IMAGE DATABASES

| Publication | Year | Mode | Dim | # | GT |
|-------------------------------|------|------|-----|-----|----|
| Davatzikos <i>et al.</i> [51] | 1996 | SA | 3D | 6 | N |
| Dale <i>et al.</i> [52] | 1999 | A | 3D | 100 | C |
| Smith [53] | 2002 | A | 3D | 45 | C |
| Zhuang <i>et al.</i> [54] | 2006 | A | 3D | 49 | C |
| Joshi <i>et al.</i> [55] | 2007 | A | 3D | 6 | N |
| Tu <i>et al.</i> [56] | 2007 | A | 3D | 28 | C |
| Huang <i>et al.</i> [57] | 2009 | A | 3D | 36 | C |
| Liu <i>et al.</i> [58] | 2009 | A | 3D | 38 | N |
| Li <i>et al.</i> [59] | 2011 | A | 3D | 5 | N |
| Hashioka <i>et al.</i> [60] | 2012 | SA | 3D | 14 | C |

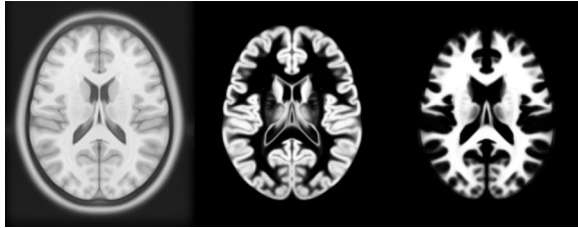


Fig. 10. Segmentation results of the brain showing the gray matter and white matter are shown here. The goal of such work in this figure is to analyze the volume, and the deformable model proves useful in isolating the voxels that belong to the brain. After identifying the desired portion of the brain with a deformable model, calculating the volume becomes a trivial task [52].

deforms to fit the data. Through the combination of these two energies, deformable models can be used for many situations. Some of the most common shape analysis applications of deformable models are in the areas of segmentation and volume analysis, along with shape matching and registration.

Table IV exemplifies applications of deformable model to human brain analysis. It includes methods starting with the early application by Davatzikos *et al.* [51] which was used to identify the central sulci and interhemispheric fissures in the brain. No methods that are primarily based on deformable model analysis have been used primarily for medical diagnostics or classification.

Davatzikos *et al.* [51] proposed one of the earliest methods for analyzing the cortical surface of the brain using deformable models. They used deformable models to identify similar landmarks on different brains for alignment. Their results showed that deformable models could be used to register two different brains with one another, and in order to select cortical and subcortical landmarks on the brain cortex.

Dale *et al.* [52] used a simplified deformable model to segment the cortex of the brain (similar to Fig. 10). The algorithm proved to be a robust method of identifying the cortex of the brain with an average accuracy of 96% across a wide variety of subjects. In 2002, Smith [53] introduced the brain extraction tool (BET). An intensity model is used to initialize the surface model, which is then refined to extract the brain. It was shown to be a fast and accurate method of extraction, having a mean percentage error of about 7% over 45 datasets. Zhuang *et al.* [54] used a model-based level set to perform skull stripping on pediatric and youth brains. The approach showed good accuracy

using the DICE metrics with notable improvements over the BET proposed several years before by Smith [53].

Joshi *et al.* [55] used deformable models to register sulci along with a coregistration of brain volume data. Results showed a statistical improvement over the AIR [61], [62] and HAMMER [63], [64] methods. Tu *et al.* [56] use deformable models to aid in segmenting specific locations found in the brain. The discriminative model they developed played a major role in obtaining clear segmentations. Additionally, the segmentation could be further improved by adjusting the smoothness of the model and constraining the shape with a global shape model.

Huang *et al.* [57] proposed the use of deformable models to segment the cortex, gray matter, and CSF of the human brain. They showed good results when the data was analyzed using the DICE metric. They concluded that deformable models led to improved segmentation accuracy and robustness when applied using a hybrid approach against, as opposed to using only geometric or statistical features. On real clinical MRI datasets, the hybrid approach demonstrated an improved accuracy over other state-of-the-art approaches.

Liu *et al.* [58] suggested a deformable model that driven by radial basis functions to be used for automated extraction of the brain. This model proved to be an accurate and fast technique, having a similar accuracy to the BET proposed by Smith [53]. Li *et al.* [59] proposed an alternative method for the automated extraction of the brain using a deformable model. Their method was an extension of the human brain extraction tool and was found to more reliably extract brains through the inclusion of a deformable model. Hashioka *et al.* [60] proposed a method that utilized active contour modeling (ACM), also commonly referred to as “snakes,” for the extraction of the cortex in the neonatal children. The results showed a sensitivity of 98.5% with a false positive ratio of 13.8%. While their results were largely successful when an optimal head contour was present, they noted that a nonoptimal contour performed less robustly.

While deformable models may not be in the forefront of diagnosis classifications, they have become an integral element of shape analysis. The primary advantage is in the area of shape segmentation, in which these models excel. Deformable models are also very adaptable at isolating complex regions of shapes for further analysis. Deformable models provide useful and accurate ways to identify and segment locations in the brain which is a critical step in analyzing the shape of the brain. The major drawback of using deformable model analysis is that it does not often provide many metrics for directly examining the brain for the purpose of classification or matching.

VI. SPHERICAL HARMONICS

Dealing with the orientation of the brain and aligning two brain objects with one another to compare differences in shape can prove challenging and time consuming. SPHARM, a popular method of shape analysis, can be used to remove these factors. SPHARM analysis [65], [66] considers 3-D surface data as a linear combination of specific basis functions. Additionally, SPHARM provides a rotation invariant common coordinate system in which shapes can be analyzed. The main goal of

SPHARM is to decompose a 3-D object into concentric, or unit, spheres. This process is what discards the orientation information that primarily accompanies a 3-D shape representation of an object. The result is a shape descriptor that is both descriptive and invariant to orientation.

Consideration of the analysis of the entire brain for purposes of identifying differences in shape between different structures is one of the major advantages of SPHARMs. The volume changes in the brain are intuitive features that can be used to describe illness, disorders, and atrophy. The area that SPHARM seeks to address is the structural changes inherent to the surface of the brain. This is an area that SPHARM analysis seeks to address. The use of SPHARM applied to brain analysis was first proposed by Gerig *et al.* [65] for the analysis of the lateral ventricles of the brain. SPHARM was originally developed as a technique for model-based segmentation and data storage; however, its applications have grown in recent years. One important factor of SPHARM analysis is that it relies primarily on the surface of a shape and manifold properties. Due to this, only shapes without holes or disconnects in their surfaces can be accurately analyzed.

SPHARM is a global-based shape analysis technique that is hierarchical in nature. Any shape can be parameterized by a set of basis functions, and these basis functions are referred to as SPHARMs. SPHARM is based on Laplace's equation and involves a mathematical solution of the angular components of the equation. SPHARMs were first discovered by Simon de Laplace in 1782, although it would take several centuries before they were applied to the shape analysis of the brain.

SPHARM basis functions Y_l^m , $-l \leq m \leq l$ of degree l and m are defined on $\theta \in [0; \pi] \times \phi \in [0; 2\pi]$ by the following definitions [65]:

$$\begin{aligned} Y_l^m(\theta, \phi) &= \sqrt{\frac{2l+1}{4\pi} \frac{(l-m)!}{(l+m)!}} P_l^m(\cos \theta) e^{im\phi} \\ Y_l^{-m}(\theta, \phi) &= (-1)^m Y_l^m(\theta, \phi) \end{aligned} \quad (1)$$

where Y_l^m denotes the complex conjugate of Y_l^m . P_l^m describes the associated Legendre polynomials given as

$$P_l^m(\omega) = \frac{(-1)^m}{2^l l!} (1 - \omega^2)^{\frac{m}{2}} \frac{d^{m+l}}{d\omega^{m+l}} (\omega^2 - l^2). \quad (2)$$

The surface is then decomposed from the Cartesian coordinate functions and is represented as $v(\theta, \phi) = (x(\theta, \phi), y(\theta, \phi), z(\theta, \phi))^T$. To express a surface using SPHARMs the following equation is used:

$$v(\theta, \phi) = \sum_{l=0}^{\infty} \sum_{m=-l}^l c_l^m Y_l^m(\theta, \phi) \quad (3)$$

where the coefficients c_l^m are 3-D vectors that are typically obtained through solving a least-squares problem for the points. As previously mentioned, these basis functions allow for a hierarchical description of the surface of a shape. The more coefficients are used in the reconstruction, the more detail is present in the final constructed shape.

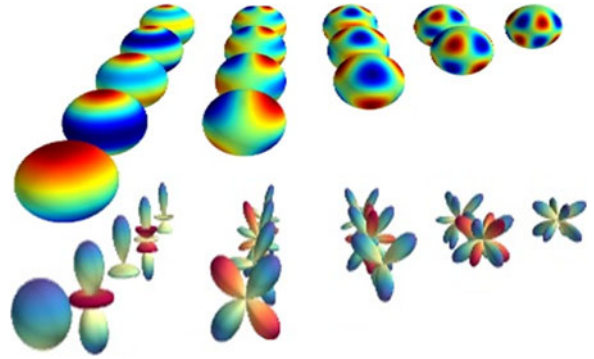


Fig. 11. Decomposition of an object, as described by Gerig *et al.* [65]. In the upper section of the image the SPHARM are plotted overlayed on top of a unit sphere, and below the polar plot of the unit spheres are shown to give a more detailed understanding of the actual information contained within each sphere.

Table IV lists applications of SPHARM to human brain analysis. It includes methods starting with the early application by Keleman [67], along with notable applications, e.g., Gerig *et al.* [65], which have shown SPHARM as a potential method for classifying neurological disorders. SPHARM has been widely applied as a method for potential diagnosis.

Brechbühler *et al.* [78] demonstrated the usage of SPHARM as a method for parameterizing closed surfaces of 3-D objects. In 1999, Keleman [67] demonstrated an ability of SPHARM to analyze shape deformations in neuro-radiological data. Keleman used training data to compute SPHARM representations of the brain which were then simplified using PCA and applied to segment a cortex. Their results showed that SPHARM was a promising technique for improving standard brain segmentations because of the included 3-D forces SPHARM offered.

Gerig *et al.* [65] proposed one of the most significant applications of SPHARM. It was used to analyze the volume similarity between twin brains and demonstrated that SPHARM shape measures reveal new information in addition to size measurements. They proposed that this information might become relevant for an improved understanding of the structural differences not only in normal populations, but also in comparisons between healthy controls and autistic patients. A sample example of the deformation of an object is shown in Fig. 11. Styner and Gerig [79] later proposed a framework package based on SPHARM analysis entitled SPHARM-PDM that could be used for analysis of a multitude of brain structures. This SPHARM-PDM package has been used for examining various brain structures, including work by Kim *et al.* [76] on the hippocampus, and by Paniagua *et al.* [20] (previously mentioned) on the lateral ventricles in neonates.

Chung *et al.* [66] proposed a method to analyze the computed SPHARM coefficients to identify autism in subjects. While the SPHARM coefficients did not generate reliable results, their work showed the ability to accurately and efficiently encode neurological information using a weighted-SPHARM. Chung *et al.* [70] continued their application to explore statistically significant differences between autistic and control subjects using the coefficients. While their work showed some areas of statistical difference, the locations were largely random. This study did

TABLE V
AUTOMATED (A) OR SEMIAUTOMATED (SA) SPHARM ANALYSIS: GROUND TRUTH (GT) FROM CLINICIAN (C) OR NONCLINICIAN (N) EXPERTS; DIMENSIONALITY (DIM) AND SIZES (#) OF EXPERIMENTAL IMAGE DATABASES

| Publication | Year | Mode | Dim | # | GT |
|--------------------------------|------|------|-----|-----|----|
| Keleman <i>et al</i> [67] | 1999 | A | 3D | 21 | N |
| Gerig <i>et al</i> [65] | 2001 | A | 3D | 20 | C |
| Chung <i>et al</i> [66] | 2007 | A | 3D | 28 | C |
| Uthama <i>et al</i> [68] | 2007 | A | 3D | 40 | C |
| Abdallah <i>et al</i> [69] | 2008 | A | 3D | 18 | C |
| Chung <i>et al</i> [70] | 2008 | A | 3D | 28 | C |
| Uthama <i>et al</i> [71] | 2008 | A | 3D | 20 | C |
| Esmail-Zadeh <i>et al</i> [72] | 2010 | A | 3D | 95 | N |
| Nitzken <i>et al</i> [73] | 2011 | A | 3D | 45 | C |
| Nitzken <i>et al</i> [74] | 2011 | A | 3D | 30 | C |
| Geng <i>et al</i> [75] | 2011 | A | 3D | 5 | N |
| Kim <i>et al</i> [76] | 2011 | A | 3D | n/a | C |
| Paniagua <i>et al</i> [20] | 2013 | A | 3D | 90 | C |
| Hosseini <i>et al</i> [77] | 2013 | A | 3D | 69 | C |

show that the weighted SPHARM provides better smoothing in cortical applications than other comparative methods.

Uthama *et al.* [68] proposed the analysis of the ventricle geometry using SPHARM between Parkinson's disease (PD) and control patients. They showed that a statistically significant comparison ($p < 0.05$) of controls and PD subjects could be made using SPHARM, and that it was able to detect subtle changes in synthetic and clinical brain ventricle data. Uthama *et al.* [71] also proposed the use of SPHARM to perform fMRI spatial analysis. They demonstrated differences in the way PD patients and healthy controls respond to an increased task demand. The analysis illustrated that the inability to respond to task demand was reflected in the failure of PD subjects to increase basal ganglia output, and a reliance on cerebellar and cortical activity to enable successful performance.

Abdallah *et al.* [69] applied a parameterization to 3-D meshes, and then used SPHARM application to improve the shape detection of the ventricles. Results showed that a parameterization of a shape followed by SPHARM analysis can lead to improve comparisons and better shape descriptors.

Esmail-Zadeh *et al.* [72] use SPHARM to analyze the hippocampus to classify subjects as either normal or epileptic. Their results showed that in an optimum case, a 90.32% rate of classification of left and right anterior temporal lobes could be achieved when validated using the leave-one-out method.

Nitzken *et al.* [73], [80] proposed an alternative use SPHARM by using the SPHARM reconstruction error to classify autism (see Fig. 12). Classification accuracies on a test population of 100% could be achieved and illustrates a potentially effective way of classifying autism in subjects. Nitzken *et al.* [74], [81] later expanded this theory to the classification of dyslexia. A variation was further used to examine changes related to aging in the human brain [82].

Geng *et al.* [75] demonstrated the use of SPHARM coefficients to perform nonrigid registration of brain white matter and fiber tracts. This method performed better than standard second-order registration methods, although this could also be attributed to the use of higher orders when applying SPHARM. Overall, it was found that SPHARM provided a notable

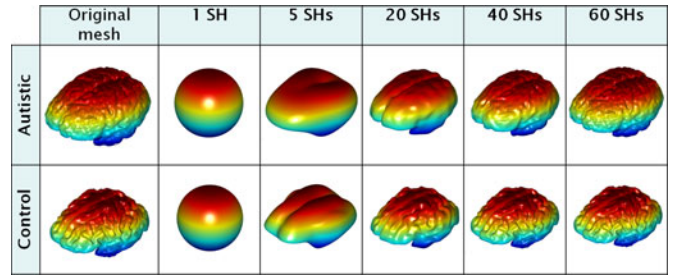


Fig. 12. Method proposed by Nitzken [73] for the approximation of the 3D brain cortex shape for autistic (A) and normal subjects (C).

TABLE VI
AUTOMATED (A) OR SEMIAUTOMATED (SA) VOXEL- AND DEFORMATION-BASED MORPHOMETRY ANALYSIS: GROUND TRUTH (GT) FROM CLINICIAN (C) OR NONCLINICIAN (N) EXPERTS; DIMENSIONALITY (DIM) AND SIZES (#) OF EXPERIMENTAL IMAGE DATABASES

| Publication | Year | Mode | Dim | # | GT |
|----------------------------|------|------|-----|-----|----|
| Chung <i>et al</i> [83] | 2002 | A | 3D | 28 | C |
| Leow <i>et al</i> [84] | 2006 | A | 3D | 17 | C |
| Lepore <i>et al</i> [85] | 2007 | A | 3D | 30 | C |
| Afzali <i>et al</i> [86] | 2010 | A | 3D | 31 | C |
| Wang <i>et al</i> [87] | 2012 | A | 3D | 2 | C |
| Yang <i>et al</i> [88] | 2012 | A | 3D | 60 | C |
| Fletcher <i>et al</i> [89] | 2013 | A | 3D | 285 | C |
| Shi <i>et al</i> [90] | 2013 | A | 3D | 35 | C |

improvement. In 2013, Hosseini *et al.* [77] proposed a further expansion of SPHARM to a 4-D representation of subcortical structures. This new 4-D SPHARM is entitled HyperSPHARM and is intended to serve as a method of tracking changes over time using SPHARM. This allows SPHARM to directly compete with applications typically reserved to methods such as voxel- and deformation-based morphometry.

SPHARM is one of the most beneficial methods of shape analysis for providing meaningful global analyses of objects. SPHARM excels in brain analysis areas that involve large surfaces, such as the cortex and white matter. The major drawbacks to SPHARM analysis are that it can be difficult to localize the SPHARM analysis to understand select locations. It also struggles with applications such as segmentation and automated identification of objects in 2-D images. SPHARM's greatest strength comes in its ability to distinguish between shapes and its applications such as clinical diagnosis classification.

VII. VOXEL- AND DEFORMATION-BASED MORPHOMETRY

Voxel-based morphometry (VBM) is another technique for examining the entire brain [91], [92]. Table VI lists applications of morphometry-based techniques to human brain analysis. VBM is a technique wherein brains between subjects are generally warped, aligned, and normalized in order to remove large differences between the brains, and a volume is then compared across each brain on a voxel by voxel basis. In VBM-smoothed values of the voxels or an averaging of a voxel and its neighbors are typically used. The major usage for VBM is the detection of differences and similarities for images between two populations or shapes [86]. Deformation-based morphometry (DBM) is a similar form of statistical analysis to VBM. However, instead

of measuring the changes between voxels, the changes on the deformation fields are used. The most common variant of DBM in brain shape analysis is tensor-based morphometry (TBM), which is based on the Jacobian determinants. While DBM and more specifically TBM are able to detect more subtle changes between brains, they introduce a significantly higher degree of computational complexity when compared to VBM, because the warping often involves highly nonlinear algorithms. Both VBM and TBM are commonly used in calculating cortical thickness measurements as well.

In 2001, Ashburner *et al.* [93] made a case for VBM in response to criticism posed in Dr. Bookstein's article "Voxel-Based Morphometry Should Not Be Used with Imperfectly Registered Images" [91]. He explains that VBM was a method originally intended to explore cortical thickness that benefits from not being affected by volume changes, the major weakness of volumetric analysis. While acknowledging the partial volume effect as a potential issue, Ashburner also details how modern normalization techniques allow for high-resolution image alignments and warping. He also discusses that VBM is not subject to the issues of landmark selection as found in other analysis methods like Procrustes analysis. In summary, VBM is a useful and reliable method for examining the volume of the brain and its subcomponents, while avoiding the traditional pitfalls associated with volumetric measurements.

Afzali *et al.* [86] explored the differences between using VBM and the tractography of diffusion tensor MRIs for patients with epilepsy. Compared to the tractography methods, VBM showed a consistently accurate performance in analyzing the volume of the hippocampus and frontal lobe of the brain. Afzali does discuss the downside of partial volume effects and increased statistical analysis complexity for VBM. However, he notes that with modern computing power the second fact becomes increasingly less significant. It is also important to note that modern techniques have greatly reduced partial volume effects.

Chung *et al.* [83] introduced a tensor-based model for analyzing the brain surface in 2002. Chung applied a diffusion smoothing operator that is based on a standard Laplace–Beltrami operator to the tensors of the cortex and brain stem to determine local differences. The approach demonstrated that TBM could detect a localized regions of difference on the shapes of two clinical groups. Wang *et al.* [87] applied a multivariate TBM to the lateral vents and the hippocampus. Wang demonstrated a straightforward framework for performing TBM operations on subcomponents of the brain to be used by other researchers.

Lepore *et al.* [85] applied a generalized TBM method to HIV/AIDS patients to examine differences between the corpus callosum and brain surfaces of individuals. Lepore also explored the use of multivariate tensors and discussed how increasing the number of parameters for these tensors could improve the multivariate statistics. Lepore commented how TBM is useful in both registration and statistical analysis, illustrating the multiple use cases for many brain analysis applications.

Leow *et al.* [84] proposed using TBM to identify changes in the brains of aging subjects. Leow's results showed that in Alzheimer's patients, there were reliable brain shape changes in the tensors over time relative to baseline controls. Leow also

illustrated several methods for correcting distortion in TBM techniques. Fletcher *et al.* [89] combined TBM and boundary-based methods to track longitudinal brain changes in subjects. This method was compared to those that do not involve boundary detection, and demonstrated how the inclusion of boundary parameters helped to correct for noise at the tissue boundaries. It also helped to remove bias-correction, which may occur from warping algorithms, and added only minimal performance degradation. Fletcher, like Leow, also explored the proposition of using TBM to detect Alzheimer's in patients. Yang *et al.* [88] used VBM for the application of Alzheimer's as well. Yang studied the changes of VBM measurements in patients over a three-year period. The study showed that atrophy clusters in the brain could be detected in patients who had been diagnosed with Alzheimer's.

Shi *et al.* [90] used TBM to examine the effects of prematurity in the brains of newborns. Different from other methods, Shi registered the surface fluid of the brain instead of the cortex, and applied a TBM approach to this surface fluid. The statistical analysis showed common clusters of significant difference between the brains of the subjects. Shi also showed that the TBM approach was sensitive enough to measure the largely smooth surface of the surface fluid and discern small, but meaningful differences.

VIII. ADDITIONAL METHODS OF SHAPE ANALYSIS

Table VII details additional applications of shape analysis. It includes additional methods such as graph-matching, symmetry-based analysis, Laplace–Beltrami analysis, and volumetric analysis. Many different methods have been applied as potential methods of diagnosis or classification.

A. Distance Mapping

Distance mapping is a technique that has similarities to geodesic distance and medial axis analysis. It differs in that more generalized distance metrics and locations are often computed and examined. He *et al.* [94] proposed a method of brain analysis using distance mapping (see Fig. 13). They examined the statistical differences in distances at the border of a segmented corpus callosum in autistic patients. They hypothesized that a statistical mean difference between segmented images could be discovered; however, it was ultimately concluded that no meaningful statistical difference in shape between subjects could be found using the proposed method.

El-Baz *et al.* [95] proposed an alternative distance mapping technique based on the fast marching method. They used this technique to approximate the thickness of the white matter in autistic patients. They expanded their work to improve the accuracy and explore the technique in different brain abnormalities [117]–[123].

B. Entropy-Based Particle Systems

Cates *et al.* [96] introduced a novel approach to brain shape analysis using an entropy-based system. Points are modeled on the surface of the brain as particles. These particles are then

TABLE VII
AUTOMATED (A) OR SEMIAUTOMATED (SA) ADDITIONAL METHODS OF SHAPE ANALYSIS: GROUND TRUTH (GT) FROM CLINICIAN (C) OR NONCLINICIAN (N)
EXPERTS; DIMENSIONALITY (DIM) AND SIZES (#) OF EXPERIMENTAL IMAGE DATABASES

| Method | Publication | Year | Mode | Dim | # | GT |
|--------------------------------|---------------------------------|------|------|-----|-----|----|
| Distance Mapping | He <i>et al.</i> [94] | 2007 | SA | 2D | 10 | N |
| Distance Mapping | El-Baz <i>et al.</i> [95] | 2007 | A | 3D | 30 | C |
| Entropy-based Particle Systems | Cates <i>et al.</i> [96] | 2009 | A | 3D | 56 | C |
| Graph Matching | Geraud <i>et al.</i> [97] | 1995 | SA | 2D | n/a | N |
| Graph Matching | Yang <i>et al.</i> [98] | 2007 | A | 3D | 120 | N |
| Graph Matching | Long <i>et al.</i> [99] | 2012 | SA | 2D | 60 | C |
| Homologous Model | Yamaguchi <i>et al.</i> [100] | 2009 | A | 3D | 4 | N |
| Homologous Model | Yamaguchi <i>et al.</i> [101] | 2010 | A | 3D | 11 | N |
| Laplace-Beltrami | Angenent <i>et al.</i> [102] | 1999 | A | 3D | 1 | C |
| Laplace-Beltrami | Lai <i>et al.</i> [103] | 2011 | A | 2D | 32 | N |
| Laplace-Beltrami | Shishegar <i>et al.</i> [104] | 2011 | A | 3D | 78 | C |
| Laplace-Beltrami | Germanaud <i>et al.</i> [105] | 2012 | A | 3D | 151 | N |
| Reeb Analysis | Makram <i>et al.</i> [106] | 2008 | A | 3D | 12 | C |
| Reeb Analysis | Shi <i>et al.</i> [107] | 2011 | A | 3D | 200 | C |
| Spectral Matching | Lombaert <i>et al.</i> [108] | 2011 | A | 3D | 36 | N |
| Spectral Matching | Lombaert <i>et al.</i> [109] | 2013 | A | 3D | 12 | N |
| Symmetry-based | Prima <i>et al.</i> [110] | 2002 | A | 3D | 250 | C |
| Symmetry-based | Gefen <i>et al.</i> [111] | 2004 | A | 2D | 232 | N |
| Symmetry-based | Liu <i>et al.</i> [112] | 2007 | A | 2D | 3 | N |
| Symmetry-based | Feng <i>et al.</i> [113] | 2008 | A | 2D | 1 | N |
| Symmetry-based | Fournier <i>et al.</i> [114] | 2011 | A | 3D | 37 | N |
| Volume Analysis | Herman <i>et al.</i> [115] | 1988 | A | 3D | n/a | N |
| Volume Analysis | Wagenknecht <i>et al.</i> [116] | 2008 | A | 3D | n/a | N |

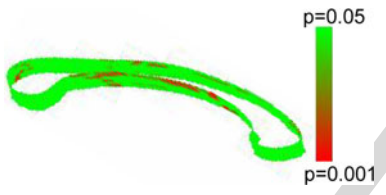


Fig. 13. Method proposed by He *et al.* [94] using distance mapping to examine areas of significant difference along the outer edge of the corpus callosum.

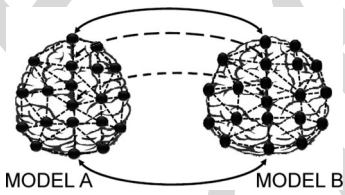


Fig. 14. Method proposed by Yamaguchi *et al.* [100] illustrating the concept of homologous modeling on two brains.

optimized and negative energy is measured to create a distribution of each unique shape. The technique is useful in both 2- and 3-D analysis. The computational efficiency of the approach is based on the number of particles used. Cates applied the approach to the examination of the hippocampus. The advantages to the technique showed results consistent with many other techniques, while requiring a minimum amount of parameter tuning. Due to this fact it could be easily adapted to the brain curvature.

C. Graph Matching

Graph matching techniques involve converting more complex information into a more simplified graph-based representation. Similarities in the graphs are then used to identify, segment, and analyze the more complex information. Geraud *et al.* [97] proposed a method of graph matching analysis. They utilized a Markovian relaxation on a watershed-based adjacency graph to improve the segmentation of neighboring structures in the brain. The results showed a good initial approach to the application of graph matching in the area of segmentation and identification.

Yang *et al.* [98] proposed that two graph-matching techniques can be used to constrain a search neighborhood and the genetic algorithms can be used to optimize sulci labeling. They were

able to achieve satisfactory identification rates for finding sulci using the proposed graph-matching strategy.

Long *et al.* [99] suggested that the brain shape could be decomposed to a graph by subdividing the images into a tree structure containing various properties of the specific brain. By manually selecting important locations for placing the subdivision structures, the brain could be successfully classified for cognitive impairment due to Alzheimer's disease.

D. Homologous Modeling

Homologous modeling is a mesh-based technique in which items having the same number of analysis points in the same locations on two different models can be examined. The technique has been applied to many different applications, but due to implementation complexity is rarely applied to the whole brain. However, it may also be appropriate for the analysis of other discrete brain structures (e.g., corpus callosum, amygdala, or hippocampus).

Yamaguchi *et al.* [100] demonstrated a method based on a homologous model to calculate a sulcal-distribution index for brains to identify brain fissures (see Fig. 14). A mean displacement of 1.3 ± 0.7 mm was found. Their results suggested that

a homologous model could be used to correspond the sulci and gyri among the evaluating brains effectively. Yamaguchi *et al.* [101] proposed a later method to statistically quantify the brain shape using a homologous model. The work examined the changes in the frontal and occipital lobes between male and female subjects. A significant difference ($p < 0.05$) was detected in the sample population and the model was able to successfully detect the locations in the brain that differ significantly.

E. Laplace–Beltrami

Laplace–Beltrami methods comprise any methods that rely heavily on the Laplace–Beltrami operator. The Laplace–Beltrami operator of a smooth function f on a Riemannian manifold M and is defined as $\Delta f = \text{div}(\text{grad}f)$, where div and grad are the divergence and gradient operators of the manifold M [104]. This technique is most commonly used in smoothing applications or curvature analysis.

Angenent *et al.* [102] was the first researcher to propose brain analysis using a Laplace–Beltrami model. Angenent hypothesized that a brain could be flattened by using a Laplace–Beltrami operator on the brain surface. The technique was shown to be an efficient method of flattening the brain.

Lai *et al.* [103] used Laplace–Beltrami nodal curves, and geodesic curve evolutions to segment to the corpus callosum. In small datatests, the method appeared to show positive results and be robust.

Shishegar *et al.* [104] analyzed the first 20 eigenvalues of the Laplace–Beltrami spectrum to classify epilepsy. In the best testing results, Shishegar acheived a 91.9% true positive rate and a 33.3% false positive rate using out of normal range classifiers and cross validation, illustrating that while there were difficulties, it was a promising method.

Germanaud *et al.* [105] computed the eigenfunctions of the Laplace–Beltrami operator to decompose meshes for left- and right-handed subjects. Germanaud was able to detect shallow folds and rare deep folds in the brain which lead to the quantification and classification of brains using the Spangy method.

F. Reeb Graph

A Reeb graph describes the connectivity of the level sets of an object [124]. Visually, a constructed Reeb graph looks similar to a medial axis skeleton. Makram *et al.* [106] suggested a method of using Reeb graph analysis to drive an elastic registration model for the detection of maxilla malformations. The results of detection were deemed satisfactory to a clinician, but not actual values were not reported. The method illustrated the potential for Reeb graph analysis as a registration framework.

Shi *et al.* [107] used reeb graph analysis to isolate, extract, and reconstruct enhanced brain surfaces. The system was able to process cortical surfaces with the accuracy of freesurfer, but at a lower computational cost.

G. Spectral Matching

Spectral correspondence as a way to examine the shapes of objects was first pioneered by Reuter [125], [126] in 2005, and as later expanded by Rustamov [127] where they were

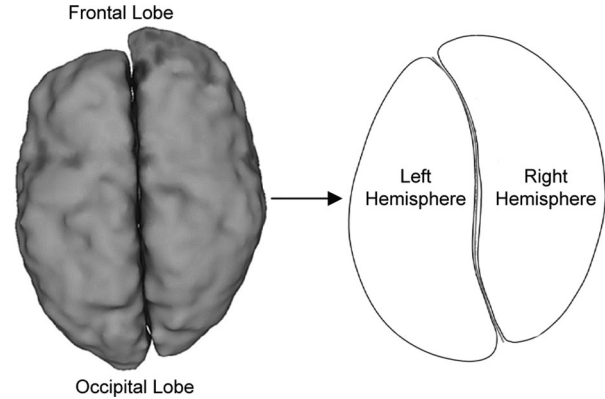


Fig. 15. As shown by Fournier *et al.* [114], the human brain has a slight asymmetry based on if subjects are right or left handed.

combined with Laplace–Beltrami operators. In 2011, Lombaert *et al.* [108] proposed a method of spectral correspondence that was applied to brain shapes. They used an eigendecomposition to match brain surfaces between subjects. Initially, the spectra are computed for each brain. These spectra are then sorted and aligned. The result allows point locations between two brains to be quickly matched. The method is primarily applicable to brain registration. Lombaert *et al.* [109] proposed an extension of this work for corresponding features on the surface of the brain, entitled FOCUSR. The surface features of each brain were used to drive the alignment. The primary advantage of FOCUSR over competing techniques is the speed required to match the brains to one another. The spectral matching technique required a mere 208 s to achieve the same accuracy as FreeSurfer, a commercial brain analysis tool, which required several hours.

H. Symmetry Analysis

Symmetry-based techniques exploit the fact that the human brain is largely symmetric along the sagittal plane, and use this information to make observations. Prima *et al.* [110] proposed an early method of symmetry-based brain analysis. Prima-analyzed brain symmetry to automatically compute the mid-saggital plane and obtain subvoxel accuracy in computing, reorienting, and recentering 3-D images in a time efficient manner.

Gefen *et al.* [111] aligned individual brain images along symmetry lines to create more accurate 3-D models. Gefen concluded that some regions yielded better restoration in 3-D models than other regions, but overall the alignment results were accurate and consistent.

Liu *et al.* [112] examined the topic of multimodality brain registration by aligning the symmetry planes of objects using affine transformations. Liu surmised that the test objects were successfully matched and the symmetry planes were accurately computed.

Feng *et al.* [113] used the symmetry properties of the brain to improve brain segmentation algorithms. Feng's algorithm, while effective at determining bilateral symmetry, was limited by only being applicable to 2-D images.

Fournier *et al.* [114] examined the asymmetries in brains of humans and chimpanzees and compared left- and right-handed individuals to search for a difference (see Fig. 15). Fournier was able to recover typical global asymmetry patterns and hypoth-

esized that future symmetry-based analysis could provide an automated way of comparing individuals.

I. Volumetric Analysis

Volumetric techniques measure the volume of an object. Herman *et al.* [115] proposed a method based on volumetric analysis to use gradient-based boundary tracking to examine the volume between control and Alzheimer's patients. Herman concluded that the gradient-based methods are superior to standard thresholding methods, but did not provide a detailed summary of the diagnostic results.

Wagenknecht *et al.* [116] used a 3-D live-wire approach to extract volumes of interest from a brain for comparison or identification. An average miscalculation rate less than 0.0039 was reported, and the proposed method showed to be accurate and robust for extracting volumes of interest and calculating various properties for them.

IX. DISCUSSION

A. Research Challenges

The brain has long been a topic of research, but utilizing shape analysis with the help of computers enables researchers to examine its shape and texture. There are several major challenges facing shape analysis methods related to the brain or other complex medical structures. The brain is a complex and very diverse organ. Unlike more rigid and well-defined objects that may be easily represented by geometric shapes, the brain suffers from large irregular variabilities. The lack of overall consistency in the brain requires the techniques that analyze it to be flexible, and be able to adaptable to changes in contrast, shape, varying degrees of noise, and abnormality. This illustrates why techniques that rely on predetermined templates or shape models may suffer from difficulty in brain applications. This problem of consistency and complexity is the driving issue that leads to many of the challenges. These challenges can be summarized as follows:

- 1) Due to the size and complexity of the brain and other medical objects, mesh-based approaches often require a significantly large number of nodes or points of reference to perform an accurate surface or shape analysis. Even with modern computing, the complexity of the brain still poses a computational efficiency challenge.
- 2) Medial axis and other skeleton-based analysis may require a large amount of branches and complex paths to accurately represent all of the distinct locations in the human brain.
- 3) The known shape analysis and diagnostic techniques for the brain largely rely on the accuracy of brain segmentation and ability to properly determine structures in the brain. Even with the combination and fusion of modern techniques (e.g., active contours, deformable models, SPHARM, and geodesic distances), identification and segmentation accuracies still suffer significant errors when applied to large sets of data.
- 4) Computer-aided diagnostic systems have faced great difficulty in accurately classifying neurological diseases based on shape metrics over the past decades. This is largely due

to the lack of consistency found across different subjects, but is also due to the difficulty in properly registering and aligning brains so that like areas can be examined.

B. Comparisons and Trends

While there is a high degree of merit in all applications of shape analysis to the brain, some techniques are more suited to specific applications than others. There are four generalized applications of shape analysis techniques with the brain: examination of individual sulci and their curvatures on the brain, examination of the entire human brain and white matter as a whole, registration of brain shapes amongst subjects, and examination of the subcomponents of the brain (e.g., corpus callosum, ventricles, hippocampus). Due to the wide variety of shapes and curvatures in the human brain, many techniques can be used with an array of different brain applications. However, it should be noted that most of the techniques are more commonly used in one or two areas.

Geodesic distances, medial axis, skeletal analysis, and Laplace–Beltrami methods are the most common methods used for examination of the individual sulci and brain curvature, with geodesic distances between the most prevalent in modern applications. SPHARM, voxel- and tensor-based morphometry, volume analysis, symmetry-based modeling, and deformable models are the most common for analysis of the brain and white matter. However, SPHARM is generally reserved for mesh-based applications, and deformable models are often preferred for registration and segmentation applications. While having some uses in whole brain shape analysis, Procrustes analysis, homologous modeling, graph matching, and symmetry-based modeling are most commonly used for brain registration and segmentation applications. Voxel- and tensor-based morphometry, medial axis, skeletal analysis, SPHARM, and distance mapping are the most preferable methods for the examination of subcomponents of the brain, and while typically not always used exclusively, geodesic distances are often combined with these methods. Voxel- and tensor-based morphometry and SPHARM also have significant applications in brain shape registration. It should be specifically noted that deformable models have a high degree of applicability to all of the mentioned analysis methods, and are often combined with or frequently used in many forms of brain shape analysis.

Longitudinal studies and those that examining comparisons between populations tend to most commonly use SPHARM or morphometry-based approaches, because these approaches often take factors of data alignment into account. Geodesic distances can also contribute to longitudinal studies. Deformable models, medial axis, and geodesic distance analysis are good methodologies for examining subcortical structures or legions in the brain along with intricate details about specific anatomy. Cortical thickness studies are most suited for morphometry or distance-based techniques as these provide the most straightforward approaches for measurement studies. In summary, some methods are more suited to specific applications; however, unique studies may need to explore a combination of techniques and approaches due to the abnormality of the brain shape.

To address the aforementioned challenges, recent trends in shape analysis of the brain involve the following aspects:

- 1) Many of the methods discussed were initially applicable to 2-D analysis, but in recent years nearly all methods have evolved for use in 3-D applications.
- 2) Deformable model methods [57]–[59] have seen an increase in usage and have additionally taken the place of many segmentation methods in the past five years, leading to an improved accuracy in brain segmentation. These advances will undoubtedly help to push forward new and improved shape analysis techniques.
- 3) More complex techniques such as SPHARM, started by Gerig *et al.* [65], have been further developed by others [69], [70], [72]–[74] in recent years and have shown great promise in advancing the field for analysis of the cortex and white matter, along with analysis of subcomponents of the brain. These methods have illustrated the potential for utilizing methods that are parameter invariant to solve many of the difficult alignment and registration errors that are often associated with the brain.
- 4) Automation has become increasingly important in modern methods, and the rate of semiautomated and manual methods has drastically decreased. Modern methods are generally expected to perform in an automated manner, and the reduction in human interaction has resulted in an increase in the accuracy for newer techniques.
- 5) Methods such as medial axis analysis [19] and geodesic distances [38] are now more frequently combined with other techniques leading to more accurate segmentation, registration, and classification of the human brain and its various subcomponents, such as the ventricles and corpus callosum.

X. CONCLUSION

This survey details the numerous methods for solving the complex problem of brain shape analysis. Early techniques, which suffered from lower accuracies, slow computation times, and significant user input, have given rise to complicated modern techniques that offer high degrees of automation and improved accuracy. Methods such as SPHARM, deformation-based morphometry, and deformable models will likely become the dominant modes for use in brain shape analysis going forward. Geodesic distances, medial axis, and Laplace–Beltrami operations, among others, will become methods used to support and enhance these dominant modes of brain shape analysis. An amalgamation of techniques opens new opportunities for researchers and engineers to develop more advanced analysis methods. Exciting new opportunities, such as HyperSPHARM and 4-D analysis techniques, provide a look into the future of where modern techniques and amalgamations may be headed. In conclusion, the future of the field of shape analysis for the brain is evolving rapidly, and new techniques will develop and emerge as technology continues to progress.

REFERENCES

- [1] M. Casanova, A. El-Baz, and J. Suri, *Imaging the Brain in Autism*. New York, NY, USA: Springer-Verlag, 2013.
- [2] V. Barras, A. Simons III, and M. Arbib, “Synthetic event-related potentials: A computational bridge between neurolinguistic models and experiments,” *Neural Netw.*, vol. 37, no. 0, pp. 66–92, 2013.
- [3] R. Lande, “Quantitative genetic analysis of multivariate evolution, applied to brain: Body size allometry,” *Evolution*, vol. 33, no. 1, pp. 402–416, 1979.
- [4] R. Desimone, S. Schein, J. Moran, and L. Ungerleider, “Contour, color, and shape analysis beyond the striate cortex,” *Vis. Res.*, vol. 25, no. 3, pp. 441–452, 1985.
- [5] J. Martin, A. Pentland, and R. Kikinis, “Shape analysis of brain structures using physical and experimental modes,” in *Proc. IEEE Comput. Soc. Conf. Comput. Vis. Pattern Recognit.*, Jun. 1994, pp. 752–755.
- [6] M. Delfour and J.-P. Zolsio, *Shapes and Geometries: Metrics, Analysis, Differential Calculus, and Optimization*, (Advances in Design and Control), 2nd ed. Philadelphia, PA, USA: SIAM, Dec. 2010.
- [7] H. Poincaré, *Analysis Situs*, (Séries Journal de l’Ecole polytechnique II sér), 1st ed. Paris, France: Gauthier-Villars, 1895.
- [8] L. de Floriani and M. Spagnuolo, *Shape Analysis and Structuring, (Mathematics and Visualization)*, 1st ed. New York, NY, USA: Springer, Nov. 2010.
- [9] D. Guliato and R. Rangayyan, *Modeling and Analysis of Shape: With Applications in Computer-Aided Diagnosis of Breast Cancer*, (Synthesis Lectures on Biomedical Engineering), 1st ed. San Mateo, CA, USA: Morgan Kaufmann, Jan. 2011.
- [10] D. Attali, J.-D. Boissonnat, and H. Edelsbrunner, “Stability and computation of medial axes—A state-of-the-art report,” in *Mathematical Foundations of Scientific Visualization, Computer Graphics, and Massive Data Exploration*. New York, NY, USA: Springer-Verlag, 2009.
- [11] H. Blum, “A transformation for extracting new descriptors of shape,” *Models Percept. Speech Visual Form*, vol. 19, no. 5, pp. 362–380, 1967.
- [12] H. Blum, “Biological shape and visual science (Part I),” *J. Theoret. Biol.*, vol. 38, no. 2, pp. 205–287, 1973.
- [13] M. Naf, O. Kubler, R. Kikinis, M. E. Shenton, and G. Szekely, “Characterization and recognition of 3D organ shape in medical image analysis using skeletonization,” in *Proc. Math. Methods Biomed. Image Anal. Workshop.*, Jun. 1996, pp. 139–150.
- [14] P. Golland, W. Grimson, and R. Kikinis, “Statistical shape analysis using fixed topology skeletons: Corpus callosum study,” in *Information Processing in Medical Imaging*. New York, NY, USA: Springer-Verlag, 1999, pp. 382–387.
- [15] S. M. Pizer, D. S. Fritsch, P. A. Yushkevich, V. E. Johnson, and E. L. Chaney, “Segmentation, registration, and measurement of shape variation via image object shape,” *IEEE Trans. Med. Imag.*, vol. 18, no. 10, pp. 851–865, Oct. 1999.
- [16] P. Golland, “Statistical shape analysis of anatomical structures” Ph.D. dissertation, Dept. Electr. Eng. Comput. Sci., Massachusetts Inst. Technol., Cambridge, MA, USA, Aug. 2001.
- [17] M. Styner and G. Gerig, “Three-dimensional medial shape representation incorporating object variability,” in *Proc. IEEE Comput. Soc. Conf. Comput. Vis. Pattern Recognit.*, vol. 2, pp. II–651–II–656.
- [18] K. Gorczowski, M. Styner, J.-Y. Jeong, J. S. Marron, J. Piven, H. C. Hazlett, S. M. Pizer, and G. Gerig, “Statistical shape analysis of multi-object complexes,” in *Proc. IEEE Conf. Comput. Vis. Pattern Recognit.*, Jun. 2007, pp. 1–8.
- [19] A. Elnakib, M. F. Casanova, G. Gimel’farb, A. E. Switala, and A. El-Baz, “Autism diagnostics by centerline-based shape analysis of the corpus callosum,” in *Proc. IEEE Int. Symp. Biomed. Imag., Nano Macro*, Apr. 2011, pp. 1843–1846.
- [20] B. Paniagua, A. Lyall, J. B. Berger, C. Vachet, R. M. Hamer, S. Woolson, W. Lin, J. Gilmore, and M. Styner, “Lateral ventricle morphology analysis via mean latitude axis,” *Proc. Soc. Photo Opt. Instrum. Eng.*, vol. 8672, Mar. 2013.
- [21] A. Elnakib, M. Casanova, G. Gimel’farb, A. El-Baz, and K. Suzuki, “Autism diagnostics by 3D shape analysis of the corpus callosum,” in *Machine Learning in Computer-Aided Diagnosis: Medical Imaging Intelligence and Analysis*, K. Suzuki, Ed. Hershey, PA, USA: IGI Global, 2012, pp. 315–335.
- [22] A. Elnakib, M. Casanova, G. Gimel’farb, A. Switala, and A. El-Baz, “Dyslexia diagnostics by 3-D shape analysis of the corpus callosum,” *IEEE Trans. Inf. Technol. Biomed.*, vol. 16, no. 4, pp. 700–708, Jul. 2012.
- [23] A. Elnakib, A. El-Baz, M. Casanova, G. Gimel’farb, and A. Switala, “Image-based detection of corpus callosum variability for more accurate discrimination between dyslexic and normal brains,” in *Proc. IEEE Int. Symp. Biomed. Imag., Nano Macro*, 2010, pp. 109–112.
- [24] A. Elnakib, A. El-Baz, M. Casanova, G. Gimel’farb, and A. Switala, “Image-based detection of corpus callosum variability for more accurate

- discrimination between autistic and normal brains," in *Proc. 17th IEEE Int. Conf. Image Process.*, 2010, pp. 4337–4340.
- [25] M. F. Casanova, A. El-Baz, A. Elnakib, J. Giedd, J. M. Rumsey, E. L. Williams, and A. E. Switala, "Corpus callosum shape analysis with application to dyslexia," *Transl. Neurosci.*, vol. 1, no. 2, pp. 124–130, Jun. 2010.
- [26] M. F. Casanova, A. El-Baz, A. Elnakib, A. E. Switala, E. L. Williams, D. L. Williams, N. J. Minshew, and T. E. Conturo, "Quantitative analysis of the shape of the corpus callosum in patients with autism and comparison individuals," *Autism*, vol. 15, no. 2, pp. 223–238, Mar. 2011.
- [27] A. El-Baz, A. Elnakib, M. Casanova, G. Gimelfarb, A. Switala, D. Jordan, and S. Rainey, "Accurate automated detection of autism related corpus callosum abnormalities," *J. Med. Syst.*, vol. 35, no. 5, pp. 929–939, 2011.
- [28] L. D. Griffin, "The intrinsic geometry of the cerebral cortex," *J. Theoret. Biol.*, vol. 166, no. 3, pp. 261–273, 1994.
- [29] N. Khaneja, M. I. Miller, and U. Grenander, "Dynamic programming generation of curves on brain surfaces," *IEEE Trans. Pattern Anal. Mach. Intell.*, vol. 20, no. 11, pp. 1260–1265, Nov. 1998.
- [30] M. Berger and B. Gostiaux, *Differential Geometry: Manifolds and Curves and And Surfaces*, (Series Graduate texts in mathematics). New York, NY, USA: Springer-Verlag, 1988.
- [31] Y. Wang, B. S. Peterson, and L. H. Staib, "3D brain surface matching based on geodesics and local geometry," *Comput. Vis. Image Understand.*, vol. 89, no. 23, pp. 252–271, 2003.
- [32] J. Pastore, E. Moler, and V. Ballarin, "Segmentation of brain magnetic resonance images through morphological operators and geodesic distance," *Digital Signal Process.*, vol. 15, no. 2, pp. 153–160, 2005.
- [33] A. Huang, R. Abugharbieh, R. Tam, and A. Traboulsee, "MRI brain extraction with combined expectation maximization and geodesic active contours," in *Proc. IEEE Int. Symp. Signal Process. Inf. Technol.*, Aug. 2006, pp. 107–111.
- [34] W. Mio, J. C. Bowers, M. K. Hurdal, and X. Liu, "Modeling brain anatomy with 3D arrangements of curves," in *Proc. IEEE 11th Int. Conf. Comput. Vis.*, Oct. 2007, pp. 1–8.
- [35] J. A. Butman and M. G. Linguraru, "Assessment of ventricle volume from serial MRI scans in communicating hydrocephalus," in *Proc. 5th IEEE Int. Symp. Biomed. Imag., Nano*, May 2008, pp. 49–52.
- [36] J. Hua, Z. Lai, M. Dong, X. Gu, and H. Qin, "Geodesic distance-weighted shape vector image diffusion," *IEEE Trans. Vis. Comput. Graph.*, vol. 14, no. 6, pp. 1643–1650, Nov. 2008.
- [37] X. Liang and J. Zhang, "White matter integrity analysis along cingulum paths in mild cognitive impairment—A geodesic distance approach," in *Proc. 2nd Int. Conf. Bioinformat. Biomed. Eng.*, May 2008, pp. 510–513.
- [38] A. A. Joshi, D. W. Shattuck, H. Damasio, and R. M. Leahy, "Geodesic curvature flow on surfaces for automatic sulcal delineation," in *Proc. 9th IEEE Int. Symp. Biomed. Imag.*, May 2012, pp. 430–433.
- [39] R. Kimmel and N. Kiryati, *Finding Shortest Paths On Surfaces By Fast Global Approximation And Precise Local Refinement*. Citeseer, 1994.
- [40] R. Kimmel, A. Amir, and A. M. Bruckstein, "Finding shortest paths on surfaces using level sets propagation," *IEEE Trans. Pattern Anal. Mach. Intell.*, vol. 17, no. 6, pp. 635–640, Jun. 1995.
- [41] R. Kimmel and J. A. Sethian, "Computing geodesic paths on manifolds," *Proc. Nat. Acad. Sci.*, vol. 95, no. 15, pp. 8431–8435, 1998.
- [42] E. Tripp, *The Meridian Handbook of Classical Mythology*. New York, NY, USA: Penguin, 1974.
- [43] A. W. Toga and P. M. Thompson, "The role of image registration in brain mapping," *Image Vis. Comput.*, vol. 19, no. 1–2, pp. 3–24, Jan. 2001.
- [44] N. Duta, A. K. Jain, and M. P. Dubuisson-Jolly, "Learning 2-D shape models," *Proc. Comput. Vis. Pattern Recognit., IEEE Comput. Soc. Conf.*, vol. 2, pp. 8–14, 1999.
- [45] X. Penin, C. Berge, and M. Baylac, "Ontogenetic study of the skull in modern humans and the common chimpanzees: Neotenic hypothesis reconsidered with a tridimensional procrustes analysis," *Amer. J. Phys. Anthropol.*, vol. 118, no. 1, pp. 50–62, 2002.
- [46] T. Bienvenu, F. Guy, W. Coudryzer, E. Gilissen, G. Roualdès, P. Vignaud, and M. Brunet, "Assessing endocranial variations in great apes and humans using 3-D data from virtual endocasts," *Amer. J. Phys. Anthropol.*, vol. 145, no. 2, pp. 231–246, 2011.
- [47] N. Duta, A. K. Jain, and M. P. Dubuisson-Jolly, "Automatic Construction of 2-D Shape Models," *IEEE Trans. Pattern Anal. Mach. Intell.*, vol. 23, no. 5, pp. 433–446, May 2001.
- [48] T. McInerney and D. Terzopoulos, "Deformable models in medical image analysis," in *Proc. Math. Methods Biomed. Image Anal.*, 1996, *Proc. Workshop*, Jun. 1996, pp. 171–180.
- [49] C. Xu and J. L. Prince, "Snakes, shapes, and gradient vector flow," *IEEE Trans. Image Process.*, vol. 7, no. 3, pp. 359–369, Mar. 1998.
- [50] C. Xu and J. L. Prince, "Gradient vector flow deformable models," in *Handbook of Medical Imaging*. San Diego, CA, USA: Academic, 2000, pp. 159–169.
- [51] C. Davatzikos, "Spatial transformation and registration of brain images using elastically deformable models," *Comput. Vis. Image Understand.*, vol. 66, no. 2, pp. 207–222, 1997.
- [52] A. Dale, B. Fischl, and M. Sereno, "Cortical surface-based analysis—Part I: Segmentation and surface reconstruction," *Neuroimage*, vol. 9, no. 2, pp. 179–194, 1999.
- [53] S. M. Smith, "Fast robust automated brain extraction," *Hum. Brain Mapp.*, vol. 17, no. 3, pp. 143–155, Nov. 2002.
- [54] A. H. Zhuang, D. J. Valentino, and A. W. Toga, "Skull-stripping magnetic resonance brain images using a model-based level set," *Neuroimage*, vol. 32, no. 1, pp. 79–92, Aug. 2006.
- [55] A. A. Joshi, D. W. Shattuck, P. M. Thompson, and R. M. Leahy, "Surface-constrained volumetric brain registration using harmonic mappings," *IEEE Trans. Med. Imag.*, vol. 26, no. 12, pp. 1657–1669, Dec. 2007.
- [56] Z. Tu, K. L. Narr, P. Dollar, I. DiNov, P. M. Thompson, and A. W. Toga, "Brain anatomical structure segmentation by hybrid discriminative/generative models," *IEEE Trans. Med. Imag.*, vol. 27, no. 4, pp. 495–508, Apr. 2008.
- [57] A. Huang, R. Abugharbieh, and R. Tam, "A hybrid geometric statistical deformable model for automated 3-D segmentation in brain MRI," *IEEE Trans. Biomed. Eng.*, vol. 56, no. 7, pp. 1838–1848, Jul. 2009.
- [58] J. X. Liu, Y. S. Chen, and L. F. Chen, "Accurate and robust extraction of brain regions using a deformable model based on radial basis functions," *J. Neurosci. Methods*, vol. 183, no. 2, pp. 255–266, 2009.
- [59] J. Li, X. Liu, J. Zhuo, R. P. Gullapalli, and J. M. Zara, "A deformable surface model based automatic rat brain extraction method," in *Proc. IEEE Int. Symp. Biomed. Imag., Nano Macro*, Apr. 2011, pp. 1741–1745.
- [60] A. Hashioka, S. Kobashi, K. Kuramoto, Y. Wakata, K. Ando, R. Ishikura, T. Ishikawa, S. Hirota, and Y. Hata, "Shape and appearance knowledge based brain segmentation for neonatal MR images," in *Proc. World Autom. Congr.*, Jun. 2012, pp. 1–6.
- [61] R. P. Woods, S. T. Grafton, C. J. Holmes, S. R. Cherry, and J. C. Mazziotta, "Automated image registration—Part I: General methods and intrasubject, intramodality validation," *J. Comput. Assist. Tomogr.*, vol. 22, no. 1, pp. 139–152, 1998.
- [62] R. P. Woods, S. T. Grafton, J. D. Watson, N. L. Sicotte, and J. C. Mazziotta, "Automated image registration—Part II: Intersubject validation of linear and nonlinear models," *J. Comput. Assist. Tomogr.*, vol. 22, no. 1, pp. 153–165, 1998.
- [63] D. Shen and C. Davatzikos, "HAMMER: Hierarchical attribute matching mechanism for elastic registration," in *Proc. IEEE Workshop Math. Methods Biomed. Image Anal.*, 2001, pp. 29–36.
- [64] T. Liu, D. Shen, and C. Davatzikos, "Deformable registration of cortical structures via hybrid volumetric and surface warping," *Neuroimage*, vol. 22, no. 4, pp. 1790–1801, Aug. 2004.
- [65] G. Gerig, M. Styner, D. Jones, D. Weinberger, and J. Lieberman, "Shape analysis of brain ventricles using SPHARM," in *Proc. IEEE Workshop Math. Methods Biomed. Image Anal.*, 2001, pp. 171–178.
- [66] M. K. Chung, K. M. Dalton, and R. J. Davidson, "Encoding neuroanatomical information using weighted spherical harmonic representation," in *Proc. 14th Workshop Statist. Signal Process.*, Aug. 2007, pp. 146–150.
- [67] A. Kelemen, G. Székely, and G. Gerig, "Elastic Model-Based Segmentation of 3D Neuroradiological Data Sets," *IEEE Trans. Med. Imag.*, vol. 18, no. 10, pp. 828–839, Oct. 1999.
- [68] A. Uthama, R. Abugharbieh, A. Traboulsee, and M. J. McKeown, "Invariant SPHARM shape descriptors for complex geometry in MR region of interest analysis," in *Proc. 29th Annu. Int. Conf. IEEE Eng. Med. Biol. Soc.*, Aug. 2007, pp. 1322–1325.
- [69] A. Ben Abdallah, F. Ghorbel, H. Essabbah, and M. H. Bedoui, "Chapter 9: Shape analysis of left ventricle using invariant 3D spherical harmonics shape descriptors," in *Proc. 3rd Int. Conf. Geometr. Model. Imag.*, Jul. 2008, pp. 53–58.
- [70] M. K. Chung, K. M. Dalton, and R. J. Davidson, "Tensor-based cortical surface morphometry via weighted spherical harmonic representation," *IEEE Trans. Med. Imag.*, vol. 27, no. 8, pp. 1143–1151, Aug. 2008.
- [71] A. Uthama, R. Abugharbieh, S. J. Palmer, A. Traboulsee, and M. J. McKeown, "SPHARM-based spatial fMRI characterization with

- intersubject anatomical variability reduction," *IEEE J. Sel. Topics Signal Process.*, vol. 2, no. 6, pp. 907–918, Dec. 2008.
- [72] M. Esmaeil-Zadeh, H. Soltanian-Zadeh, and K. Jafari-Khouzani, "SPHARM-based shape analysis of hippocampus for lateralization in mesial temporal lobe epilepsy," in *Proc. 8th Iran. Conf. Electr. Eng.*, May 2010, pp. 39–44.
- [73] M. Nitzken, M. F. Casanova, G. Gimel'farb, F. Khalifa, A. Elnakib, A. E. Switala, and A. El-Baz, "3-D shape analysis of the brain cortex with application to autism," in *Proc. IEEE Int. Symp. Biomed. Imag. Nano Macro*, Apr. 2011, pp. 1847–1850.
- [74] M. Nitzken, M. F. Casanova, G. Gimel'farb, A. Elnakib, F. Khalifa, A. E. Switala, and A. El-Baz, "3D shape analysis of the brain cortex with application to dyslexia," in *Proc. 18th IEEE Int. Conf. Image Process.*, Sep. 2011, pp. 2657–2660.
- [75] X. Geng, T. J. Ross, H. Gu, W. Shin, W. Zhan, Y.-P. Chao, C.-P. Lin, N. Schuff, and Y. Yang, "Diffeomorphic image registration of diffusion MRI using spherical harmonics," *IEEE Trans. Med. Imag.*, vol. 30, no. 3, pp. 747–758, Mar. 2011.
- [76] H. Kim, T. Mansi, A. Bernasconi, and N. Bernasconi, "Vertex-wise shape analysis of the hippocampus: Disentangling positional differences from volume changes," *Med. Image Comput. Comput. Assist. Interv.*, vol. 14, Pt. 2, pp. 352–359, 2011.
- [77] A. Hosseinibor, M. K. Chung, S. Schaefer, C. van Reekum, L. Peschke-Schmitz, M. Sutterer, A. L. Alexander, and R. J. Davidson, "4D hyperspherical harmonic (hyperspharm) representation of multiple disconnected brain subcortical structures," in *Proc. 16th Int. Conf. Med. Image Comput. Comput. Assist. Interv.*, Sep. 2013, pp. 598–605.
- [78] C. H. Brechbuhler, G. Gerig, and O. Kubler, "Parametrization of closed surfaces for 3-D shape description," *Comput. Vis. Image Understand.*, vol. 61, no. 2, pp. 154–170, 1995.
- [79] M. Styner, I. Oguz, S. Xu, C. Brechbuhler, D. Pantazis, J. J. Levitt, M. E. Shenton, and G. Gerig, "Framework for the statistical shape analysis of brain structures using SPHARM-PDM," *Insight J.*, vol. 1071, no. 1071, pp. 242–250, 2006.
- [80] M. Nitzken, M. Casanova, F. Khalifa, G. Sokhadze, and A. El-Baz, "Shape-based detection of cortex variability for more accurate discrimination between autistic and normal brains," in *Multi Modality State-of-the-Art Medical Image Segmentation and Registration Methodologies*, A. S. El-Baz, R. Acharya U, A. F. Laine, and J. S. Suri, Eds. New York, NY, USA: Springer-Verlag, 2011, pp. 161–185.
- [81] A. Elnakib, M. Nitzken, M. Casanova, H. Park, G. Gimel'farb, and A. El-Baz, "Quantification of age-related brain cortex change using 3d shape analysis," in *Proc. 21st Int. Conf. Pattern Recognit.*, 2012, pp. 41–44.
- [82] E. L. Williams, A. El-Baz, M. Nitzken, A. E. Switala, and M. F. Casanova, "Spherical harmonic analysis of cortical complexity in autism and dyslexia," *Transl. Neurosci.*, vol. 3, no. 1, pp. 36–40, Mar. 2012.
- [83] M. K. Chung, K. J. Worsley, and A. C. Evans, "Tensor-based brain surface modeling and analysis," in *Proc. IEEE Comput. Soc. Conf. Comput. Vis. Pattern Recognit.*, 2003, vol. 1, pp. I–467–I–473.
- [84] A. D. Leow, A. D. Klunder, C. R. JackJr., A. Toga, A. Dale, M. A. Bernstein, P. J. Britson, J. L. Gunter, C. P. Ward, J. L. Whitwell, B. J. Borowski, A. S. Fleisher, N. C. Fox, D. Harvey, J. Kornak, N. Schuff, C. Studholme, G. Alexander, and M. W. Weiner Thompson, "Longitudinal stability of MRI for mapping brain change using tensor-based morphometry," *NeuroImage*, vol. 31, no. 2, pp. 627–640, 2006.
- [85] N. Lepore, C. Brun, Y. Y. Chou, M. C. Chiang, R. A. Dutton, K. M. Hayashi, E. Luders, O. L. Lopez, H. J. Aizenstein, A. W. Toga, J. T. Becker, and P. M. Thompson, "Generalized tensor-based morphometry of HIV/AIDS using multivariate statistics on deformation tensors," *IEEE Trans. Med. Imag.*, vol. 27, no. 1, pp. 129–141, Jan. 2008.
- [86] M. Afzali and H. Soltanian-Zadeh, "Comparison of voxel-based morphometry (VBM) And tractography of diffusion tensor MRI (DT-MRI) in temporal lobe epilepsy," in *Proc. 18th Iran. Conf. Electr. Eng.*, 2010, pp. 18–23.
- [87] Y. Wang, T. F. Chan, A. W. Toga, and P. M. Thompson, "Shape analysis with multivariate tensor-based morphometry and holomorphic differentials," in *Proc. IEEE 12th Int. Conf. Comput. Vis.*, 2009, pp. 2349–2356.
- [88] H. Yang, W. Liu, H. Xia, Z. Zhou, and L. Tong, "Longitudinal change of the grey matter of mild cognitive impairment patients over 3 years by using voxel-based morphometry," in *Proc. 5th Int. Conf. Biomed. Eng. Informat.*, 2012, pp. 304–308.
- [89] E. Fletcher, A. Knaack, B. Singh, E. Lloyd, E. Wu, O. Carmichael, and C. DeCarli, "Combining boundary-based methods with tensor-based morphometry in the measurement of longitudinal brain change," *IEEE Trans. Med. Imag.*, vol. 32, no. 2, pp. 223–236, Feb. 2013.
- [90] J. Shi, Y. Wang, R. Ceschin, X. An, M. D. Nelson, A. Panigrahy, and N. Lepore, "Surface fluid registration and multivariate tensor-based morphometry in newborns—The effects of prematurity on the putamen," in *Proc. Asia-Pacific Signal Inf. Process. Assoc. Annu. Summit Conf.*, 2012, pp. 1–8.
- [91] F. L. Bookstein, "'Voxel-based morphometry' should not be used with imperfectly registered images," *Neuroimage*, vol. 14, no. 6, pp. 1454–1462, Dec. 2001.
- [92] U. Grenander and M. I. Miller, "Computational anatomy: An emerging discipline," *Quart. Appl. Math.*, vol. 56, no. 4, pp. 617–694, 1998.
- [93] J. Ashburner and K. J. Friston, "Why voxel-based morphometry should be used," *Neuroimage*, vol. 14, no. 6, pp. 1238–1243, 2001.
- [94] Q. He, Y. Duan, J. Miles, and N. Takahashi, "Statistical shape analysis of the corpus callosum in subtypes of autism," in *7th IEEE Int. Conf. Proc. Bioinform. Bioeng.*, Oct. 2007, pp. 1087–1091.
- [95] A. El-Baz, M. F. Casanova, G. Gimel'farb, M. Mott, and A. E. Switala, "Autism diagnostics by 3-D texture analysis of cerebral white matter gyrfications," *Med. Image Comput. Comput. Assist. Interv.*, vol. 10, Pt 2, pp. 882–890, 2007.
- [96] J. Cates, P. T. Fletcher, M. Styner, M. Shenton, and R. Whitaker, "Shape modeling and analysis with entropy-based particle systems," *Inf. Process. Med. Imag.*, vol. 20, pp. 333–345, 2007.
- [97] T. Geraud, J. F. Mangin, I. Bloch, and H. Maitre, "Segmenting internal structures in 3-D MR images of the brain by Markovian relaxation on a watershed based adjacency graph," in *Proc. Int. Conf. Image Process.*, Oct. 1995, vol. 3, pp. 548–551.
- [98] F. Yang and F. Kruggel, "Optimization algorithms for labeling brain sulci based on graph matching," in *Proc. IEEE 11th Int. Conf. Comput. Vis.*, Oct. 2007, pp. 1–7.
- [99] S. S. Long and L. B. Holder, "Graph based MRI brain scan classification and correlation discovery," in *Proc. IEEE Symp. Computat. Intell. Bioinform. Computat. Biol.*, May 2012, pp. 335–342.
- [100] K. Yamaguchi, S. Kobashi, I. Mohri, S. Imawaki, M. Tamiike, and Y. Hata, "Brain shape homologous modeling using sulcal-distribution index in MR images," in *Proc. Syst., Man Cybern., IEEE Int. Conf.*, Oct. 2009, pp. 1102–1106.
- [101] K. Yamaguchi, S. Kobashi, K. Kuramoto, Y. T. Kitamura, S. Imawaki, and Y. Hata, "Statistical quantification of brain shape deformation with homologous brain shape modeling," in *Proc. World Autom. Congr.*, Sep. 2010, pp. 1–6.
- [102] S. Angenent, S. Haker, A. Tannenbaum, and R. Kikinis, "On the Laplace-Beltrami operator and brain surface flattening," *IEEE Trans. Med. Imag.*, vol. 18, no. 8, pp. 700–711, Aug. 1999.
- [103] R. Lai, Y. Shi, N. Sicotte, and A. W. Toga, "Automated corpus callosum extraction via Laplace–Beltrami nodal parcellation and intrinsic geodesic curvature flows on surfaces," in *Proc. IEEE Int. Conf. Comput. Vis.*, Nov. 2011, pp. 2034–2040.
- [104] R. Shishegar, H. Soltanian-Zadeh, and S. R. Moghadasi, "Hippocampal shape analysis in epilepsy using Laplace–Beltrami spectrum," in *Proc. 19th Iran. Conf. Electr. Eng.*, May 2011, p. 1.
- [105] D. Germanaud, J. Lefevre, R. Toro, C. Fischer, J. Dubois, L. Hertz-Pannier, and J. F. Mangin, "Larger is twistier: Spectral analysis of gyration (SPANGY) applied to adult brain size polymorphism," *Neuroimage*, vol. 63, no. 3, pp. 1257–1272, Nov. 2012.
- [106] M. Makram, H. Kamel, and M. Emma, "3D elastic registration using a balanced multi resolution reeb graph: Application for a detection of a maxilla facial malformation," in *Proc. Int. Conf. Comput. Commun. Eng.*, May 2008, pp. 1063–1071.
- [107] Y. Shi, R. Lai, and A. Toga, "Cortical surface reconstruction via unified reeb analysis of geometric and topological outliers in magnetic resonance images," *IEEE Trans. Med. Imag.*, 2012.
- [108] H. Lombaert, L. Grady, J. R. Polimeni, and F. Cheriet, "Fast brain matching with spectral correspondence," *Inf. Process. Med. Imag.*, vol. 22, pp. 660–673, 2011.
- [109] H. Lombaert, L. Grady, J. R. Polimeni, and F. Cheriet, "FOCUSR: Feature oriented correspondence using spectral regularization—A method for precise surface matching," *IEEE Trans. Pattern Anal. Mach. Intell.*, vol. 35, no. 9, pp. 2143–2160, Sep. 2013.
- [110] S. Prima, S. Ourselin, and N. Ayache, "Computation of the mid-sagittal plane in 3D brain images," *IEEE Trans. Med. Imag.*, vol. 21, no. 2, pp. 122–138, Feb. 2002.

- [111] S. Gefen, Y. Fan, L. Bertrand, and J. NissaNov, "Symmetry-based 3D brain reconstruction," in *Proc. IEEE Int. Symp. Biomed. Imag., Nano Macro*, Apr. 2004, pp. 744–747.
- [112] X. Liu, C. Imielinska, A. F. Laine, and A. D'Ambrosio, "Symmetry based multi-modality registration of the brain imagery," in *Proc. IEEE Int. Symp. Signal Process. Inf. Technol.*, Dec. 2007, pp. 807–812.
- [113] J. Feng, F. Desheng, and B. Shuoben, "Brain image segmentation based on bilateral symmetry information," in *Proc. 2nd Int. Conf. Bioinformat. Biomed. Eng.*, May 2008, pp. 1951–1954.
- [114] M. Fournier, B. Combes, N. Roberts, S. Keller, T. J. Crow, W. D. Hopkins, and S. Prima, "Surface-based method to evaluate global brain shape asymmetries in human and chimpanzee brains," in Apr. 2, 2011, pp. 310–316.
- [115] G. T. Herman, M. I. Kohn, and R. E. Gur, "Computerized three-dimensional volume analysis from magnetic resonance images for characterization of brain disorders," in *Proc. Biomed. Eng., Proc. Spec. Symp. Matur. Technol. Emerg. Horiz.*, Nov. 1988, pp. 65–67.
- [116] G. Wagkenknecht and S. Winter, "Volume-of-interest segmentation of cortical regions for multimodal brain analysis," in *Proc. IEEE Nuclear Sci. Symp. Conf. Rec.*, Oct. 2008, pp. 4368–4372.
- [117] M. F. Casanova, A. El-Baz, M. Mott, G. Mannheim, H. Hassan, R. Fahmi, J. Giedd, J. M. Rumsey, A. E. Switala, and A. Farag, "Reduced gyral window and corpus callosum size in autism: Possible macroscopic correlates of a minicolumnopathy," *J. Autism. Dev. Disord.*, vol. 39, no. 5, pp. 751–764, May 2009.
- [118] M. F. Casanova, A. S. El-Baz, J. Giedd, J. M. Rumsey, and A. E. Switala, "Increased white matter gyral depth in dyslexia: Implications for cortico-cortical connectivity," *J. Autism. Dev. Disord.*, vol. 40, no. 1, pp. 21–29, Jan. 2010.
- [119] A. El-Baz, M. Casanova, G. Gimel'farb, M. Mott, A. Switala, E. Vanbogaert, and R. McCracken, "A new CAD system for early diagnosis of dyslexic brains," in *Proc. 15th IEEE Int. Conf. Image Process.*, 2008, pp. 1820–1823.
- [120] A. El-Baz, M. Casanova, G. Gimel'farb, M. Mott, A. Switala, E. Vanbogaert, and R. McCracken, "Dyslexia diagnostics by 3D texture analysis of cerebral white matter gyrfications," in *Proc. 19th Int. Conf. Pattern Recognit.*, 2008, pp. 1–4.
- [121] A. El-Baz, M. Casanova, G. Gimel'farb, M. Mott, and A. Switala, "A new image analysis approach for automatic classification of autistic brains," in *Proc. 4th IEEE Int. Symp. Biomed. Imag.*, 2007, pp. 352–355.
- [122] A. El-Baz, M. Casanova, G. Gimel'farb, M. Mott, and A. Switala, "An MRI-based diagnostic framework for early diagnosis of dyslexia," *Int. J. Comput. Assist. Radiol. Surg.*, vol. 3, no. 3–4, pp. 181–189, 2008.
- [123] R. Fahmi, A. El-Baz, H. Abd El Munim, A. Farag, and M. Casanova, "Classification techniques for autistic Vs. typically developing brain using MRI data," in *Proc. 4th IEEE Int. Symp. Biomed. Imag., Nano Macro*, 2007, pp. 1348–1351.
- [124] H. Doraiswamy and V. NataraJan, "Efficient algorithms for computing Reeb graphs," *Computat. Geometry*, vol. 42, no. 67, pp. 606–616, 2009.
- [125] M. Reuter, F.-E. Wolter, and N. Peinecke, "Laplace-spectra as fingerprints for shape matching," in *Proc. 2005 ACM Symp. Solid Phys. Model.*, NY, USA: ACM, 2005, pp. 101–106.
- [126] M. Reuter, F.-E. Wolter, and N. Peinecke, "Laplace–Beltrami spectra as shape-DNA of surfaces and solids," *Comput.-Aided Design*, vol. 38, no. 4, pp. 342–366, 2006.
- [127] R. M. Rustamov, "Laplace–Beltrami eigenfunctions for deformation invariant shape representation," in *Proc. 5th Eurograph. Symp. Geometry Process.*, 2007, pp. 225–233.



Matthew J. Nitzken (M'10) received the B.S. and M.Eng. degrees in 2009 and 2010, respectively, from the University of Louisville, Louisville, KY, USA.

He is currently a Doctoral Candidate in the electrical and computer engineering program at the University of Louisville. He has a strong focus in the fields of shape analysis, computer-aided detection and diagnosis, and the understanding of complex brain disorders. His primary area of expertise is in 2-dimensional and 3-dimensional shape analysis, and over the years he has worked extensively in brain, lung, heart, and prostate analysis. He has more than 20 combined publications and book chapters and has submitted numerous patents in the field of brain and lung shape analysis. His work has had the opportunity to be presented at conferences in countries around the world, including the United States, Germany, Spain, and Japan, among others.



Manuel F. Casanova received the B.S. degree from the University of Puerto Rico, Puerto, Rico, in 1975, the M.D. degree from the School of Medicine, University of Puerto Rico, in 1979, and the Internship and Residency Neurology from the University District Hospital, in 1983.

From 1983 to 1986, he was Clinical and Research Fellow at The Johns Hopkins University, MD, USA. He is currently the Gottfried and Gisela Kolbe Endowed Chair in psychiatry in the University of Louisville, Louisville, KY, USA. Dr. Casanova was

a Magisterial Speaker at the World Autism Congress in 2010 and the recipient of an EUREKA award from the National Institute of Mental Health. He has received the titles of Stanley Scholar from the United States and an Honorary Professor degree from the University of Krasnoyarsk, Russia. He is one of the founding members for the International Autism Institute. He serves on the Editorial Board of 20 journals and has published more than 200 peer reviewed articles and 70 book chapters.



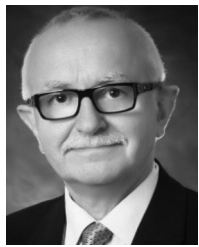
Georgy Gimel'farb received the Ph.D. degree from the Ukrainian Academy of Sciences in 1969 and an advanced Doctor of Engineering degree from the Higher Certifying Commission of the USSR in 1991. After working for a long time in the Glushkov Institute of Cybernetics of the Ukrainian Academy of Sciences, he joined in 1997 the University of Auckland (New Zealand) where he is currently a Professor of Computer Science and a Codirector of the Intelligent Vision Systems Laboratory. He authored or coauthored more than 45 journal articles, 260 papers

in peer-reviewed conference proceedings, 65 book chapters, two textbooks, and four books, including the monograph "Image Textures and Gibbs Random Fields" (Kluwer Academic, 1999). His research interests include probabilistic image modeling, statistical pattern recognition, texture analysis in medical and remotely sensed images, and computer stereo vision. In 1997, he received a prestigious State Premium of Ukraine in Science and Technology for fundamental and applied results in image and signal recognition.



Tamer Inanc (M'xx) received the M.S. and Ph.D. degrees from Department of Electrical Engineering, Pennsylvania State University, State College, PA, USA, in 1996 and 2002, respectively, under supervision of Prof. M. Sznaier.

After receiving the Ph.D. degree, he did a Postdoctoral Scholarship at California Institute of Technology, Pasadena, CA, USA, between 2002 and 2004 under the supervision of Prof. R. M. Murray. He started working as an Assistant Professor in 2004 at Department of Electrical and Computer Engineering, University of Louisville, Louisville, KY, USA. He has been working as an Associate Professor at the same department since 2010. His research interests include control systems, robust identification, active vision systems, autonomous robotics, biometrics and control systems and identification applications to bioengineering problems.



Jacek M. Zurada (LF'96) received the M.S. and Ph.D. degrees in 1968 and 1975, respectively from the Gdansk Institute of Technology, Gdansk, Poland.

He currently serves as a Professor of electrical and computer engineering at the University of Louisville, Louisville, KY, USA. He authored or coauthored several books and more than 370 papers in the area of computational intelligence, neural networks and machine learning, logic rule extraction, and bioinformatics, and delivered numerous presentations and seminars throughout the world. His work has been cited

more than 7400 times.

Dr. Zurada currently serves as IEEE V-President for Technical Activities (TAB Chair) and also chairs the IEEE TAB Management Committee. He was the Editor-in-Chief of the IEEE TRANSACTIONS ON NEURAL NETWORKS (1997–03), Associate Editor of the IEEE TRANSACTIONS ON CIRCUITS AND SYSTEMS and was member of the Editorial Board of The Proceedings of the IEEE. In 2004–05, he was the President of the IEEE Computational Intelligence Society. He is an Associate Editor of *Neurocomputing*, *Neural Networks*, and of several other international journals. He holds the title of a Professor in Poland, the Membership of the Polish Academy of Sciences, and has been awarded numerous awards, including the Joe Desch Award in 2013 and four honorary professorships of Chinese universities, including of Sichuan University in Chengdu. He is a Board of Directors Member of IEEE, IEEE CIS, and IJCNN.



Ayman El-Baz (M'05) received the B.S. and M.S. degrees in electrical engineering from Mansoura University, Egypt, in 1997 and 2000, respectively, and the Ph.D. degree in electrical engineering from the University of Louisville, KY, USA, in 2006.

He Associate Professor in the Department of Bioengineering at the University of Louisville, KY. Dr. El-Baz has twelve years of hands-on experience in the fields of bioimaging modeling and computer-assisted diagnostic systems. He has developed new techniques for analyzing 3D medical images. His work has been

reported at several prestigious international conferences (e.g., CVPR, ICCV, MICCAI, etc.) and in journals (e.g., IEEE TMI, IEEE TIP, IEEE TBME, IEEE TITB, Brain, etc.). His work related to novel image analysis techniques for lung cancer and autism diagnosis have earned him multiple awards, including: first place at the annual Research Louisville 2002, 2005, 2006, 2007, 2008, 2010, 2011 and 2012 meetings, and the "Best Paper Award in Medical Image Processing" from the prestigious ICGST International Conference on Graphics, Vision and Image Processing (GVIP-2005). He has authored or coauthored more than 300 technical articles.

IEEE
proof

Shape Analysis of the Human Brain: A Brief Survey

Matthew J. Nitzken, *Member, IEEE*, Manuel F. Casanova, Georgy Gimel'farb, Tamer Inanc, *Member, IEEE*, Jacek M. Zurada, *Life Fellow, IEEE*, and Ayman El-Baz, *Member, IEEE*

Abstract—The survey outlines and compares popular computational techniques for quantitative description of shapes of major structural parts of the human brain, including medial axis and skeletal analysis, geodesic distances, Procrustes analysis, deformable models, spherical harmonics, and deformation morphometry, as well as other less widely used techniques. Their advantages, drawbacks, and emerging trends, as well as results of applications, in particular, for computer-aided diagnostics, are discussed.

Index Terms—Brain, diagnostics, shape analysis.

I. INTRODUCTION

THE human brain belongs to the most complex anatomical structure in the human body. Individual brains vary substantially, and therefore analyzing the brain presents a real challenge [1]. Fig. 1 illustrates the complexity of the brain represented in a three-dimensional (3-D) mesh format. Computer-aided medical diagnostics call for the quantitative analysis of many structural parts of the brain, such as the cortex, ventricles, corpus callosum, hippocampus, brain stem, and gyrfications.

This survey focuses primarily on applications of various shape analysis techniques to the human brain. Methods of shape analysis for the human brain include techniques such as medial axis and skeletal analysis, geodesic distances, Procrustes analysis, deformable models, SPHARM, deformation-based morphometry, symmetry-based analysis, Laplace-Beltrami operators, and homologous modeling, among other techniques.

In 1979, Lande [3] proposed to analyze the shape of the brain by measuring the brain volume. While the volumetric analysis of brain scans arguably does not yield sound discriminatory features, it was a key starting point for shape analysis related to the brain. Later on, Desimone *et al.* [4] and Martin *et al.* [5]

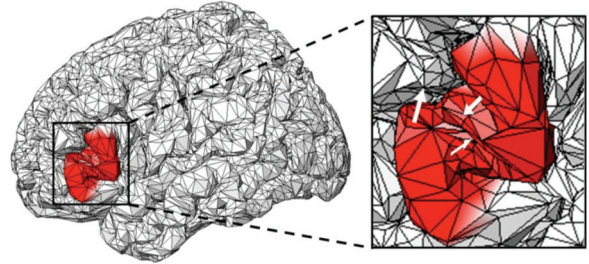


Fig. 1. 3-D mesh brain representation (the expanded section details its complexity and variability due to multiple different structures and gyrfications). Courtesy of Barras *et al.* [2].

proposed two more elaborate shape analysis frameworks. The first framework examined color, shape, and texture of the cortex on 2-D scans of the brain. The second framework performed a more advanced analysis, by examining pregenerated mesh models of the brain ventricles. To more accurately represent the brain, the meshes were decomposed using eigenvectors, that were obtained in a way similar to conventional principal component analysis (PCA). These early frameworks for examining the shapes of brain constructs did not produce reliable descriptors of brain-related health or behavioral disorders, such as autism and Alzheimer's disorder. However, they inspired extensive subsequent research that helped to push the current field of brain shape analysis into the forefront of research and development for computer-assisted medical diagnostics.

Generally, shape analysis is applied to digital geometric models of surfaces and/or volumes of objects-of-interest in order to detect similarities or differences between the objects [6]. Typically, shape analysis is fully automated or is a combination of automated and manual processing, and it is closely paired with some kind of object segmentation. Segmented objects are represented in a variety of digital formats including volumes, point clouds, and meshes. Most typically, the outer boundary (or surface) of an object, or a manifold representing this object, is examined.¹

Surface analysis, formally called surface interrogation, and computer-aided design systems, explicitly examine intrinsic and extrinsic geometric properties of surfaces of objects and manifolds, including visual pleasantness, technical smoothness, and geometric constraints [8]. It is often used to detect surface imperfections, analyze shapes, or visualize different forms.

Shape analysis techniques can be primarily classified into first- and second-order types, each containing large numbers of congruency-based, intrinsic, and graph-based shape descriptors [8]. The first-order methods typically rely on surface normal

Manuscript received March 25, 2013; revised September 12, 2013 and November 08, 2013; accepted December 20, 2013. Date of publication; date of current version.

M. J. Nitzken and A. El-Baz are with the BioImaging Laboratory, Bioengineering Department, University of Louisville, Louisville, KY 40292 USA (e-mail: mnjitz02@louisville.edu; aelba01@louisville.edu).

M. F. Casanova is with the Department of Psychiatry, University of Louisville, Louisville, KY 40202 USA (e-mail: m0cas02@louisville.edu).

G. Gimel'farb is with the Department of Computer Science, University of Auckland, Auckland 1142, New Zealand (e-mail: g.gimelfarb@auckland.ac.nz).

T. Inanc is with the Department of Electrical and Computer Engineering, University of Louisville, Louisville, KY 40292 USA (e-mail: t.inanc@louisville.edu).

J. M. Zurada is with the Electrical and Computer Engineering Department, University of Louisville, Louisville, KY 40292 USA and also with the Spoleczna Akademia Nauk, 90-011 Lodz, Poland (e-mail: jacek.zurada@louisville.edu).

Color versions of one or more of the figures in this paper are available online at <http://ieeexplore.ieee.org>.

Digital Object Identifier 10.1109/JBHI.2014.2298139

¹By Henri Poincaré [7], a manifold is the level set of a continuously differentiable function between Euclidean spaces that satisfies the non-degeneracy hypothesis of the implicit function theorem. In a simplified version, it can be thought of as an object with no holes or discontinuities.

vectors, inflections, and other intrinsic descriptors, obtained, e.g., by the Laplace–Beltrami analysis or the more popular geodesic path analysis. Some congruency methods fall into this category, such as the shape distribution and symmetry analysis.

Second-order analysis generally is based on the surface curvature and second derivatives. Typical descriptors are produced by moment analysis, spherical harmonics (SPHARMs), and Procrustes analysis, being invariant with respect to congruency and medial axis, skeletal, and Reeb graph analysis, which also heavily rely on the curvature. Importantly, many second-order analysis methods incorporate first-order techniques.

Both categories of shape analysis depend critically on shape interrogation, or extraction of structural characteristics of a shape from its geometric model [8], and remeshing, i.e., repartitioning of primitive components to fit best the original shape. Most commonly, vertex–vertex or face–vertex methods are used to construct the meshes. The vertex–vertex method deals with a point cloud, where the points relate to critical junctures in an object, while the face–vertex method exploits faces that interconnect vertices in a specific and controlled manner [9]. A widely known example of the latter is Delaunay triangulation, in which every face is a triangle and the final mesh consists of a large number of interconnected triangular faces. While the remeshing helps to preserve the original shape of the object, it can also be used to enhance some features of the shape. A primitive (such as a triangle that minimally characterizes the shape) can locally fit any such feature.

Some of the most popular shape analysis techniques, for application to the human brain, are detailed and compared below. These include 1) the medial axis and skeletal analysis, which is commonly used for surface (2-D) and volume (3-D) reconstruction in complex models; 2) geodesic distances to compare different brains in detail by using intrinsic and graph based analysis; 3) Procrustes analysis that can provide accurate and quick statistical evaluation of shapes in rigid objects; 4) deformable models evolving to fit boundaries of complex objects; 5) more recent 3-D surface approximation with SPHARMs in order to analyze the brain shape in detail; 6) the use of morphometry-based techniques to accurately analyze the volume of objects; 7) an examination of alternative and lesser used techniques.

II. MEDIAL AXIS AND SKELETAL ANALYSIS

Medial axes of complex 2-D/3-D graphical models are widely used for surface reconstruction and dimensionality reduction. A medial axis, or a skeleton of an object, is defined as the set of internal points with more than one closest point on the object's surface (see Fig. 2). Generally, it is represented by a polygon or a similar simple construction of concatenated arcs and parabolas that follow the would-be centerline of the object. The medial axis and skeletal graphs facilitate indexing, matching, segmenting, or associating objects with one another. Medial axis analysis has a wide range of uses that can be used in many anatomical applications outside of the brain, such as virtual colonoscopies.

The notion of a skeleton of a 2-D or 3-D shape was first introduced by Blum *et al.* [11], [12]. The underlying idea was to place a primitive shape inside an object, such as a ball. The

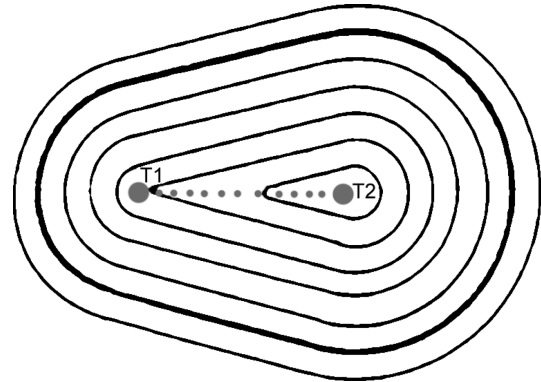


Fig. 2. Medial axis of a 2-D object: the outer black line shows the boundary of the object and the central dark line connecting the points T1 and T2. Inner isolines indicate the same distances from the boundary [10].

TABLE I
AUTOMATED (A) OR SEMIAUTOMATED (SA) MEDIAL AXIS ANALYSIS: GROUND TRUTH (GT) FROM CLINICIAN (C) OR NONCLINICIAN (N) EXPERTS; DIMENSIONALITY (DIM) AND SIZES (#) OF EXPERIMENTAL IMAGE DATABASES

| Publication | Year | Mode | Dim | # | GT |
|-----------------------------|------|------|-----|-----|----|
| Naf <i>et al</i> [13] | 1996 | A | 3D | n/a | N |
| Golland <i>et al</i> [14] | 1999 | A | 2D | 66 | C |
| Pizer <i>et al</i> [15] | 1999 | SA | 2D | 20 | C |
| Golland <i>et al</i> [16] | 2001 | A | 3D | 30 | C |
| Styner <i>et al</i> [17] | 2001 | A | 3D | 20 | C |
| Gorcowski <i>et al</i> [18] | 2007 | A | 3D | 70 | C |
| Elnakib <i>et al</i> [19] | 2011 | A | 3D | 34 | C |
| Paniagua <i>et al</i> [20] | 2013 | A | 3D | 90 | C |

primitive is then inflated it until reaching the object's surface, and this process is repeated until the object is filled with the maximum-size primitives. Connected centers of the primitives form the skeleton that represents geometric properties of the object's interior, such as bends and elongations, and reveals the geometric structure, or constituent parts of the object, and gives information about the object's position, orientation, and size.

Table I indexes applications of skeletons for human brain analysis, starting from the novel proposal by Naf *et al.* [13]. Naf classified various organs, including the brain, after characterizing their structure in 3-D images with Voronoi diagrams and skeletons. Excepting [15], all the methods in Table I were used for medical diagnostics or classification.

Golland *et al.* [14] analyzed skeletons of the corpus callosum in 2-D images in order to classify cases of schizophrenia. The initial skeletons were refined using snakes, or active contours, which evolved from different randomly chosen starting points. Then, the curvature angles and the width of the skeleton were used as discriminatory features. The angles were calculated between each set of adjacent points along the sampled medial axis, and the width was defined as the radial distance from the medial axis point to the surface boundary. Sampling more points of the skeleton provided finer details, but also increased the analysis time. The approach was tested on clinical datasets for normal and schizophrenic patients. A relatively high accuracy (more than 70% in the best case) was obtained for identifying schizophrenia in patients by statistical shape analysis of the corpus callosum and hippocampus [16] (the accuracy of a linear

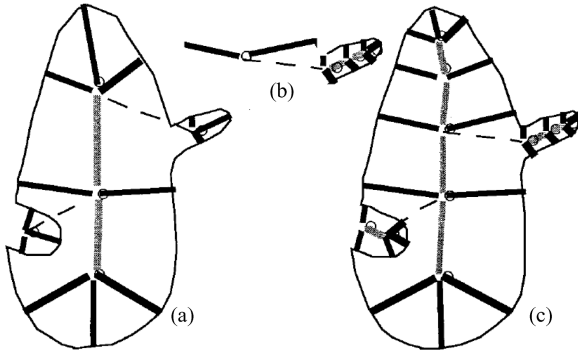


Fig. 3. Shown is a visual representation of Pizer's [15] medial axis approach. Due to the complexity of the shape, it is initialized with three skeletons (a). These are then individually examined (b) to create a composite skeleton of the parent figure (c).

classifier in determining schizophrenic patients on the training data proved to be consistently higher than the one using cross validation).

As noted in [14] and [16], the main advantages and drawbacks of skeletons relate to their compact and intuitive shape representation that can be used for segmentation, tracking, and object recognition, as well as their high sensitivity to noise in the object's boundary, respectively. The complex and spatially variant structure of the brain leads to a large amount of noise along the typical shape boundary. To overcome this challenge, frequently the typical general shapes of the objects are known in advance from segmented training samples and methods using fixed topology skeletons have been proposed in [14] and [16]. The significant benefit of such skeletons is that they can be adjusted to each current object of similar shape and optimized for accuracy.

Pizer *et al.* [15] proposed another method of quantifying object shapes in 2-D images that can be used in a variety of applications, including different brain structures. In this case, the skeletons were used to register brain shapes and compare the brain ventricles and brain stem. These structures could then be quantitatively described using a combination of the medial axes and distance analysis.

Golland's works [14], [16] dealt primarily with the corpus callosum of the shape that typically featured no extending appendages. Contrastingly, Pizer's medial axis analysis was focused on the brain ventricles, shapes of which (and thus their skeletons) often have one or more appendages. The skeletal appendages extend outward to include additional information about the more complex shapes. In Pizer's case, the medial axis analysis was modified to incorporate intersection points where multiple skeletons can be fused together, as, e.g., in Fig. 3. The resulting more complex skeletons proved to be useful for solving various problems, including segmentation and image registration [15]. Both Pizer's and Golland's approaches can be easily extended from 2-D to 3-D objects, at the expense of increased computational time due to the calculation of 3-D distances.

Styner and Gerig [17] expanded Pizer's concepts and analyzed the brain ventricles in 3-D images using Voronoi skeletons and PCA to obtain discriminatory features of shape changes and

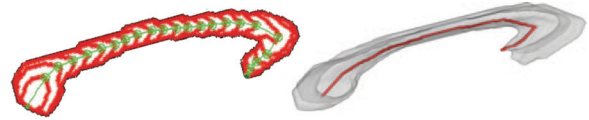


Fig. 4. Elnakib *et al.* [19] skeleton extraction method showing the centerline extraction method on the left and the final extracted centerline on the right.

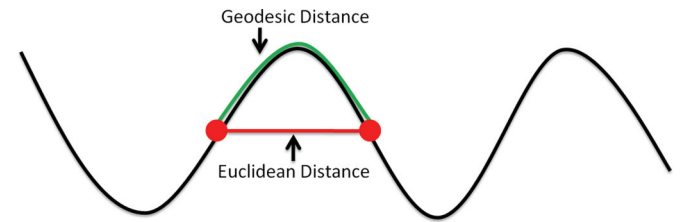


Fig. 5. Visual representation of a simple geodesic distance. The two points on the curve (shown as red circles) are connected by Euclidean (red straight line) and geodesic (green curved line) distance lines. Note how the geodesic distance follows the arc of the curve.

locality. SPHARMs were used to analyze similarities between the skeletons and compare twin ventricles. Similar to Pizer's implementation, Styner and Gerig's skeletons contain many detailed branches and intersections that represented the shape of the object. To reduce the effect of the noise in the outer object's boundary of the shape, the shape was smoothed by using PCA to include only dominant characteristics of shapes. After this initial simplification, the Voronoi skeleton was constructed using standard medial axis computation. Then PCA was used once again to "prune" smaller and less important branches of the skeleton.

Gorcowski *et al.* [18] used skeletons to analyze shapes and poses of five brain structures in order to classify autism. The mean classification accuracy on the basis of only poses, only shapes, or combined poses and shapes was 56%, 60%, and 64%, respectively, for an image database of 46 autistic and 24 control subjects. Although the combined features gave better results, the overall classification rate was rather low.

Elnakib *et al.* [19] obtained notably better classification accuracy, using a method shown in Fig. 4, for autistic and control subjects by analyzing the corpus callosum centerline: the study correctly classified 94% autistic and 88% control subjects at the 85% confidence level, 94% autistic and 82% control subjects at the 90% confidence level, and 82% autistic and 76.5% control subjects at the 95% confidence level for the database of 17 autistic and 17 normal subjects. They further extended their centerline extraction implementations [21]–[24] to examine more aspects of the corpus callosum and its 3-D centerline as applied to autism and dyslexia. This study was also explored by Casanova *et al.* [25], [26] and El-Baz *et al.* [27].

Paniagua *et al.* [20] used SPHARMs to calculate the mean latitude axis of ventricles in neonates. While this is not a full medial axis computation, it can be computed in a straightforward manner when using SPHARM. Importantly, Paniagua introduced a fusion of the medial axis technique with SPHARM analysis to achieve a diagnostic classification in neonatal subjects. This is

consistent with the modern trend of combining techniques for better accuracy.

In total, the medial axis and skeletal analysis are important for examining basic locations and shapes of structural parts of the brain. The main advantages of this method are that it creates simple representations of objects along with similarity measures and accurate descriptions for very complex shapes. These are useful in applications such as object classification and matching for medical diagnostics or understanding of object structure and construction. The limited use of the object's surface is the major drawback of the skeletal analysis that significantly decreases the usefulness of the medial axes and skeletons in applications dealing with the surface characteristics and/or small variations in shapes.

III. GEODESIC DISTANCES

Of primary interest in the analysis of the brain is the ability to make detailed comparisons of different brains. This often requires some form of nonrigid registration of the two surfaces of interest, or surface matching. A popular approach to this shape analysis problem is the use of geodesic distances. Geodesic distances can serve as an important geometric measurement of the brain and can help to provide a means of understanding complex shapes. Geodesic distances can serve to deliver a wealth of information about the surface geometry of a shape [8]. One of the first uses of geodesic distances, as applied to the brain, was by Griffin [28] in 1994. Griffin proposed the use of geodesic distance to characterize the cortical shape of the brain. This was later expanded on by Khaneja [29] who used geodesic distance to examine the curvature of sulci in the brain.

Geodesic distance is a combination of intrinsic and graph-based analysis. It is defined as the length of the graph of a geodesic between two vertices within an object [30]. It is the shortest path between two points that can be found in a curved space (such as the surface of a sphere) and has a wide array of practical uses. If you have ever boarded a plane to travel between continents there is a strong likelihood that you have traveled on a geodesic path, because these are the shortest distances between two points. In the sulci of the brain, geodesic paths that connect two points in a single sulcus will often follow the curvature of the sulcus [31]. The detection of geodesic paths is also heavily utilized on the surfaces of meshes for common graphics operations such as mesh segmentation, watermarking, editing, and smoothing [8].

Table II lists the applications of geodesic distance to the human brain analysis. Early application methods by Wang *et al.* [31] analyze the individual sulci of the brain. No methods that are primarily based on geodesic distance analysis have been used solely for medical diagnostics or classification.

The geodesic distance can be defined in a number of ways, although the most common calculations are for the Gaussian curvature and the mean surface curvature of an object. These metrics allow features of the brain, such as the gyrus and sulcus, to be easily calculated by examining each point. Information about the convex and concave areas of the sulci can be determined by examining the sign of the Gaussian curvature to

TABLE II
AUTOMATED (A) OR SEMIAUTOMATED (SA) GEODESIC DISTANCE ANALYSIS:
GROUND TRUTH (GT) FROM CLINICIAN (C) OR NONCLINICIAN (N) EXPERTS;
DIMENSIONALITY (DIM) AND SIZES (#) OF EXPERIMENTAL IMAGE DATABASES

| Publication | Year | Mode | Dim | # | GT |
|--------------------|------|------|-----|-----|----|
| Wang et al [31] | 2003 | A | 3D | n/a | N |
| Pastore et al [32] | 2005 | SA | 2D | 200 | N |
| Huang et al [33] | 2006 | A | 3D | 36 | C |
| Mio et al [34] | 2007 | A | 3D | 14 | C |
| Butman et al [35] | 2008 | SA | 3D | 12 | C |
| Hua et al [36] | 2008 | A | 3D | 20 | N |
| Liang et al [37] | 2008 | A | 3D | 34 | C |
| Joshi et al [38] | 2012 | A | 3D | 12 | N |

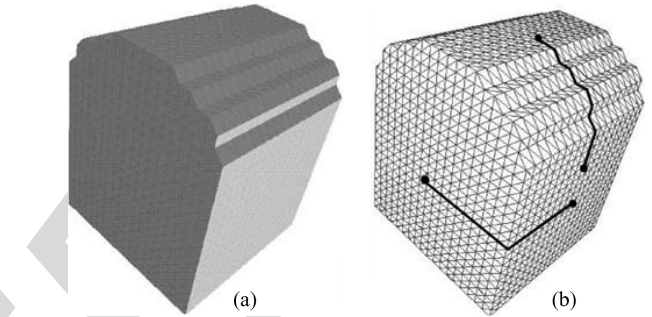


Fig. 6. Illustration showing the calculated geodesic distance between two points on a synthetic surface. (a) Original synthetic surface. (b) Synthetic surface overlayed with geodesic distances between four example points, calculated using the fast marching method [31], [41].

determine if the value is greater than or less than the mean surface curvature.

Once the points of interest are determined, the geodesic distance can be computed using a number of different methods [39]–[41]. One of the most popular is the fast marching method proposed by Kimmel and Sethian [41]. This method has gained wide acceptance due to the speed of the calculations, and its easy applicability to a vast array of applications, which include 2- and 3-D structures. An example of the result of the fastmarching method is illustrated on a synthetic surface in Fig. 6.

Wang *et al.* [31] proposed the use of geodesic distance analysis to analyze the sulci and gyral fissures of the brain for matching brains. Locations were classified and compared between subjects. Areas where the sulci and gyri were similar could then be detected in the brain. Their results showed that surface correspondences could be found between brains, and that the fissures could be consistently identified across brains. Pastore *et al.* [32] used geodesic distances to improve the segmentation accuracy (see Fig. 7) of the sulci and gyri in the brain. They found that geodesic distances proved to be a precise, efficient, and versatile method for segmenting the external boundary of the brain because the gyrfications of the brain have large curvatures and this feature is carried over into the MRI images.

Huang *et al.* [33] proposed a method for the extraction of brain for comparison of contours using geodesic distances. Results they obtained showed that geodesic distances could aid in making extractions consistent across datasets, and the proposed method achieved a tight brain mask around the brain cortex.

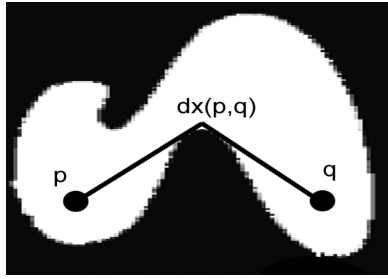


Fig. 7. Example of a geodesic distance calculation between two points (p and q) on the boundary of a 2-D MRI scan [32]. The area has been zoomed and binarized so that the curvature can be clearly seen.

Mio *et al.* [34] used geodesic distances to compare brains by comparing the decomposed geodesic curvature of each brain. Their work illustrated how geodesic distance could be successfully used to quantify morphological similarity and differences, and to identify particular regions where shape similarity and divergence were the most pronounced.

Butman *et al.* [35] identified the brain ventricles and computed the volume of hydrocephalus in subjects using geodesic distance. Similar to the results of Huang, Butman showed that segmentation results were robust throughout datasets and able to classify hydrocephalus.

Hua *et al.* [36] combined geodesic distances with vector image diffusion, a method of examining intrinsic geometric characteristics (e.g., mean curvatures) using a multiscale diffusion and scale space, to match brains of different subjects. This method was shown to be superior to anisotropic diffusion and SIFT curvature matching algorithms in finding stable keypoints. Liang *et al.* [37] approximated the curved cingulum bundle using diffusion tensor imaging (DTI) tractography and geodesic distances. Although there were many limitations found, a significant reduction in fractional anisotropy values, within specific anatomical regions, were detected when using geodesic distances.

Joshi *et al.* [38] analyzed the sulcal curvature in the cortex of the human brain using geodesic curvature. They concluded that geodesic curvature showed promising prospects for analyzing the sulcal curvature in case of small temporal lobe lesions. In the literature and application, geodesic distances are most often used to examine the curvatures of locations of the brain and to locate key points that can be identified due to their curved nature. Geodesic distances have proven to be a useful shape analysis tool in segmentation, registration, and analysis, and are also unique in that they incorporate aspects of first- and second-order analysis.

Geodesic distances have a large number of applications, but primary advantages are their applications in segmentation and the identification of locations in the shapes of brains. This method provides an excellent metric for examining curvature and localized areas of objects, and can provide many discriminatory metrics for classification. Their major drawbacks are their generally localized nature, and the fact that it is difficult to examine large and complex objects that have numerous inflections in their curvature. Three-dimensional analysis of shapes

TABLE III
AUTOMATED (A) OR SEMIAUTOMATED (SA) PROCRUSTES ANALYSIS: GROUND TRUTH (GT) FROM CLINICIAN (C) OR NONCLINICIAN (N) EXPERTS; DIMENSIONALITY (DIM) AND SIZES (#) OF EXPERIMENTAL IMAGE DATABASES

| Publication | Year | Mode | Dim | # | GT |
|---------------------|------|------|-----|-----|----|
| Duta et al [44] | 1999 | A | 2D | 28 | C |
| Penin et al [45] | 2002 | SA | 3D | N/A | N |
| Bienvenu et al [46] | 2011 | A | 3D | 144 | N |

such as the cortex and white matter of the brain prove more challenging for a solely geodesic analysis.

IV. PROCRUSTES ANALYSIS

Procrustes analysis is a statistical form of congruent shape analysis that primarily focuses on the distributions of sets of shapes. It is interesting to note that Procrustes was a rogue and bandit who was the son of Poseidon in ancient Greek mythology [42]. He was known for either stretching people or cutting off their limbs to force them to fit within a statically sized iron bed. The process of Procrustes analysis thereby refers to shape analysis in which properties such as translation, rotation, and scaling are removed so that the shape can be fit into a common reference frame. The process is inherently congruent. Procrustes analysis is most commonly performed by superimposing shapes on top of one another and then applying uniform properties so that geometric transformation of the objects are removed and the shapes can be compared. Procrustes analysis has also served an important role in shape warping, especially as applied to the brain [43].

Table III exemplifies applications of procrustes analysis to brain analysis. It includes methods starting with the early application by Duta *et al.* [44] which analyzes the properties of the skull structure. Bienvenu *et al.* [46] used Procrustes analysis primarily for medical diagnostics or classification.

Nicolae Duta *et al.* [44] proposed a method for the basis of Procrustes analysis in 2-D shape models in medical image analysis. Duta defines the main reasons for the use of Procrustes analysis as a convenient way to compute a prototype (average shape) from a set of simultaneously aligned shapes. Once the point correspondences are found, there exists an analytical or exact solution to the alignment problem.

Mathematically, Procrustes analysis seeks a solution to the following problem: assume we are given a set of m shape instances where $S_k = (x_i^k, y_i^k)_{i=1 \dots n_k}^{k=1 \dots m}$ that is represented by a set of landmarks or boundary points. This set is partitioned into a set of clusters and for each shape cluster a mean shape, or prototype, must be computed. The set of prototypes can then be used for segmentation or the calculation of other metrics. One such metric is a Procrustes residual, which is defined as a deviation in landmarks on a specific object from the consensus of a group, or the prototypes. Duta illustrated the usage of Procrustes analysis for the segmentation of objects and registration of different objects following segmentation. They also introduced algorithms for global and local similarity measures using Procrustes analysis.

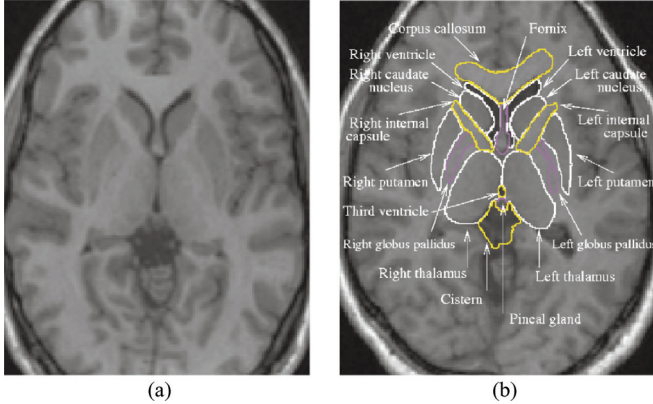


Fig. 8. (a) Magnetic resonance image of the human brain. Neuroanatomic structures of the brain are highlighted by a neuroanatomist (b) Structures shown in yellow are able to be accurately classified by Procrustes analysis. Image courtesy of Duta *et al.* [47].

Penin *et al.* [45] proposed a method for the study of the skull of humans and brains as compared to other primates through the use of tri-dimensional Procrustes analysis. In this study, 29 key features were identified as common landmarks between the different skulls, and the shapes were defined as Procrustes residuals. A Procrustes residual is a deviation in a landmark from the consensus of a group. One downside noted by Penin was that in Procrustes analysis the size and shape are calculated as independent vectors when using traditional shape theory, meaning that normalization of objects is often required during preprocessing.

Bienvenu *et al.* [46] proposed a similar method for examining endocranial variations. Bienvenu found that Procrustes analysis was more favorable in examining the skull, as it has less variability than the cortical surface itself, and is therefore less subjective to the noise introduced by the large differences in the cortex. Similar to Penin, Bienvenu selected specific landmarks commonly found on the enocranial surface and generated a prototype. This prototype was then used to examine the differences between males and females of different species. It was found that Procrustes analysis was capable of determining not only the gender, but the species as well due to the large variation in the landmarks of the prototypes.

In a follow up to his previous work, Duta examined the automated construction of shape models using Procrustes analysis [47]. This study determined that the major advantage of Procrustes analysis, as applied to the brain, is that Procrustes analysis is a reliable method of classifying and segmenting anatomical structures in relatively rigid objects including the ventricles and corpus callosum of the brain (see Fig. 8). It struggles with more complex structures of the brain, specifically the gray and white matter. Procrustes analysis therefore provides an accurate and fast method of analysis in objects that do not have significant variation. This limits its applicability to only specific cases; however, it is a useful measure for examining the shape of the brain and its more rigid structures.

One of the more direct problems related to Procrustes analysis is the method of selecting landmarks on the brain. Because of

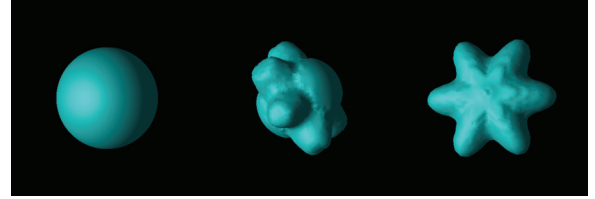


Fig. 9. Illustration of a 3-D deformable model as it contracts on a star-like object [50]. Three frames of progression are shown starting at the left with the original spherical model. The model gradually deforms around the object until it has converged on the star in the center.

the variability in sulci and notable landmarks on the brain, there may be an impact on the resulting analysis. Furthermore, the selection of landmarks could introduce a bias into the analysis. If landmarks are not appropriately located, areas may either be over- or undercompensated for, adding an additional degree of complication to this form of analysis. It is likely one of the driving reasons that this methodology has only seen moderate modern adoption.

Procrustes analysis, while useful, does not provide an in-depth analysis of complex objects as some other methods. Discussion of deformable models and SPHARMs will illustrate examples of some of the more popular techniques for identifying mathematical differences between 3-D shapes that the human eye is unlikely to be able to classify.

V. DEFORMABLE MODELS

Deformable models, also known as active surfaces, are a model-based technique that combines geometry, physics, and approximation theory in order to offer a unique and powerful approach to image analysis [48]. Deformable models have proven useful in a variety of applications for the brain including segmentation, shape representation, matching, and motion tracking. Unlike more rigid methods of analysis, deformable models are capable of accommodating for significant variability in shapes (see Fig. 9), like the brain, over time and across different individuals. While deformable models were originally used in the field of computer vision, their application to the analysis of complex medical objects, such as the brain, was quickly realized by the scientific community. In their 2-D forms, deformable models are often referred to as active contours or snakes [49], [50].

Deformable models have mathematical foundations in geometry, physics, and shape approximation theory [48]–[50]. Geometry is used to represent an object's shape, and deformable models commonly make use of complex geometric representations, such as splines, that offer flexibility and many degrees of freedom. Physics is applied to impose constraints controlling how that shape can vary, with respect to properties such as space and time. The name “deformable models” is most closely associated with the incorporation of this elasticity theory at a physical level. Therefore, deformable models are most commonly constructed inside a Lagrangian dynamics setting that is able to respond naturally to constraints and applied forces. As a model deforms in the Lagrangian setting, the deformation energy will give rise to internal elastic forces. Potential energy functions for the external model are defined so that the model

TABLE IV

AUTOMATED (A) OR SEMIAUTOMATED (SA) DEFORMABLE MODEL ANALYSIS:
GROUND TRUTH (GT) FROM CLINICIAN (C) OR NONCLINICIAN (N) EXPERTS;
DIMENSIONALITY (DIM) AND SIZES (#) OF EXPERIMENTAL IMAGE DATABASES

| Publication | Year | Mode | Dim | # | GT |
|-------------------------------|------|------|-----|-----|----|
| Davatzikos <i>et al.</i> [51] | 1996 | SA | 3D | 6 | N |
| Dale <i>et al.</i> [52] | 1999 | A | 3D | 100 | C |
| Smith [53] | 2002 | A | 3D | 45 | C |
| Zhuang <i>et al.</i> [54] | 2006 | A | 3D | 49 | C |
| Joshi <i>et al.</i> [55] | 2007 | A | 3D | 6 | N |
| Tu <i>et al.</i> [56] | 2007 | A | 3D | 28 | C |
| Huang <i>et al.</i> [57] | 2009 | A | 3D | 36 | C |
| Liu <i>et al.</i> [58] | 2009 | A | 3D | 38 | N |
| Li <i>et al.</i> [59] | 2011 | A | 3D | 5 | N |
| Hashioka <i>et al.</i> [60] | 2012 | SA | 3D | 14 | C |

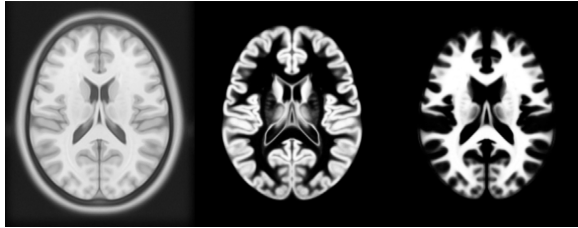


Fig. 10. Segmentation results of the brain showing the gray matter and white matter are shown here. The goal of such work in this figure is to analyze the volume, and the deformable model proves useful in isolating the voxels that belong to the brain. After identifying the desired portion of the brain with a deformable model, calculating the volume becomes a trivial task [52].

deforms to fit the data. Through the combination of these two energies, deformable models can be used for many situations. Some of the most common shape analysis applications of deformable models are in the areas of segmentation and volume analysis, along with shape matching and registration.

Table IV exemplifies applications of deformable model to human brain analysis. It includes methods starting with the early application by Davatzikos *et al.* [51] which was used to identify the central sulci and interhemispheric fissures in the brain. No methods that are primarily based on deformable model analysis have been used primarily for medical diagnostics or classification.

Davatzikos *et al.* [51] proposed one of the earliest methods for analyzing the cortical surface of the brain using deformable models. They used deformable models to identify similar landmarks on different brains for alignment. Their results showed that deformable models could be used to register two different brains with one another, and in order to select cortical and subcortical landmarks on the brain cortex.

Dale *et al.* [52] used a simplified deformable model to segment the cortex of the brain (similar to Fig. 10). The algorithm proved to be a robust method of identifying the cortex of the brain with an average accuracy of 96% across a wide variety of subjects. In 2002, Smith [53] introduced the brain extraction tool (BET). An intensity model is used to initialize the surface model, which is then refined to extract the brain. It was shown to be a fast and accurate method of extraction, having a mean percentage error of about 7% over 45 datasets. Zhuang *et al.* [54] used a model-based level set to perform skull stripping on pediatric and youth brains. The approach showed good accuracy

using the DICE metrics with notable improvements over the BET proposed several years before by Smith [53].

Joshi *et al.* [55] used deformable models to register sulci along with a coregistration of brain volume data. Results showed a statistical improvement over the AIR [61], [62] and HAMMER [63], [64] methods. Tu *et al.* [56] use deformable models to aid in segmenting specific locations found in the brain. The discriminative model they developed played a major role in obtaining clear segmentations. Additionally, the segmentation could be further improved by adjusting the smoothness of the model and constraining the shape with a global shape model.

Huang *et al.* [57] proposed the use of deformable models to segment the cortex, gray matter, and CSF of the human brain. They showed good results when the data was analyzed using the DICE metric. They concluded that deformable models led to improved segmentation accuracy and robustness when applied using a hybrid approach against, as opposed to using only geometric or statistical features. On real clinical MRI datasets, the hybrid approach demonstrated an improved accuracy over other state-of-the-art approaches.

Liu *et al.* [58] suggested a deformable model that driven by radial basis functions to be used for automated extraction of the brain. This model proved to be an accurate and fast technique, having a similar accuracy to the BET proposed by Smith [53]. Li *et al.* [59] proposed an alternative method for the automated extraction of the brain using a deformable model. Their method was an extension of the human brain extraction tool and was found to more reliably extract brains through the inclusion of a deformable model. Hashioka *et al.* [60] proposed a method that utilized active contour modeling (ACM), also commonly referred to as “snakes,” for the extraction of the cortex in the neonatal children. The results showed a sensitivity of 98.5% with a false positive ratio of 13.8%. While their results were largely successful when an optimal head contour was present, they noted that a nonoptimal contour performed less robustly.

While deformable models may not be in the forefront of diagnosis classifications, they have become an integral element of shape analysis. The primary advantage is in the area of shape segmentation, in which these models excel. Deformable models are also very adaptable at isolating complex regions of shapes for further analysis. Deformable models provide useful and accurate ways to identify and segment locations in the brain which is a critical step in analyzing the shape of the brain. The major drawback of using deformable model analysis is that it does not often provide many metrics for directly examining the brain for the purpose of classification or matching.

VI. SPHERICAL HARMONICS

Dealing with the orientation of the brain and aligning two brain objects with one another to compare differences in shape can prove challenging and time consuming. SPHARM, a popular method of shape analysis, can be used to remove these factors. SPHARM analysis [65], [66] considers 3-D surface data as a linear combination of specific basis functions. Additionally, SPHARM provides a rotation invariant common coordinate system in which shapes can be analyzed. The main goal of

SPHARM is to decompose a 3-D object into concentric, or unit, spheres. This process is what discards the orientation information that primarily accompanies a 3-D shape representation of an object. The result is a shape descriptor that is both descriptive and invariant to orientation.

Consideration of the analysis of the entire brain for purposes of identifying differences in shape between different structures is one of the major advantages of SPHARMs. The volume changes in the brain are intuitive features that can be used to describe illness, disorders, and atrophy. The area that SPHARM seeks to address is the structural changes inherent to the surface of the brain. This is an area that SPHARM analysis seeks to address. The use of SPHARM applied to brain analysis was first proposed by Gerig *et al.* [65] for the analysis of the lateral ventricles of the brain. SPHARM was originally developed as a technique for model-based segmentation and data storage; however, its applications have grown in recent years. One important factor of SPHARM analysis is that it relies primarily on the surface of a shape and manifold properties. Due to this, only shapes without holes or disconnects in their surfaces can be accurately analyzed.

SPHARM is a global-based shape analysis technique that is hierarchical in nature. Any shape can be parameterized by a set of basis functions, and these basis functions are referred to as SPHARMs. SPHARM is based on Laplace's equation and involves a mathematical solution of the angular components of the equation. SPHARMs were first discovered by Simon de Laplace in 1782, although it would take several centuries before they were applied to the shape analysis of the brain.

SPHARM basis functions Y_l^m , $-l \leq m \leq l$ of degree l and m are defined on $\theta \in [0; \pi] \times \phi \in [0; 2\pi]$ by the following definitions [65]:

$$\begin{aligned} Y_l^m(\theta, \phi) &= \sqrt{\frac{2l+1}{4\pi} \frac{(l-m)!}{(l+m)!}} P_l^m(\cos \theta) e^{im\phi} \\ Y_l^{-m}(\theta, \phi) &= (-1)^m Y_l^m(\theta, \phi) \end{aligned} \quad (1)$$

where Y_l^m denotes the complex conjugate of Y_l^m . P_l^m describes the associated Legendre polynomials given as

$$P_l^m(\omega) = \frac{(-1)^m}{2^l l!} (1 - \omega^2)^{\frac{m}{2}} \frac{d^{m+l}}{d\omega^{m+l}} (\omega^2 - l^2). \quad (2)$$

The surface is then decomposed from the Cartesian coordinate functions and is represented as $v(\theta, \phi) = (x(\theta, \phi), y(\theta, \phi), z(\theta, \phi))^T$. To express a surface using SPHARMs the following equation is used:

$$v(\theta, \phi) = \sum_{l=0}^{\infty} \sum_{m=-l}^l c_l^m Y_l^m(\theta, \phi) \quad (3)$$

where the coefficients c_l^m are 3-D vectors that are typically obtained through solving a least-squares problem for the points. As previously mentioned, these basis functions allow for a hierarchical description of the surface of a shape. The more coefficients are used in the reconstruction, the more detail is present in the final constructed shape.

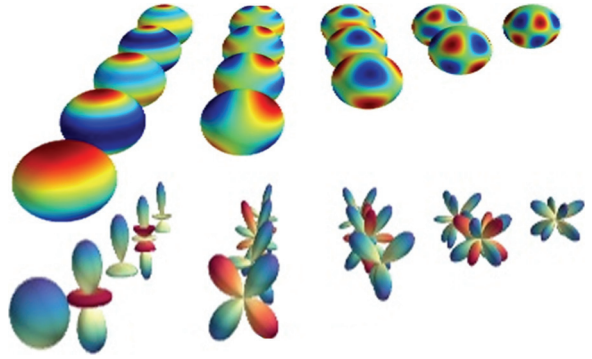


Fig. 11. Decomposition of an object, as described by Gerig *et al.* [65]. In the upper section of the image the SPHARM are plotted overlayed on top of a unit sphere, and below the polar plot of the unit spheres are shown to give a more detailed understanding of the actual information contained within each sphere.

Table IV lists applications of SPHARM to human brain analysis. It includes methods starting with the early application by Keleman [67], along with notable applications, e.g., Gerig *et al.* [65], which have shown SPHARM as a potential method for classifying neurological disorders. SPHARM has been widely applied as a method for potential diagnosis.

Brechbühler *et al.* [78] demonstrated the usage of SPHARM as a method for parameterizing closed surfaces of 3-D objects. In 1999, Keleman [67] demonstrated an ability of SPHARM to analyze shape deformations in neuro-radiological data. Keleman used training data to compute SPHARM representations of the brain which were then simplified using PCA and applied to segment a cortex. Their results showed that SPHARM was a promising technique for improving standard brain segmentations because of the included 3-D forces SPHARM offered.

Gerig *et al.* [65] proposed one of the most significant applications of SPHARM. It was used to analyze the volume similarity between twin brains and demonstrated that SPHARM shape measures reveal new information in addition to size measurements. They proposed that this information might become relevant for an improved understanding of the structural differences not only in normal populations, but also in comparisons between healthy controls and autistic patients. A sample example of the deformation of an object is shown in Fig. 11. Styner and Gerig [79] later proposed a framework package based on SPHARM analysis entitled SPHARM-PDM that could be used for analysis of a multitude of brain structures. This SPHARM-PDM package has been used for examining various brain structures, including work by Kim *et al.* [76] on the hippocampus, and by Paniagua *et al.* [20] (previously mentioned) on the lateral ventricles in neonates.

Chung *et al.* [66] proposed a method to analyze the computed SPHARM coefficients to identify autism in subjects. While the SPHARM coefficients did not generate reliable results, their work showed the ability to accurately and efficiently encode neurological information using a weighted-SPHARM. Chung *et al.* [70] continued their application to explore statistically significant differences between autistic and control subjects using the coefficients. While their work showed some areas of statistical difference, the locations were largely random. This study did

TABLE V
AUTOMATED (A) OR SEMIAUTOMATED (SA) SPHARM ANALYSIS: GROUND TRUTH (GT) FROM CLINICIAN (C) OR NONCLINICIAN (N) EXPERTS; DIMENSIONALITY (DIM) AND SIZES (#) OF EXPERIMENTAL IMAGE DATABASES

| Publication | Year | Mode | Dim | # | GT |
|--------------------------------|------|------|-----|-----|----|
| Keleman <i>et al</i> [67] | 1999 | A | 3D | 21 | N |
| Gerig <i>et al</i> [65] | 2001 | A | 3D | 20 | C |
| Chung <i>et al</i> [66] | 2007 | A | 3D | 28 | C |
| Uthama <i>et al</i> [68] | 2007 | A | 3D | 40 | C |
| Abdallah <i>et al</i> [69] | 2008 | A | 3D | 18 | C |
| Chung <i>et al</i> [70] | 2008 | A | 3D | 28 | C |
| Uthama <i>et al</i> [71] | 2008 | A | 3D | 20 | C |
| Esmail-Zadeh <i>et al</i> [72] | 2010 | A | 3D | 95 | N |
| Nitzken <i>et al</i> [73] | 2011 | A | 3D | 45 | C |
| Nitzken <i>et al</i> [74] | 2011 | A | 3D | 30 | C |
| Geng <i>et al</i> [75] | 2011 | A | 3D | 5 | N |
| Kim <i>et al</i> [76] | 2011 | A | 3D | n/a | C |
| Paniagua <i>et al</i> [20] | 2013 | A | 3D | 90 | C |
| Hosseini <i>et al</i> [77] | 2013 | A | 3D | 69 | C |

show that the weighted SPHARM provides better smoothing in cortical applications than other comparative methods.

Uthama *et al.* [68] proposed the analysis of the ventricle geometry using SPHARM between Parkinson's disease (PD) and control patients. They showed that a statistically significant comparison ($p < 0.05$) of controls and PD subjects could be made using SPHARM, and that it was able to detect subtle changes in synthetic and clinical brain ventricle data. Uthama *et al.* [71] also proposed the use of SPHARM to perform fMRI spatial analysis. They demonstrated differences in the way PD patients and healthy controls respond to an increased task demand. The analysis illustrated that the inability to respond to task demand was reflected in the failure of PD subjects to increase basal ganglia output, and a reliance on cerebellar and cortical activity to enable successful performance.

Abdallah *et al.* [69] applied a parameterization to 3-D meshes, and then used SPHARM application to improve the shape detection of the ventricles. Results showed that a parameterization of a shape followed by SPHARM analysis can lead to improve comparisons and better shape descriptors.

Esmail-Zadeh *et al.* [72] use SPHARM to analyze the hippocampus to classify subjects as either normal or epileptic. Their results showed that in an optimum case, a 90.32% rate of classification of left and right anterior temporal lobes could be achieved when validated using the leave-one-out method.

Nitzken *et al.* [73], [80] proposed an alternative use SPHARM by using the SPHARM reconstruction error to classify autism (see Fig. 12). Classification accuracies on a test population of 100% could be achieved and illustrates a potentially effective way of classifying autism in subjects. Nitzken *et al.* [74], [81] later expanded this theory to the classification of dyslexia. A variation was further used to examine changes related to aging in the human brain [82].

Geng *et al.* [75] demonstrated the use of SPHARM coefficients to perform nonrigid registration of brain white matter and fiber tracts. This method performed better than standard second-order registration methods, although this could also be attributed to the use of higher orders when applying SPHARM. Overall, it was found that SPHARM provided a notable

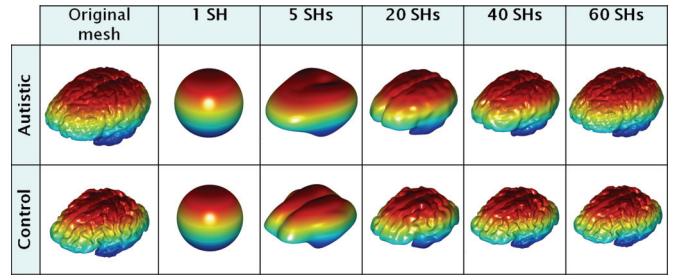


Fig. 12. Method proposed by Nitzken [73] for the approximation of the 3D brain cortex shape for autistic (A) and normal subjects (C).

TABLE VI
AUTOMATED (A) OR SEMIAUTOMATED (SA) VOXEL- AND DEFORMATION-BASED MORPHOMETRY ANALYSIS: GROUND TRUTH (GT) FROM CLINICIAN (C) OR NONCLINICIAN (N) EXPERTS; DIMENSIONALITY (DIM) AND SIZES (#) OF EXPERIMENTAL IMAGE DATABASES

| Publication | Year | Mode | Dim | # | GT |
|----------------------------|------|------|-----|-----|----|
| Chung <i>et al</i> [83] | 2002 | A | 3D | 28 | C |
| Leow <i>et al</i> [84] | 2006 | A | 3D | 17 | C |
| Lepore <i>et al</i> [85] | 2007 | A | 3D | 30 | C |
| Afzali <i>et al</i> [86] | 2010 | A | 3D | 31 | C |
| Wang <i>et al</i> [87] | 2012 | A | 3D | 2 | C |
| Yang <i>et al</i> [88] | 2012 | A | 3D | 60 | C |
| Fletcher <i>et al</i> [89] | 2013 | A | 3D | 285 | C |
| Shi <i>et al</i> [90] | 2013 | A | 3D | 35 | C |

improvement. In 2013, Hosseini *et al.* [77] proposed a further expansion of SPHARM to a 4-D representation of subcortical structures. This new 4-D SPHARM is entitled HyperSPHARM and is intended to serve as a method of tracking changes over time using SPHARM. This allows SPHARM to directly compete with applications typically reserved to methods such as voxel- and deformation-based morphometry.

SPHARM is one of the most beneficial methods of shape analysis for providing meaningful global analyses of objects. SPHARM excels in brain analysis areas that involve large surfaces, such as the cortex and white matter. The major drawbacks to SPHARM analysis are that it can be difficult to localize the SPHARM analysis to understand select locations. It also struggles with applications such as segmentation and automated identification of objects in 2-D images. SPHARM's greatest strength comes in its ability to distinguish between shapes and its applications such as clinical diagnosis classification.

VII. VOXEL- AND DEFORMATION-BASED MORPHOMETRY

Voxel-based morphometry (VBM) is another technique for examining the entire brain [91], [92]. Table VI lists applications of morphometry-based techniques to human brain analysis. VBM is a technique wherein brains between subjects are generally warped, aligned, and normalized in order to remove large differences between the brains, and a volume is then compared across each brain on a voxel by voxel basis. In VBM-smoothed values of the voxels or an averaging of a voxel and its neighbors are typically used. The major usage for VBM is the detection of differences and similarities for images between two populations or shapes [86]. Deformation-based morphometry (DBM) is a similar form of statistical analysis to VBM. However, instead

of measuring the changes between voxels, the changes on the deformation fields are used. The most common variant of DBM in brain shape analysis is tensor-based morphometry (TBM), which is based on the Jacobian determinants. While DBM and more specifically TBM are able to detect more subtle changes between brains, they introduce a significantly higher degree of computational complexity when compared to VBM, because the warping often involves highly nonlinear algorithms. Both VBM and TBM are commonly used in calculating cortical thickness measurements as well.

In 2001, Ashburner *et al.* [93] made a case for VBM in response to criticism posed in Dr. Bookstein's article "Voxel-Based Morphometry Should Not Be Used with Imperfectly Registered Images" [91]. He explains that VBM was a method originally intended to explore cortical thickness that benefits from not being affected by volume changes, the major weakness of volumetric analysis. While acknowledging the partial volume effect as a potential issue, Ashburner also details how modern normalization techniques allow for high-resolution image alignments and warping. He also discusses that VBM is not subject to the issues of landmark selection as found in other analysis methods like Procrustes analysis. In summary, VBM is a useful and reliable method for examining the volume of the brain and its subcomponents, while avoiding the traditional pitfalls associated with volumetric measurements.

Afzali *et al.* [86] explored the differences between using VBM and the tractography of diffusion tensor MRIs for patients with epilepsy. Compared to the tractography methods, VBM showed a consistently accurate performance in analyzing the volume of the hippocampus and frontal lobe of the brain. Afzali does discuss the downside of partial volume effects and increased statistical analysis complexity for VBM. However, he notes that with modern computing power the second fact becomes increasingly less significant. It is also important to note that modern techniques have greatly reduced partial volume effects.

Chung *et al.* [83] introduced a tensor-based model for analyzing the brain surface in 2002. Chung applied a diffusion smoothing operator that is based on a standard Laplace–Beltrami operator to the tensors of the cortex and brain stem to determine local differences. The approach demonstrated that TBM could detect a localized regions of difference on the shapes of two clinical groups. Wang *et al.* [87] applied a multivariate TBM to the lateral vents and the hippocampus. Wang demonstrated a straightforward framework for performing TBM operations on subcomponents of the brain to be used by other researchers.

Lepore *et al.* [85] applied a generalized TBM method to HIV/AIDS patients to examine differences between the corpus callosum and brain surfaces of individuals. Lepore also explored the use of multivariate tensors and discussed how increasing the number of parameters for these tensors could improve the multivariate statistics. Lepore commented how TBM is useful in both registration and statistical analysis, illustrating the multiple use cases for many brain analysis applications.

Leow *et al.* [84] proposed using TBM to identify changes in the brains of aging subjects. Leow's results showed that in Alzheimer's patients, there were reliable brain shape changes in the tensors over time relative to baseline controls. Leow also

illustrated several methods for correcting distortion in TBM techniques. Fletcher *et al.* [89] combined TBM and boundary-based methods to track longitudinal brain changes in subjects. This method was compared to those that do not involve boundary detection, and demonstrated how the inclusion of boundary parameters helped to correct for noise at the tissue boundaries. It also helped to remove bias-correction, which may occur from warping algorithms, and added only minimal performance degradation. Fletcher, like Leow, also explored the proposition of using TBM to detect Alzheimer's in patients. Yang *et al.* [88] used VBM for the application of Alzheimer's as well. Yang studied the changes of VBM measurements in patients over a three-year period. The study showed that atrophy clusters in the brain could be detected in patients who had been diagnosed with Alzheimer's.

Shi *et al.* [90] used TBM to examine the effects of prematurity in the brains of newborns. Different from other methods, Shi registered the surface fluid of the brain instead of the cortex, and applied a TBM approach to this surface fluid. The statistical analysis showed common clusters of significant difference between the brains of the subjects. Shi also showed that the TBM approach was sensitive enough to measure the largely smooth surface of the surface fluid and discern small, but meaningful differences.

VIII. ADDITIONAL METHODS OF SHAPE ANALYSIS

Table VII details additional applications of shape analysis. It includes additional methods such as graph-matching, symmetry-based analysis, Laplace–Beltrami analysis, and volumetric analysis. Many different methods have been applied as potential methods of diagnosis or classification.

A. Distance Mapping

Distance mapping is a technique that has similarities to geodesic distance and medial axis analysis. It differs in that more generalized distance metrics and locations are often computed and examined. He *et al.* [94] proposed a method of brain analysis using distance mapping (see Fig. 13). They examined the statistical differences in distances at the border of a segmented corpus callosum in autistic patients. They hypothesized that a statistical mean difference between segmented images could be discovered; however, it was ultimately concluded that no meaningful statistical difference in shape between subjects could be found using the proposed method.

El-Baz *et al.* [95] proposed an alternative distance mapping technique based on the fast marching method. They used this technique to approximate the thickness of the white matter in autistic patients. They expanded their work to improve the accuracy and explore the technique in different brain abnormalities [117]–[123].

B. Entropy-Based Particle Systems

Cates *et al.* [96] introduced a novel approach to brain shape analysis using an entropy-based system. Points are modeled on the surface of the brain as particles. These particles are then

TABLE VII
AUTOMATED (A) OR SEMIAUTOMATED (SA) ADDITIONAL METHODS OF SHAPE ANALYSIS: GROUND TRUTH (GT) FROM CLINICIAN (C) OR NONCLINICIAN (N)
EXPERTS; DIMENSIONALITY (DIM) AND SIZES (#) OF EXPERIMENTAL IMAGE DATABASES

| Method | Publication | Year | Mode | Dim | # | GT |
|--------------------------------|---------------------------------|------|------|-----|-----|----|
| Distance Mapping | He <i>et al.</i> [94] | 2007 | SA | 2D | 10 | N |
| Distance Mapping | El-Baz <i>et al.</i> [95] | 2007 | A | 3D | 30 | C |
| Entropy-based Particle Systems | Cates <i>et al.</i> [96] | 2009 | A | 3D | 56 | C |
| Graph Matching | Geraud <i>et al.</i> [97] | 1995 | SA | 2D | n/a | N |
| Graph Matching | Yang <i>et al.</i> [98] | 2007 | A | 3D | 120 | N |
| Graph Matching | Long <i>et al.</i> [99] | 2012 | SA | 2D | 60 | C |
| Homologous Model | Yamaguchi <i>et al.</i> [100] | 2009 | A | 3D | 4 | N |
| Homologous Model | Yamaguchi <i>et al.</i> [101] | 2010 | A | 3D | 11 | N |
| Laplace-Beltrami | Angenent <i>et al.</i> [102] | 1999 | A | 3D | 1 | C |
| Laplace-Beltrami | Lai <i>et al.</i> [103] | 2011 | A | 2D | 32 | N |
| Laplace-Beltrami | Shishegar <i>et al.</i> [104] | 2011 | A | 3D | 78 | C |
| Laplace-Beltrami | Germanaud <i>et al.</i> [105] | 2012 | A | 3D | 151 | N |
| Reeb Analysis | Makram <i>et al.</i> [106] | 2008 | A | 3D | 12 | C |
| Reeb Analysis | Shi <i>et al.</i> [107] | 2011 | A | 3D | 200 | C |
| Spectral Matching | Lombaert <i>et al.</i> [108] | 2011 | A | 3D | 36 | N |
| Spectral Matching | Lombaert <i>et al.</i> [109] | 2013 | A | 3D | 12 | N |
| Symmetry-based | Prima <i>et al.</i> [110] | 2002 | A | 3D | 250 | C |
| Symmetry-based | Gefen <i>et al.</i> [111] | 2004 | A | 2D | 232 | N |
| Symmetry-based | Liu <i>et al.</i> [112] | 2007 | A | 2D | 3 | N |
| Symmetry-based | Feng <i>et al.</i> [113] | 2008 | A | 2D | 1 | N |
| Symmetry-based | Fournier <i>et al.</i> [114] | 2011 | A | 3D | 37 | N |
| Volume Analysis | Herman <i>et al.</i> [115] | 1988 | A | 3D | n/a | N |
| Volume Analysis | Wagenknecht <i>et al.</i> [116] | 2008 | A | 3D | n/a | N |

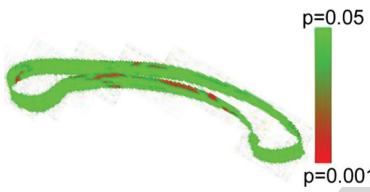


Fig. 13. Method proposed by He *et al.* [94] using distance mapping to examine areas of significant difference along the outer edge of the corpus callosum.

optimized and negative energy is measured to create a distribution of each unique shape. The technique is useful in both 2- and 3-D analysis. The computational efficiency of the approach is based on the number of particles used. Cates applied the approach to the examination of the hippocampus. The advantages to the technique showed results consistent with many other techniques, while requiring a minimum amount of parameter tuning. Due to this fact it could be easily adapted to the brain curvature.

C. Graph Matching

Graph matching techniques involve converting more complex information into a more simplified graph-based representation. Similarities in the graphs are then used to identify, segment, and analyze the more complex information. Geraud *et al.* [97] proposed a method of graph matching analysis. They utilized a Markovian relaxation on a watershed-based adjacency graph to improve the segmentation of neighboring structures in the brain. The results showed a good initial approach to the application of graph matching in the area of segmentation and identification.

Yang *et al.* [98] proposed that two graph-matching techniques can be used to constrain a search neighborhood and the genetic algorithms can be used to optimize sulci labeling. They were

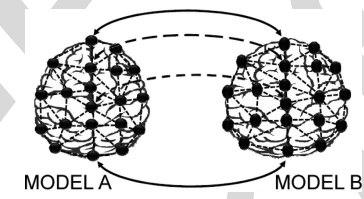


Fig. 14. Method proposed by Yamaguchi *et al.* [100] illustrating the concept of homologous modeling on two brains.

able to achieve satisfactory identification rates for finding sulci using the proposed graph-matching strategy.

Long *et al.* [99] suggested that the brain shape could be decomposed to a graph by subdividing the images into a tree structure containing various properties of the specific brain. By manually selecting important locations for placing the subdivision structures, the brain could be successfully classified for cognitive impairment due to Alzheimer's disease.

D. Homologous Modeling

Homologous modeling is a mesh-based technique in which items having the same number of analysis points in the same locations on two different models can be examined. The technique has been applied to many different applications, but due to implementation complexity is rarely applied to the whole brain. However, it may also be appropriate for the analysis of other discrete brain structures (e.g., corpus callosum, amygdala, or hippocampus).

Yamaguchi *et al.* [100] demonstrated a method based on a homologous model to calculate a sulcal-distribution index for brains to identify brain fissures (see Fig. 14). A mean displacement of 1.3 ± 0.7 mm was found. Their results suggested that

a homologous model could be used to correspond the sulci and gyri among the evaluating brains effectively. Yamaguchi *et al.* [101] proposed a later method to statistically quantify the brain shape using a homologous model. The work examined the changes in the frontal and occipital lobes between male and female subjects. A significant difference ($p < 0.05$) was detected in the sample population and the model was able to successfully detect the locations in the brain that differ significantly.

E. Laplace–Beltrami

Laplace–Beltrami methods comprise any methods that rely heavily on the Laplace–Beltrami operator. The Laplace–Beltrami operator of a smooth function f on a Riemannian manifold M and is defined as $\Delta f = \text{div}(\text{grad}f)$, where div and grad are the divergence and gradient operators of the manifold M [104]. This technique is most commonly used in smoothing applications or curvature analysis.

Angenent *et al.* [102] was the first researcher to propose brain analysis using a Laplace–Beltrami model. Angenent hypothesized that a brain could be flattened by using a Laplace–Beltrami operator on the brain surface. The technique was shown to be an efficient method of flattening the brain.

Lai *et al.* [103] used Laplace–Beltrami nodal curves, and geodesic curve evolutions to segment to the corpus callosum. In small datatests, the method appeared to show positive results and be robust.

Shishegar *et al.* [104] analyzed the first 20 eigenvalues of the Laplace–Beltrami spectrum to classify epilepsy. In the best testing results, Shishegar acheived a 91.9% true positive rate and a 33.3% false positive rate using out of normal range classifiers and cross validation, illustrating that while there were difficulties, it was a promising method.

Germanaud *et al.* [105] computed the eigenfunctions of the Laplace–Beltrami operator to decompose meshes for left- and right-handed subjects. Germanaud was able to detect shallow folds and rare deep folds in the brain which lead to the quantification and classification of brains using the Spangy method.

F. Reeb Graph

A Reeb graph describes the connectivity of the level sets of an object [124]. Visually, a constructed Reeb graph looks similar to a medial axis skeleton. Makram *et al.* [106] suggested a method of using Reeb graph analysis to drive an elastic registration model for the detection of maxilla malformations. The results of detection were deemed satisfactory to a clinician, but not actual values were not reported. The method illustrated the potential for Reeb graph analysis as a registration framework.

Shi *et al.* [107] used reeb graph analysis to isolate, extract, and reconstruct enhanced brain surfaces. The system was able to process cortical surfaces with the accuracy of freesurfer, but at a lower computational cost.

G. Spectral Matching

Spectral correspondence as a way to examine the shapes of objects was first pioneered by Reuter [125], [126] in 2005, and as later expanded by Rustamov [127] where they were

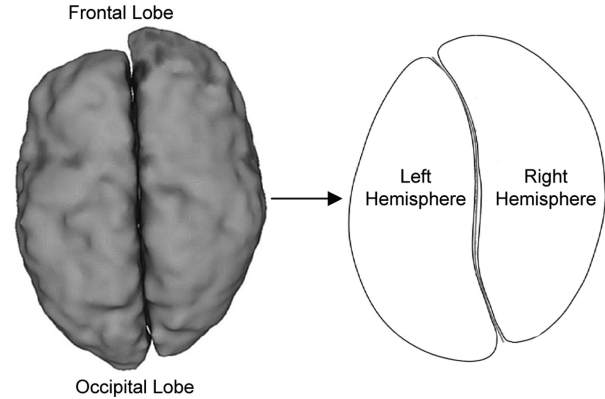


Fig. 15. As shown by Fournier *et al.* [114], the human brain has a slight asymmetry based on if subjects are right or left handed.

combined with Laplace–Beltrami operators. In 2011, Lombaert *et al.* [108] proposed a method of spectral correspondence that was applied to brain shapes. They used an eigendecomposition to match brain surfaces between subjects. Initially, the spectra are computed for each brain. These spectra are then sorted and aligned. The result allows point locations between two brains to be quickly matched. The method is primarily applicable to brain registration. Lombaert *et al.* [109] proposed an extension of this work for corresponding features on the surface of the brain, entitled FOCUSR. The surface features of each brain were used to drive the alignment. The primary advantage of FOCUSR over competing techniques is the speed required to match the brains to one another. The spectral matching technique required a mere 208 s to achieve the same accuracy as FreeSurfer, a commercial brain analysis tool, which required several hours.

H. Symmetry Analysis

Symmetry-based techniques exploit the fact that the human brain is largely symmetric along the sagittal plane, and use this information to make observations. Prima *et al.* [110] proposed an early method of symmetry-based brain analysis. Prima-analyzed brain symmetry to automatically compute the mid-saggital plane and obtain subvoxel accuracy in computing, reorienting, and recentering 3-D images in a time efficient manner.

Gefen *et al.* [111] aligned individual brain images along symmetry lines to create more accurate 3-D models. Gefen concluded that some regions yielded better restoration in 3-D models than other regions, but overall the alignment results were accurate and consistent.

Liu *et al.* [112] examined the topic of multimodality brain registration by aligning the symmetry planes of objects using affine transformations. Liu surmised that the test objects were successfully matched and the symmetry planes were accurately computed.

Feng *et al.* [113] used the symmetry properties of the brain to improve brain segmentation algorithms. Feng's algorithm, while effective at determining bilateral symmetry, was limited by only being applicable to 2-D images.

Fournier *et al.* [114] examined the asymmetries in brains of humans and chimpanzees and compared left- and right-handed individuals to search for a difference (see Fig. 15). Fournier was able to recover typical global asymmetry patterns and hypoth-

esized that future symmetry-based analysis could provide an automated way of comparing individuals.

I. Volumetric Analysis

Volumetric techniques measure the volume of an object. Herman *et al.* [115] proposed a method based on volumetric analysis to use gradient-based boundary tracking to examine the volume between control and Alzheimer's patients. Herman concluded that the gradient-based methods are superior to standard thresholding methods, but did not provide a detailed summary of the diagnostic results.

Wagenknecht *et al.* [116] used a 3-D live-wire approach to extract volumes of interest from a brain for comparison or identification. An average miscalculation rate less than 0.0039 was reported, and the proposed method showed to be accurate and robust for extracting volumes of interest and calculating various properties for them.

IX. DISCUSSION

A. Research Challenges

The brain has long been a topic of research, but utilizing shape analysis with the help of computers enables researchers to examine its shape and texture. There are several major challenges facing shape analysis methods related to the brain or other complex medical structures. The brain is a complex and very diverse organ. Unlike more rigid and well-defined objects that may be easily represented by geometric shapes, the brain suffers from large irregular variabilities. The lack of overall consistency in the brain requires the techniques that analyze it to be flexible, and be able to adaptable to changes in contrast, shape, varying degrees of noise, and abnormality. This illustrates why techniques that rely on predetermined templates or shape models may suffer from difficulty in brain applications. This problem of consistency and complexity is the driving issue that leads to many of the challenges. These challenges can be summarized as follows:

- 1) Due to the size and complexity of the brain and other medical objects, mesh-based approaches often require a significantly large number of nodes or points of reference to perform an accurate surface or shape analysis. Even with modern computing, the complexity of the brain still poses a computational efficiency challenge.
- 2) Medial axis and other skeleton-based analysis may require a large amount of branches and complex paths to accurately represent all of the distinct locations in the human brain.
- 3) The known shape analysis and diagnostic techniques for the brain largely rely on the accuracy of brain segmentation and ability to properly determine structures in the brain. Even with the combination and fusion of modern techniques (e.g., active contours, deformable models, SPHARM, and geodesic distances), identification and segmentation accuracies still suffer significant errors when applied to large sets of data.
- 4) Computer-aided diagnostic systems have faced great difficulty in accurately classifying neurological diseases based on shape metrics over the past decades. This is largely due

to the lack of consistency found across different subjects, but is also due to the difficulty in properly registering and aligning brains so that like areas can be examined.

B. Comparisons and Trends

While there is a high degree of merit in all applications of shape analysis to the brain, some techniques are more suited to specific applications than others. There are four generalized applications of shape analysis techniques with the brain: examination of individual sulci and their curvatures on the brain, examination of the entire human brain and white matter as a whole, registration of brain shapes amongst subjects, and examination of the subcomponents of the brain (e.g., corpus callosum, ventricles, hippocampus). Due to the wide variety of shapes and curvatures in the human brain, many techniques can be used with an array of different brain applications. However, it should be noted that most of the techniques are more commonly used in one or two areas.

Geodesic distances, medial axis, skeletal analysis, and Laplace–Beltrami methods are the most common methods used for examination of the individual sulci and brain curvature, with geodesic distances between the most prevalent in modern applications. SPHARM, voxel- and tensor-based morphometry, volume analysis, symmetry-based modeling, and deformable models are the most common for analysis of the brain and white matter. However, SPHARM is generally reserved for mesh-based applications, and deformable models are often preferred for registration and segmentation applications. While having some uses in whole brain shape analysis, Procrustes analysis, homologous modeling, graph matching, and symmetry-based modeling are most commonly used for brain registration and segmentation applications. Voxel- and tensor-based morphometry, medial axis, skeletal analysis, SPHARM, and distance mapping are the most preferable methods for the examination of subcomponents of the brain, and while typically not always used exclusively, geodesic distances are often combined with these methods. Voxel- and tensor-based morphometry and SPHARM also have significant applications in brain shape registration. It should be specifically noted that deformable models have a high degree of applicability to all of the mentioned analysis methods, and are often combined with or frequently used in many forms of brain shape analysis.

Longitudinal studies and those that examining comparisons between populations tend to most commonly use SPHARM or morphometry-based approaches, because these approaches often take factors of data alignment into account. Geodesic distances can also contribute to longitudinal studies. Deformable models, medial axis, and geodesic distance analysis are good methodologies for examining subcortical structures or legions in the brain along with intricate details about specific anatomy. Cortical thickness studies are most suited for morphometry or distance-based techniques as these provide the most straightforward approaches for measurement studies. In summary, some methods are more suited to specific applications; however, unique studies may need to explore a combination of techniques and approaches due to the abnormality of the brain shape.

To address the aforementioned challenges, recent trends in shape analysis of the brain involve the following aspects:

- 1) Many of the methods discussed were initially applicable to 2-D analysis, but in recent years nearly all methods have evolved for use in 3-D applications.
- 2) Deformable model methods [57]–[59] have seen an increase in usage and have additionally taken the place of many segmentation methods in the past five years, leading to an improved accuracy in brain segmentation. These advances will undoubtedly help to push forward new and improved shape analysis techniques.
- 3) More complex techniques such as SPHARM, started by Gerig *et al.* [65], have been further developed by others [69], [70], [72]–[74] in recent years and have shown great promise in advancing the field for analysis of the cortex and white matter, along with analysis of subcomponents of the brain. These methods have illustrated the potential for utilizing methods that are parameter invariant to solve many of the difficult alignment and registration errors that are often associated with the brain.
- 4) Automation has become increasingly important in modern methods, and the rate of semiautomated and manual methods has drastically decreased. Modern methods are generally expected to perform in an automated manner, and the reduction in human interaction has resulted in an increase in the accuracy for newer techniques.
- 5) Methods such as medial axis analysis [19] and geodesic distances [38] are now more frequently combined with other techniques leading to more accurate segmentation, registration, and classification of the human brain and its various subcomponents, such as the ventricles and corpus callosum.

X. CONCLUSION

This survey details the numerous methods for solving the complex problem of brain shape analysis. Early techniques, which suffered from lower accuracies, slow computation times, and significant user input, have given rise to complicated modern techniques that offer high degrees of automation and improved accuracy. Methods such as SPHARM, deformation-based morphometry, and deformable models will likely become the dominant modes for use in brain shape analysis going forward. Geodesic distances, medial axis, and Laplace–Beltrami operations, among others, will become methods used to support and enhance these dominant modes of brain shape analysis. An amalgamation of techniques opens new opportunities for researchers and engineers to develop more advanced analysis methods. Exciting new opportunities, such as HyperSPHARM and 4-D analysis techniques, provide a look into the future of where modern techniques and amalgamations may be headed. In conclusion, the future of the field of shape analysis for the brain is evolving rapidly, and new techniques will develop and emerge as technology continues to progress.

REFERENCES

- [1] M. Casanova, A. El-Baz, and J. Suri, *Imaging the Brain in Autism*. New York, NY, USA: Springer-Verlag, 2013.
- [2] V. Barras, A. Simons III, and M. Arbib, “Synthetic event-related potentials: A computational bridge between neurolinguistic models and experiments,” *Neural Netw.*, vol. 37, no. 0, pp. 66–92, 2013.
- [3] R. Lande, “Quantitative genetic analysis of multivariate evolution, applied to brain: Body size allometry,” *Evolution*, vol. 33, no. 1, pp. 402–416, 1979.
- [4] R. Desimone, S. Schein, J. Moran, and L. Ungerleider, “Contour, color, and shape analysis beyond the striate cortex,” *Vis. Res.*, vol. 25, no. 3, pp. 441–452, 1985.
- [5] J. Martin, A. Pentland, and R. Kikinis, “Shape analysis of brain structures using physical and experimental modes,” in *Proc. IEEE Comput. Soc. Conf. Comput. Vis. Pattern Recognit.*, Jun. 1994, pp. 752–755.
- [6] M. Delfour and J.-P. Zolsio, *Shapes and Geometries: Metrics, Analysis, Differential Calculus, and Optimization*, (Advances in Design and Control), 2nd ed. Philadelphia, PA, USA: SIAM, Dec. 2010.
- [7] H. Poincaré, *Analysis Situs*, (Séries Journal de l’Ecole polytechnique II sér), 1st ed. Paris, France: Gauthier-Villars, 1895.
- [8] L. de Floriani and M. Spagnuolo, *Shape Analysis and Structuring, (Mathematics and Visualization)*, 1st ed. New York, NY, USA: Springer, Nov. 2010.
- [9] D. Guliato and R. Rangayyan, *Modeling and Analysis of Shape: With Applications in Computer-Aided Diagnosis of Breast Cancer*, (Synthesis Lectures on Biomedical Engineering), 1st ed. San Mateo, CA, USA: Morgan Kaufmann, Jan. 2011.
- [10] D. Attali, J.-D. Boissonnat, and H. Edelsbrunner, “Stability and computation of medial axes—A state-of-the-art report,” in *Mathematical Foundations of Scientific Visualization, Computer Graphics, and Massive Data Exploration*. New York, NY, USA: Springer-Verlag, 2009.
- [11] H. Blum, “A transformation for extracting new descriptors of shape,” *Models Percept. Speech Visual Form*, vol. 19, no. 5, pp. 362–380, 1967.
- [12] H. Blum, “Biological shape and visual science (Part I),” *J. Theoret. Biol.*, vol. 38, no. 2, pp. 205–287, 1973.
- [13] M. Naf, O. Kubler, R. Kikinis, M. E. Shenton, and G. Szekely, “Characterization and recognition of 3D organ shape in medical image analysis using skeletonization,” in *Proc. Math. Methods Biomed. Image Anal. Workshop.*, Jun. 1996, pp. 139–150.
- [14] P. Golland, W. Grimson, and R. Kikinis, “Statistical shape analysis using fixed topology skeletons: Corpus callosum study,” in *Information Processing in Medical Imaging*. New York, NY, USA: Springer-Verlag, 1999, pp. 382–387.
- [15] S. M. Pizer, D. S. Fritsch, P. A. Yushkevich, V. E. Johnson, and E. L. Chaney, “Segmentation, registration, and measurement of shape variation via image object shape,” *IEEE Trans. Med. Imag.*, vol. 18, no. 10, pp. 851–865, Oct. 1999.
- [16] P. Golland, “Statistical shape analysis of anatomical structures” Ph.D. dissertation, Dept. Electr. Eng. Comput. Sci., Massachusetts Inst. Technol., Cambridge, MA, USA, Aug. 2001.
- [17] M. Styner and G. Gerig, “Three-dimensional medial shape representation incorporating object variability,” in *Proc. IEEE Comput. Soc. Conf. Comput. Vis. Pattern Recognit.*, vol. 2, pp. II–651–II–656.
- [18] K. Gorczowski, M. Styner, J.-Y. Jeong, J. S. Marron, J. Piven, H. C. Hazlett, S. M. Pizer, and G. Gerig, “Statistical shape analysis of multi-object complexes,” in *Proc. IEEE Conf. Comput. Vis. Pattern Recognit.*, Jun. 2007, pp. 1–8.
- [19] A. Elnakib, M. F. Casanova, G. Gimel’farb, A. E. Switala, and A. El-Baz, “Autism diagnostics by centerline-based shape analysis of the corpus callosum,” in *Proc. IEEE Int. Symp. Biomed. Imag., Nano Macro*, Apr. 2011, pp. 1843–1846.
- [20] B. Paniagua, A. Lyall, J. B. Berger, C. Vachet, R. M. Hamer, S. Woolson, W. Lin, J. Gilmore, and M. Styner, “Lateral ventricle morphology analysis via mean latitude axis,” *Proc. Soc. Photo Opt. Instrum. Eng.*, vol. 8672, Mar. 2013.
- [21] A. Elnakib, M. Casanova, G. Gimel’farb, A. El-Baz, and K. Suzuki, “Autism diagnostics by 3D shape analysis of the corpus callosum,” in *Machine Learning in Computer-Aided Diagnosis: Medical Imaging Intelligence and Analysis*, K. Suzuki, Ed. Hershey, PA, USA: IGI Global, 2012, pp. 315–335.
- [22] A. Elnakib, M. Casanova, G. Gimel’farb, A. Switala, and A. El-Baz, “Dyslexia diagnostics by 3-D shape analysis of the corpus callosum,” *IEEE Trans. Inf. Technol. Biomed.*, vol. 16, no. 4, pp. 700–708, Jul. 2012.
- [23] A. Elnakib, A. El-Baz, M. Casanova, G. Gimel’farb, and A. Switala, “Image-based detection of corpus callosum variability for more accurate discrimination between dyslexic and normal brains,” in *Proc. IEEE Int. Symp. Biomed. Imag., Nano Macro*, 2010, pp. 109–112.
- [24] A. Elnakib, A. El-Baz, M. Casanova, G. Gimel’farb, and A. Switala, “Image-based detection of corpus callosum variability for more accurate

- discrimination between autistic and normal brains," in *Proc. 17th IEEE Int. Conf. Image Process.*, 2010, pp. 4337–4340.
- [25] M. F. Casanova, A. El-Baz, A. Elnakib, J. Giedd, J. M. Rumsey, E. L. Williams, and A. E. Switala, "Corpus callosum shape analysis with application to dyslexia," *Transl. Neurosci.*, vol. 1, no. 2, pp. 124–130, Jun. 2010.
- [26] M. F. Casanova, A. El-Baz, A. Elnakib, A. E. Switala, E. L. Williams, D. L. Williams, N. J. Minshew, and T. E. Conturo, "Quantitative analysis of the shape of the corpus callosum in patients with autism and comparison individuals," *Autism*, vol. 15, no. 2, pp. 223–238, Mar. 2011.
- [27] A. El-Baz, A. Elnakib, M. Casanova, G. Gimelfarb, A. Switala, D. Jordan, and S. Rainey, "Accurate automated detection of autism related corpus callosum abnormalities," *J. Med. Syst.*, vol. 35, no. 5, pp. 929–939, 2011.
- [28] L. D. Griffin, "The intrinsic geometry of the cerebral cortex," *J. Theoret. Biol.*, vol. 166, no. 3, pp. 261–273, 1994.
- [29] N. Khaneja, M. I. Miller, and U. Grenander, "Dynamic programming generation of curves on brain surfaces," *IEEE Trans. Pattern Anal. Mach. Intell.*, vol. 20, no. 11, pp. 1260–1265, Nov. 1998.
- [30] M. Berger and B. Gostiaux, *Differential Geometry: Manifolds and Curves and And Surfaces*, (Series Graduate texts in mathematics). New York, NY, USA: Springer-Verlag, 1988.
- [31] Y. Wang, B. S. Peterson, and L. H. Staib, "3D brain surface matching based on geodesics and local geometry," *Comput. Vis. Image Understand.*, vol. 89, no. 23, pp. 252–271, 2003.
- [32] J. Pastore, E. Moler, and V. Ballarin, "Segmentation of brain magnetic resonance images through morphological operators and geodesic distance," *Digital Signal Process.*, vol. 15, no. 2, pp. 153–160, 2005.
- [33] A. Huang, R. Abugharbieh, R. Tam, and A. Traboulsee, "MRI brain extraction with combined expectation maximization and geodesic active contours," in *Proc. IEEE Int. Symp. Signal Process. Inf. Technol.*, Aug. 2006, pp. 107–111.
- [34] W. Mio, J. C. Bowers, M. K. Hurdal, and X. Liu, "Modeling brain anatomy with 3D arrangements of curves," in *Proc. IEEE 11th Int. Conf. Comput. Vis.*, Oct. 2007, pp. 1–8.
- [35] J. A. Butman and M. G. Linguraru, "Assessment of ventricle volume from serial MRI scans in communicating hydrocephalus," in *Proc. 5th IEEE Int. Symp. Biomed. Imag., Nano*, May 2008, pp. 49–52.
- [36] J. Hua, Z. Lai, M. Dong, X. Gu, and H. Qin, "Geodesic distance-weighted shape vector image diffusion," *IEEE Trans. Vis. Comput. Graph.*, vol. 14, no. 6, pp. 1643–1650, Nov. 2008.
- [37] X. Liang and J. Zhang, "White matter integrity analysis along cingulum paths in mild cognitive impairment—A geodesic distance approach," in *Proc. 2nd Int. Conf. Bioinformat. Biomed. Eng.*, May 2008, pp. 510–513.
- [38] A. A. Joshi, D. W. Shattuck, H. Damasio, and R. M. Leahy, "Geodesic curvature flow on surfaces for automatic sulcal delineation," in *Proc. 9th IEEE Int. Symp. Biomed. Imag.*, May 2012, pp. 430–433.
- [39] R. Kimmel and N. Kiryati, *Finding Shortest Paths On Surfaces By Fast Global Approximation And Precise Local Refinement*. Citeseer, 1994.
- [40] R. Kimmel, A. Amir, and A. M. Bruckstein, "Finding shortest paths on surfaces using level sets propagation," *IEEE Trans. Pattern Anal. Mach. Intell.*, vol. 17, no. 6, pp. 635–640, Jun. 1995.
- [41] R. Kimmel and J. A. Sethian, "Computing geodesic paths on manifolds," *Proc. Nat. Acad. Sci.*, vol. 95, no. 15, pp. 8431–8435, 1998.
- [42] E. Tripp, *The Meridian Handbook of Classical Mythology*. New York, NY, USA: Penguin, 1974.
- [43] A. W. Toga and P. M. Thompson, "The role of image registration in brain mapping," *Image Vis. Comput.*, vol. 19, no. 1–2, pp. 3–24, Jan. 2001.
- [44] N. Duta, A. K. Jain, and M. P. Dubuisson-Jolly, "Learning 2-D shape models," *Proc. Comput. Vis. Pattern Recognit., IEEE Comput. Soc. Conf.*, vol. 2, pp. 8–14, 1999.
- [45] X. Penin, C. Berge, and M. Baylac, "Ontogenetic study of the skull in modern humans and the common chimpanzees: Neotenic hypothesis reconsidered with a tridimensional procrustes analysis," *Amer. J. Phys. Anthropol.*, vol. 118, no. 1, pp. 50–62, 2002.
- [46] T. Bienvenu, F. Guy, W. Coudyzer, E. Gilissen, G. Roualdès, P. Vignaud, and M. Brunet, "Assessing endocranial variations in great apes and humans using 3-D data from virtual endocasts," *Amer. J. Phys. Anthropol.*, vol. 145, no. 2, pp. 231–246, 2011.
- [47] N. Duta, A. K. Jain, and M. P. Dubuisson-Jolly, "Automatic Construction of 2-D Shape Models," *IEEE Trans. Pattern Anal. Mach. Intell.*, vol. 23, no. 5, pp. 433–446, May 2001.
- [48] T. McInerney and D. Terzopoulos, "Deformable models in medical image analysis," in *Proc. Math. Methods Biomed. Image Anal.*, 1996, *Proc. Workshop*, Jun. 1996, pp. 171–180.
- [49] C. Xu and J. L. Prince, "Snakes, shapes, and gradient vector flow," *IEEE Trans. Image Process.*, vol. 7, no. 3, pp. 359–369, Mar. 1998.
- [50] C. Xu and J. L. Prince, "Gradient vector flow deformable models," in *Handbook of Medical Imaging*. San Diego, CA, USA: Academic, 2000, pp. 159–169.
- [51] C. Davatzikos, "Spatial transformation and registration of brain images using elastically deformable models," *Comput. Vis. Image Understand.*, vol. 66, no. 2, pp. 207–222, 1997.
- [52] A. Dale, B. Fischl, and M. Sereno, "Cortical surface-based analysis—Part I: Segmentation and surface reconstruction," *Neuroimage*, vol. 9, no. 2, pp. 179–194, 1999.
- [53] S. M. Smith, "Fast robust automated brain extraction," *Hum. Brain Mapp.*, vol. 17, no. 3, pp. 143–155, Nov. 2002.
- [54] A. H. Zhuang, D. J. Valentino, and A. W. Toga, "Skull-stripping magnetic resonance brain images using a model-based level set," *Neuroimage*, vol. 32, no. 1, pp. 79–92, Aug. 2006.
- [55] A. A. Joshi, D. W. Shattuck, P. M. Thompson, and R. M. Leahy, "Surface-constrained volumetric brain registration using harmonic mappings," *IEEE Trans. Med. Imag.*, vol. 26, no. 12, pp. 1657–1669, Dec. 2007.
- [56] Z. Tu, K. L. Narr, P. Dollar, I. DiNov, P. M. Thompson, and A. W. Toga, "Brain anatomical structure segmentation by hybrid discriminative/generative models," *IEEE Trans. Med. Imag.*, vol. 27, no. 4, pp. 495–508, Apr. 2008.
- [57] A. Huang, R. Abugharbieh, and R. Tam, "A hybrid geometric statistical deformable model for automated 3-D segmentation in brain MRI," *IEEE Trans. Biomed. Eng.*, vol. 56, no. 7, pp. 1838–1848, Jul. 2009.
- [58] J. X. Liu, Y. S. Chen, and L. F. Chen, "Accurate and robust extraction of brain regions using a deformable model based on radial basis functions," *J. Neurosci. Methods*, vol. 183, no. 2, pp. 255–266, 2009.
- [59] J. Li, X. Liu, J. Zhuo, R. P. Gullapalli, and J. M. Zara, "A deformable surface model based automatic rat brain extraction method," in *Proc. IEEE Int. Symp. Biomed. Imag., Nano Macro*, Apr. 2011, pp. 1741–1745.
- [60] A. Hashioka, S. Kobashi, K. Kuramoto, Y. Wakata, K. Ando, R. Ishikura, T. Ishikawa, S. Hirota, and Y. Hata, "Shape and appearance knowledge based brain segmentation for neonatal MR images," in *Proc. World Autom. Congr.*, Jun. 2012, pp. 1–6.
- [61] R. P. Woods, S. T. Grafton, C. J. Holmes, S. R. Cherry, and J. C. Mazziotta, "Automated image registration—Part I: General methods and intrasubject, intramodality validation," *J. Comput. Assist. Tomogr.*, vol. 22, no. 1, pp. 139–152, 1998.
- [62] R. P. Woods, S. T. Grafton, J. D. Watson, N. L. Sicotte, and J. C. Mazziotta, "Automated image registration—Part II: Intersubject validation of linear and nonlinear models," *J. Comput. Assist. Tomogr.*, vol. 22, no. 1, pp. 153–165, 1998.
- [63] D. Shen and C. Davatzikos, "HAMMER: Hierarchical attribute matching mechanism for elastic registration," in *Proc. IEEE Workshop Math. Methods Biomed. Image Anal.*, 2001, pp. 29–36.
- [64] T. Liu, D. Shen, and C. Davatzikos, "Deformable registration of cortical structures via hybrid volumetric and surface warping," *Neuroimage*, vol. 22, no. 4, pp. 1790–1801, Aug. 2004.
- [65] G. Gerig, M. Styner, D. Jones, D. Weinberger, and J. Lieberman, "Shape analysis of brain ventricles using SPHARM," in *Proc. IEEE Workshop Math. Methods Biomed. Image Anal.*, 2001, pp. 171–178.
- [66] M. K. Chung, K. M. Dalton, and R. J. Davidson, "Encoding neuroanatomical information using weighted spherical harmonic representation," in *Proc. 14th Workshop Statist. Signal Process.*, Aug. 2007, pp. 146–150.
- [67] A. Kelemen, G. Székely, and G. Gerig, "Elastic Model-Based Segmentation of 3D Neuroradiological Data Sets," *IEEE Trans. Med. Imag.*, vol. 18, no. 10, pp. 828–839, Oct. 1999.
- [68] A. Uthama, R. Abugharbieh, A. Traboulsee, and M. J. McKeown, "Invariant SPHARM shape descriptors for complex geometry in MR region of interest analysis," in *Proc. 29th Annu. Int. Conf. IEEE Eng. Med. Biol. Soc.*, Aug. 2007, pp. 1322–1325.
- [69] A. Ben Abdallah, F. Ghorbel, H. Essabbah, and M. H. Bedoui, "Chapter 9: Shape analysis of left ventricle using invariant 3D spherical harmonics shape descriptors," in *Proc. 3rd Int. Conf. Geometr. Model. Imag.*, Jul. 2008, pp. 53–58.
- [70] M. K. Chung, K. M. Dalton, and R. J. Davidson, "Tensor-based cortical surface morphometry via weighted spherical harmonic representation," *IEEE Trans. Med. Imag.*, vol. 27, no. 8, pp. 1143–1151, Aug. 2008.
- [71] A. Uthama, R. Abugharbieh, S. J. Palmer, A. Traboulsee, and M. J. McKeown, "SPHARM-based spatial fMRI characterization with

- intersubject anatomical variability reduction," *IEEE J. Sel. Topics Signal Process.*, vol. 2, no. 6, pp. 907–918, Dec. 2008.
- [72] M. Esmaeil-Zadeh, H. Soltanian-Zadeh, and K. Jafari-Khouzani, "SPHARM-based shape analysis of hippocampus for lateralization in mesial temporal lobe epilepsy," in *Proc. 8th Iran. Conf. Electr. Eng.*, May 2010, pp. 39–44.
- [73] M. Nitzken, M. F. Casanova, G. Gimel'farb, F. Khalifa, A. Elnakib, A. E. Switala, and A. El-Baz, "3-D shape analysis of the brain cortex with application to autism," in *Proc. IEEE Int. Symp. Biomed. Imag. Nano Macro*, Apr. 2011, pp. 1847–1850.
- [74] M. Nitzken, M. F. Casanova, G. Gimel'farb, A. Elnakib, F. Khalifa, A. E. Switala, and A. El-Baz, "3D shape analysis of the brain cortex with application to dyslexia," in *Proc. 18th IEEE Int. Conf. Image Process.*, Sep. 2011, pp. 2657–2660.
- [75] X. Geng, T. J. Ross, H. Gu, W. Shin, W. Zhan, Y.-P. Chao, C.-P. Lin, N. Schuff, and Y. Yang, "Diffeomorphic image registration of diffusion MRI using spherical harmonics," *IEEE Trans. Med. Imag.*, vol. 30, no. 3, pp. 747–758, Mar. 2011.
- [76] H. Kim, T. Mansi, A. Bernasconi, and N. Bernasconi, "Vertex-wise shape analysis of the hippocampus: Disentangling positional differences from volume changes," *Med. Image Comput. Comput. Assist. Interv.*, vol. 14, Pt. 2, pp. 352–359, 2011.
- [77] A. Hosseini, M. K. Chung, S. Schaefer, C. van Reekum, L. Peschke-Schmitz, M. Sutterer, A. L. Alexander, and R. J. Davidson, "4D hyperspherical harmonic (hyperspharm) representation of multiple disconnected brain subcortical structures," in *Proc. 16th Int. Conf. Med. Image Comput. Comput. Assist. Interv.*, Sep. 2013, pp. 598–605.
- [78] C. H. Brechbuhler, G. Gerig, and O. Kubler, "Parametrization of closed surfaces for 3-D shape description," *Comput. Vis. Image Understand.*, vol. 61, no. 2, pp. 154–170, 1995.
- [79] M. Styner, I. Oguz, S. Xu, C. Brechbuhler, D. Pantazis, J. J. Levitt, M. E. Shenton, and G. Gerig, "Framework for the statistical shape analysis of brain structures using SPHARM-PDM," *Insight J.*, vol. 1071, no. 1071, pp. 242–250, 2006.
- [80] M. Nitzken, M. Casanova, F. Khalifa, G. Sokhadze, and A. El-Baz, "Shape-based detection of cortex variability for more accurate discrimination between autistic and normal brains," in *Multi Modality State-of-the-Art Medical Image Segmentation and Registration Methodologies*, A. S. El-Baz, R. Acharya U, A. F. Laine, and J. S. Suri, Eds. New York, NY, USA: Springer-Verlag, 2011, pp. 161–185.
- [81] A. Elnakib, M. Nitzken, M. Casanova, H. Park, G. Gimel'farb, and A. El-Baz, "Quantification of age-related brain cortex change using 3d shape analysis," in *Proc. 21st Int. Conf. Pattern Recognit.*, 2012, pp. 41–44.
- [82] E. L. Williams, A. El-Baz, M. Nitzken, A. E. Switala, and M. F. Casanova, "Spherical harmonic analysis of cortical complexity in autism and dyslexia," *Transl. Neurosci.*, vol. 3, no. 1, pp. 36–40, Mar. 2012.
- [83] M. K. Chung, K. J. Worsley, and A. C. Evans, "Tensor-based brain surface modeling and analysis," in *Proc. IEEE Comput. Soc. Conf. Comput. Vis. Pattern Recognit.*, 2003, vol. 1, pp. I–467–I–473.
- [84] A. D. Leow, A. D. Klunder, C. R. JackJr., A. Toga, A. Dale, M. A. Bernstein, P. J. Britson, J. L. Gunter, C. P. Ward, J. L. Whitwell, B. J. Borowski, A. S. Fleisher, N. C. Fox, D. Harvey, J. Kornak, N. Schuff, C. Studholme, G. Alexander, and M. W. Weiner Thompson, "Longitudinal stability of MRI for mapping brain change using tensor-based morphometry," *NeuroImage*, vol. 31, no. 2, pp. 627–640, 2006.
- [85] N. Lepore, C. Brun, Y. Y. Chou, M. C. Chiang, R. A. Dutton, K. M. Hayashi, E. Luders, O. L. Lopez, H. J. Aizenstein, A. W. Toga, J. T. Becker, and P. M. Thompson, "Generalized tensor-based morphometry of HIV/AIDS using multivariate statistics on deformation tensors," *IEEE Trans. Med. Imag.*, vol. 27, no. 1, pp. 129–141, Jan. 2008.
- [86] M. Afzali and H. Soltanian-Zadeh, "Comparison of voxel-based morphometry (VBM) And tractography of diffusion tensor MRI (DT-MRI) in temporal lobe epilepsy," in *Proc. 18th Iran. Conf. Electr. Eng.*, 2010, pp. 18–23.
- [87] Y. Wang, T. F. Chan, A. W. Toga, and P. M. Thompson, "Shape analysis with multivariate tensor-based morphometry and holomorphic differentials," in *Proc. IEEE 12th Int. Conf. Comput. Vis.*, 2009, pp. 2349–2356.
- [88] H. Yang, W. Liu, H. Xia, Z. Zhou, and L. Tong, "Longitudinal change of the grey matter of mild cognitive impairment patients over 3 years by using voxel-based morphometry," in *Proc. 5th Int. Conf. Biomed. Eng. Informat.*, 2012, pp. 304–308.
- [89] E. Fletcher, A. Knaack, B. Singh, E. Lloyd, E. Wu, O. Carmichael, and C. DeCarli, "Combining boundary-based methods with tensor-based morphometry in the measurement of longitudinal brain change," *IEEE Trans. Med. Imag.*, vol. 32, no. 2, pp. 223–236, Feb. 2013.
- [90] J. Shi, Y. Wang, R. Ceschin, X. An, M. D. Nelson, A. Panigrahy, and N. Lepore, "Surface fluid registration and multivariate tensor-based morphometry in newborns—The effects of prematurity on the putamen," in *Proc. Asia-Pacific Signal Inf. Process. Assoc. Annu. Summit Conf.*, 2012, pp. 1–8.
- [91] F. L. Bookstein, "'Voxel-based morphometry' should not be used with imperfectly registered images," *Neuroimage*, vol. 14, no. 6, pp. 1454–1462, Dec. 2001.
- [92] U. Grenander and M. I. Miller, "Computational anatomy: An emerging discipline," *Quart. Appl. Math.*, vol. 56, no. 4, pp. 617–694, 1998.
- [93] J. Ashburner and K. J. Friston, "Why voxel-based morphometry should be used," *Neuroimage*, vol. 14, no. 6, pp. 1238–1243, 2001.
- [94] Q. He, Y. Duan, J. Miles, and N. Takahashi, "Statistical shape analysis of the corpus callosum in subtypes of autism," in *7th IEEE Int. Conf. Proc. Bioinform. Bioeng.*, Oct. 2007, pp. 1087–1091.
- [95] A. El-Baz, M. F. Casanova, G. Gimel'farb, M. Mott, and A. E. Switala, "Autism diagnostics by 3-D texture analysis of cerebral white matter gyrfications," *Med. Image Comput. Comput. Assist. Interv.*, vol. 10, Pt 2, pp. 882–890, 2007.
- [96] J. Cates, P. T. Fletcher, M. Styner, M. Shenton, and R. Whitaker, "Shape modeling and analysis with entropy-based particle systems," *Inf. Process. Med. Imag.*, vol. 20, pp. 333–345, 2007.
- [97] T. Geraud, J. F. Mangin, I. Bloch, and H. Maitre, "Segmenting internal structures in 3-D MR images of the brain by Markovian relaxation on a watershed based adjacency graph," in *Proc. Int. Conf. Image Process.*, Oct. 1995, vol. 3, pp. 548–551.
- [98] F. Yang and F. Kruggel, "Optimization algorithms for labeling brain sulci based on graph matching," in *Proc. IEEE 11th Int. Conf. Comput. Vis.*, Oct. 2007, pp. 1–7.
- [99] S. S. Long and L. B. Holder, "Graph based MRI brain scan classification and correlation discovery," in *Proc. IEEE Symp. Computat. Intell. Bioinform. Computat. Biol.*, May 2012, pp. 335–342.
- [100] K. Yamaguchi, S. Kobashi, I. Mohri, S. Imawaki, M. Tamiike, and Y. Hata, "Brain shape homologous modeling using sulcal-distribution index in MR images," in *Proc. Syst., Man Cybern., IEEE Int. Conf.*, Oct. 2009, pp. 1102–1106.
- [101] K. Yamaguchi, S. Kobashi, K. Kuramoto, Y. T. Kitamura, S. Imawaki, and Y. Hata, "Statistical quantification of brain shape deformation with homologous brain shape modeling," in *Proc. World Autom. Congr.*, Sep. 2010, pp. 1–6.
- [102] S. Angenent, S. Haker, A. Tannenbaum, and R. Kikinis, "On the Laplace-Beltrami operator and brain surface flattening," *IEEE Trans. Med. Imag.*, vol. 18, no. 8, pp. 700–711, Aug. 1999.
- [103] R. Lai, Y. Shi, N. Sicotte, and A. W. Toga, "Automated corpus callosum extraction via Laplace–Beltrami nodal parcellation and intrinsic geodesic curvature flows on surfaces," in *Proc. IEEE Int. Conf. Comput. Vis.*, Nov. 2011, pp. 2034–2040.
- [104] R. Shishegar, H. Soltanian-Zadeh, and S. R. Moghadasi, "Hippocampal shape analysis in epilepsy using Laplace–Beltrami spectrum," in *Proc. 19th Iran. Conf. Electr. Eng.*, May 2011, p. 1.
- [105] D. Germanaud, J. Lefevre, R. Toro, C. Fischer, J. Dubois, L. Hertz-Pannier, and J. F. Mangin, "Larger is twistier: Spectral analysis of gyration (SPANGY) applied to adult brain size polymorphism," *Neuroimage*, vol. 63, no. 3, pp. 1257–1272, Nov. 2012.
- [106] M. Makram, H. Kamel, and M. Emma, "3D elastic registration using a balanced multi resolution reeb graph: Application for a detection of a maxilla facial malformation," in *Proc. Int. Conf. Comput. Commun. Eng.*, May 2008, pp. 1063–1071.
- [107] Y. Shi, R. Lai, and A. Toga, "Cortical surface reconstruction via unified reeb analysis of geometric and topological outliers in magnetic resonance images," *IEEE Trans. Med. Imag.*, 2012.
- [108] H. Lombaert, L. Grady, J. R. Polimeni, and F. Cheriet, "Fast brain matching with spectral correspondence," *Inf. Process. Med. Imag.*, vol. 22, pp. 660–673, 2011.
- [109] H. Lombaert, L. Grady, J. R. Polimeni, and F. Cheriet, "FOCUSR: Feature oriented correspondence using spectral regularization—A method for precise surface matching," *IEEE Trans. Pattern Anal. Mach. Intell.*, vol. 35, no. 9, pp. 2143–2160, Sep. 2013.
- [110] S. Prima, S. Ourselin, and N. Ayache, "Computation of the mid-sagittal plane in 3D brain images," *IEEE Trans. Med. Imag.*, vol. 21, no. 2, pp. 122–138, Feb. 2002.

- [111] S. Gefen, Y. Fan, L. Bertrand, and J. NissaNov, "Symmetry-based 3D brain reconstruction," in *Proc. IEEE Int. Symp. Biomed. Imag., Nano Macro*, Apr. 2004, pp. 744–747.
- [112] X. Liu, C. Imielinska, A. F. Laine, and A. D'Ambrosio, "Symmetry based multi-modality registration of the brain imagery," in *Proc. IEEE Int. Symp. Signal Process. Inf. Technol.*, Dec. 2007, pp. 807–812.
- [113] J. Feng, F. Desheng, and B. Shuoben, "Brain image segmentation based on bilateral symmetry information," in *Proc. 2nd Int. Conf. Bioinformat. Biomed. Eng.*, May 2008, pp. 1951–1954.
- [114] M. Fournier, B. Combes, N. Roberts, S. Keller, T. J. Crow, W. D. Hopkins, and S. Prima, "Surface-based method to evaluate global brain shape asymmetries in human and chimpanzee brains," in Apr. 2, 2011, pp. 310–316.
- [115] G. T. Herman, M. I. Kohn, and R. E. Gur, "Computerized three-dimensional volume analysis from magnetic resonance images for characterization of brain disorders," in *Proc. Biomed. Eng., Proc. Spec. Symp. Matur. Technol. Emerg. Horiz.*, Nov. 1988, pp. 65–67.
- [116] G. Wagenknecht and S. Winter, "Volume-of-interest segmentation of cortical regions for multimodal brain analysis," in *Proc. IEEE Nuclear Sci. Symp. Conf. Rec.*, Oct. 2008, pp. 4368–4372.
- [117] M. F. Casanova, A. El-Baz, M. Mott, G. Mannheim, H. Hassan, R. Fahmi, J. Giedd, J. M. Rumsey, A. E. Switala, and A. Farag, "Reduced gyral window and corpus callosum size in autism: Possible macroscopic correlates of a minicolumnopathy," *J. Autism. Dev. Disord.*, vol. 39, no. 5, pp. 751–764, May 2009.
- [118] M. F. Casanova, A. S. El-Baz, J. Giedd, J. M. Rumsey, and A. E. Switala, "Increased white matter gyral depth in dyslexia: Implications for cortico-cortical connectivity," *J. Autism. Dev. Disord.*, vol. 40, no. 1, pp. 21–29, Jan. 2010.
- [119] A. El-Baz, M. Casanova, G. Gimel'farb, M. Mott, A. Switala, E. Vanbogaert, and R. McCracken, "A new CAD system for early diagnosis of dyslexic brains," in *Proc. 15th IEEE Int. Conf. Image Process.*, 2008, pp. 1820–1823.
- [120] A. El-Baz, M. Casanova, G. Gimel'farb, M. Mott, A. Switala, E. Vanbogaert, and R. McCracken, "Dyslexia diagnostics by 3D texture analysis of cerebral white matter gyrfications," in *Proc. 19th Int. Conf. Pattern Recognit.*, 2008, pp. 1–4.
- [121] A. El-Baz, M. Casanova, G. Gimel'farb, M. Mott, and A. Switala, "A new image analysis approach for automatic classification of autistic brains," in *Proc. 4th IEEE Int. Symp. Biomed. Imag.*, 2007, pp. 352–355.
- [122] A. El-Baz, M. Casanova, G. Gimel'farb, M. Mott, and A. Switala, "An MRI-based diagnostic framework for early diagnosis of dyslexia," *Int. J. Comput. Assist. Radiol. Surg.*, vol. 3, no. 3–4, pp. 181–189, 2008.
- [123] R. Fahmi, A. El-Baz, H. Abd El Munim, A. Farag, and M. Casanova, "Classification techniques for autistic Vs. typically developing brain using MRI data," in *Proc. 4th IEEE Int. Symp. Biomed. Imag., Nano Macro*, 2007, pp. 1348–1351.
- [124] H. Doraiswamy and V. NataraJan, "Efficient algorithms for computing Reeb graphs," *Computat. Geometry*, vol. 42, no. 67, pp. 606–616, 2009.
- [125] M. Reuter, F.-E. Wolter, and N. Peinecke, "Laplace-spectra as fingerprints for shape matching," in *Proc. 2005 ACM Symp. Solid Phys. Model.*, NY, USA: ACM, 2005, pp. 101–106.
- [126] M. Reuter, F.-E. Wolter, and N. Peinecke, "Laplace–Beltrami spectra as shape-DNA of surfaces and solids," *Comput.-Aided Design*, vol. 38, no. 4, pp. 342–366, 2006.
- [127] R. M. Rustamov, "Laplace–Beltrami eigenfunctions for deformation invariant shape representation," in *Proc. 5th Eurograph. Symp. Geometry Process.*, 2007, pp. 225–233.



Matthew J. Nitzken (M'10) received the B.S. and M.Eng. degrees in 2009 and 2010, respectively, from the University of Louisville, Louisville, KY, USA.

He is currently a Doctoral Candidate in the electrical and computer engineering program at the University of Louisville. He has a strong focus in the fields of shape analysis, computer-aided detection and diagnosis, and the understanding of complex brain disorders. His primary area of expertise is in 2-dimensional and 3-dimensional shape analysis, and over the years he has worked extensively in brain, lung, heart, and prostate analysis. He has more than 20 combined publications and book chapters and has submitted numerous patents in the field of brain and lung shape analysis. His work has had the opportunity to be presented at conferences in countries around the world, including the United States, Germany, Spain, and Japan, among others.



Manuel F. Casanova received the B.S. degree from the University of Puerto Rico, Puerto, Rico, in 1975, the M.D. degree from the School of Medicine, University of Puerto Rico, in 1979, and the Internship and Residency Neurology from the University District Hospital, in 1983.

From 1983 to 1986, he was Clinical and Research Fellow at The Johns Hopkins University, MD, USA. He is currently the Gottfried and Gisela Kolbe Endowed Chair in psychiatry in the University of Louisville, Louisville, KY, USA. Dr. Casanova was

a Magisterial Speaker at the World Autism Congress in 2010 and the recipient of an EUREKA award from the National Institute of Mental Health. He has received the titles of Stanley Scholar from the United States and an Honorary Professor degree from the University of Krasnoyarsk, Russia. He is one of the founding members for the International Autism Institute. He serves on the Editorial Board of 20 journals and has published more than 200 peer reviewed articles and 70 book chapters.

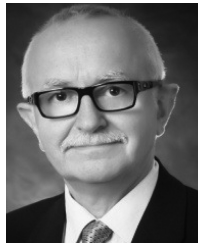


Georgy Gimel'farb received the Ph.D. degree from the Ukrainian Academy of Sciences in 1969 and an advanced Doctor of Engineering degree from the Higher Certifying Commission of the USSR in 1991. After working for a long time in the Glushkov Institute of Cybernetics of the Ukrainian Academy of Sciences, he joined in 1997 the University of Auckland (New Zealand) where he is currently a Professor of Computer Science and a Codirector of the Intelligent Vision Systems Laboratory. He authored or coauthored more than 45 journal articles, 260 papers in peer-reviewed conference proceedings, 65 book chapters, two textbooks, and four books, including the monograph "Image Textures and Gibbs Random Fields" (Kluwer Academic, 1999). His research interests include probabilistic image modeling, statistical pattern recognition, texture analysis in medical and remotely sensed images, and computer stereo vision. In 1997, he received a prestigious State Premium of Ukraine in Science and Technology for fundamental and applied results in image and signal recognition.



Tamer Inanc (M'xx) received the M.S. and Ph.D. degrees from Department of Electrical Engineering, Pennsylvania State University, State College, PA, USA, in 1996 and 2002, respectively, under supervision of Prof. M. Sznaier.

After receiving the Ph.D. degree, he did a Postdoctoral Scholarship at California Institute of Technology, Pasadena, CA, USA, between 2002 and 2004 under the supervision of Prof. R. M. Murray. He started working as an Assistant Professor in 2004 at Department of Electrical and Computer Engineering, University of Louisville, Louisville, KY, USA. He has been working as an Associate Professor at the same department since 2010. His research interests include control systems, robust identification, active vision systems, autonomous robotics, biometrics and control systems and identification applications to bioengineering problems.



Jacek M. Zurada (LF'96) received the M.S. and Ph.D. degrees in 1968 and 1975, respectively from the Gdansk Institute of Technology, Gdansk, Poland.

He currently serves as a Professor of electrical and computer engineering at the University of Louisville, Louisville, KY, USA. He authored or coauthored several books and more than 370 papers in the area of computational intelligence, neural networks and machine learning, logic rule extraction, and bioinformatics, and delivered numerous presentations and seminars throughout the world. His work has been cited

more than 7400 times.

Dr. Zurada currently serves as IEEE V-President for Technical Activities (TAB Chair) and also chairs the IEEE TAB Management Committee. He was the Editor-in-Chief of the IEEE TRANSACTIONS ON NEURAL NETWORKS (1997–03), Associate Editor of the IEEE TRANSACTIONS ON CIRCUITS AND SYSTEMS and was member of the Editorial Board of The Proceedings of the IEEE. In 2004–05, he was the President of the IEEE Computational Intelligence Society. He is an Associate Editor of *Neurocomputing*, *Neural Networks*, and of several other international journals. He holds the title of a Professor in Poland, the Membership of the Polish Academy of Sciences, and has been awarded numerous awards, including the Joe Desch Award in 2013 and four honorary professorships of Chinese universities, including of Sichuan University in Chengdu. He is a Board of Directors Member of IEEE, IEEE CIS, and IJCNN.



Ayman El-Baz (M'05) received the B.S. and M.S. degrees in electrical engineering from Mansoura University, Egypt, in 1997 and 2000, respectively, and the Ph.D. degree in electrical engineering from the University of Louisville, KY, USA, in 2006.

He is an Associate Professor in the Department of Bioengineering at the University of Louisville, KY. Dr. El-Baz has twelve years of hands-on experience in the fields of bioimaging modeling and computer-assisted diagnostic systems. He has developed new techniques for analyzing 3D medical images. His work has been

reported at several prestigious international conferences (e.g., CVPR, ICCV, MICCAI, etc.) and in journals (e.g., IEEE TMI, IEEE TIP, IEEE TBME, IEEE TITB, Brain, etc.). His work related to novel image analysis techniques for lung cancer and autism diagnosis have earned him multiple awards, including: first place at the annual Research Louisville 2002, 2005, 2006, 2007, 2008, 2010, 2011 and 2012 meetings, and the "Best Paper Award in Medical Image Processing" from the prestigious ICGST International Conference on Graphics, Vision and Image Processing (GVIP-2005). He has authored or coauthored more than 300 technical articles.

IEEE
proof